

A SYSTEMS APPROACH TO THE PASSIVE PROPERTIES
OF THE URINARY BLADDER IN THE COLLECTION PHASE

A SYSTEMS APPROACH TO THE PASSIVE PROPERTIES OF THE
URINARY BLADDER IN THE COLLECTION PHASE

PROEFSCHRIFT
TER VERKRIJGING VAN DE GRAAD VAN DOCTOR IN DE
GENEESKUNDE
AAN DE ERASMUS UNIVERSITEIT ROTTERDAM
OP GEZAG VAN DE RECTOR MAGNIFICUS
PROF. DR. B. LEIJNSE
EN VOLGENS BESLUIT VAN HET COLLEGE VAN DEKANEN.
DE OPENBARE VERDEDIGING ZAL PLAATS VINDEN OP
WOENSDAG 2 FEBRUARI 1977 DES NAMIDDAGS
TE 4.15 UUR PRECIES
DOOR
ROBERT VAN MASTRIGT
GEBOREN TE ROTTERDAM

PROMOTOR : PROF.DR. G. VAN DEN BRINK

CO-REFERENTEN: PROF.DR. N.J. BAKKER

PROF.IR. B.P.TH. VELTMAN

Dit proefschrift is opgedragen aan het Nederlandse Volk, dat ervoor betaalde.

A SYSTEMS APPROACH TO THE PASSIVE PROPERTIES
OF THE URINARY BLADDER IN THE COLLECTION PHASE

Contents

Contents	1
List of symbols	4
0. Preface	7
I. <u>Introduction</u>	8
A. Urology and Urodynamics	8
B. Anatomy and physiology of the urinary tract	9
C. Purpose and justification of the investigation	11
D. Functional approach to the urinary bladder	13
II. <u>Time dependent behaviour of the bladder wall</u>	17
A. Theory	17
1. Introduction	17
2. Visco-elasticity	18
3. Geometry of a strip of bladder wall	22
4. Determination of tissue volume	23
B. Methods	25
1. Set-up of the experimental equipment	25
2. Separation of multi-exponential signals	27
a. Statement of the problem	27
b. Constant step approximation	28
c. Operational interpretation	29
d. Test set-up	31
e. Influence of the position of the first sample	33
f. Influence of noise	35
g. Rate of convergence of algorithm	39
h. Conclusion and discussion	42
3. On-line computer analysis	44

C. Results	48
1. Order of investigated system	48
2. Relaxation constants as functions of the chemical environment	52
3. Check of conditions	57
4. Conclusion and discussion	60
D. Alternative analysis methods	61
1. Introduction	61
2. Orthonormal exponential functions	61
3. Continuous relaxation spectrum	66
4. Analogue simulation	69
5. Power series	70
6. Other models	70
7. Conclusion and discussion	71
E. Alternative measurements	72
1. Theory	72
2. Experimental equipment set-up	74
3. Results	75
4. Conclusion and discussion	78
III. <u>Length dependent behaviour of the bladder wall</u>	80
A. Theory	80
1. Conclusions from time dependent behaviour	80
2. Introduction to pulse measurements	84
3. Non-linearities	85
B. Methods	87
C. Results	90
D. Conclusion and discussion	95
IV. <u>Geometry of the urinary bladder</u>	96
A. Theory	96

B. Methods	100
C. Results	102
D. Conclusion and discussion	106
V. <u>Evaluation of total bladder model</u>	108
A. Theory	108
1. Introduction	108
2. Cystometry	110
3. Step response measurements	113
B. Methods	116
C. Results	118
VI. <u>Conclusions</u>	121
Summary	124
Samenvatting	126
References	128
Curriculum vitae	136

List of symbols

a	coefficient of exponential model	(N)
a_a	apparent coefficient of exponential model	(N)
a_0	constant in multi-exponential model	(N)
a_n	coefficient of n^{th} exponential (initial height of exponential decay curve)	(N)
$a(\gamma)$	continuous relaxation spectrum	(N)
b_n	coefficient of n^{th} orthonormal function	(N)
c_{ij}	arbitrary constant	(-)
C_{nj}	coefficient of orthonormal function	(-)
d	urinary bladder wall thickness	(m)
e	natural logarithm base	(-)
e_n	relative elastic modulus $E_n/E(I\epsilon l)$	(-)
E_n	elastic modulus of n^{th} spring	(N/m ²)
E_s	apparent elastic modulus of a spring	(N)
$E(I\epsilon l)$	elastic modulus function	(N/m ²)
IEI	elastic coefficient	(N/m ²)
F	force measured	(N)
F_a	weight of bladder strip in air	(N)
F_w	weight of bladder strip in water	(N)
g	acceleration due to gravity	(m/s ²)
i	index number	(-)
j	index number	(-)
k	number of exponential terms used	(-)
l	length of a strip of bladder wall	(m)
l_0	length of a strip of bladder wall unstrained	(m)
l_a	side of rectangular parallelepiped	(m)
l_b	side of rectangular parallelepiped	(m)
n	index number	(-)
N	number of experimental points	(-)

p	pressure in the bladder related to barometric pressure	(N/m^2)
p_0	pressure inside the sphere	(N/m^2)
p_1	pressure outside the sphere	(N/m^2)
r_0	radius of thickwalled sphere (internal)	(m)
r_1	radius of thickwalled sphere (external)	(m)
\bar{r}	mean radius of thickwalled sphere $= \frac{r_0 + r_1}{2}$	(m)
s	Laplace parameter	$(-)$
S	cross sectional area of piece of bladder wall	(m^2)
t	time	(s)
u_n	n^{th} orthonormal function	$(-)$
v	straining rate	(s^{-1})
V	volume contained by bladder	(m^3)
V_0	initial volume of bladder	(m^3)
V_t	volume of bladder wall tissue	(m^3)
x_i	independent variable of set of experimental points	(s)
y_i	dependent variable of set of experimental points	(N)
a_n	exponent in n^{th} orthonormal exponential function	(s^{-1})
β	elastic exponent	$(-)$
γ	relaxation constant	(s^{-1})
γ_n	relaxation constant in n^{th} exponential term	(s^{-1})
δ	delta function	$(-)$
δ_{ij}	Kronecker delta	$(-)$
Δt	sampling time	(s)
ϵ	strain $= \frac{l - l_0}{l_0}$	$(-)$
ϵ_1	strain of spring in mechanical model	$(-)$
ϵ_p	average level of strain applied during sinusoidal forcing	$(-)$
ϵ_s	amplitude of sinusoidal forcing	$(-)$

$ \epsilon $	amplitude of the applied strain	(-)
η_n	viscosity modulus of n^{th} dashpot	(Ns/m^2)
η_s	apparent viscosity modulus of a dashpot	(Ns)
λ	damping factor in algorithm CACM 315	(-)
μ	Poisson's ratio	(-)
ν	frequency	(s^{-1})
ρ_a	density of air	(kg/m^3)
ρ_t	density of tissue	(kg/m^3)
ρ_w	density of water	(kg/m^3)
σ	stress in the wall	(N/m^2)
σ_a	stress parallel to l_a	(N/m^2)
σ_b	stress parallel to l_b	(N/m^2)
σ_n	stress due to n^{th} spring-dashpot combination	(N/m^2)
$\sigma(a)$	standard deviation in the parameter a	(-)
σ_{noise}	standard deviation of noise	(mV)
$\sigma(r)$	tangential stress in the wall at radius r	(N/m^2)
$\bar{\tau}$	average time constant	(s)
ϕ	sum of least squares	(mV^2)

0. Preface

In 1972 a fruitful cooperation was initiated between the Urological Department of the University Hospital "Dijkzigt" and the Department of Biological and Medical Physics of the Medical Faculty of Rotterdam.

Urodynamic investigations were performed by an interdisciplinary team which consisted of B.L.R.A. Coolsaet, urologist, and W.A. van Duyl, scientist, and was later on extended with the author. In this thesis the results obtained are interpreted from a physical point of view. Since all results are due to teamwork it is not possible to separate the contributions of the various team members, except by emphasizing the different points of view. This thesis in fact should be read in conjunction with the complementary one written by B.L.R.A. Coolsaet, which presents the same material from the urological point of view. It must be made clear that the author is very much obliged to the other team members. Without their cooperation no material would exist on which this thesis could have been written.

Furthermore, the author wishes to express his gratitude to Prof.Dr. N.J. Bakker and Prof.Dr. G. van den Brink who enabled the team to perform their investigations, and the author to write this thesis.

For the performing of almost all in vitro experiments the author wishes to acknowledge the student-assistants J.W. Schouten, R.E.F. Huygen, F.H. van Rees Vellinga, W.A.M. Slierings, J.W.F. Gielisse and E.A. Tauecchio.

The author also wishes to thank his wife for the patience shown and energy expended in typing the almost unreadable manuscripts often written on the back of envelopes.

Finally the author wishes to thank R.G. van der Land, D.J. Griffiths and J.L. Grashuis for correcting the manuscript and M.G. van Kruining for typing it in its final form.

I. Introduction

A. Urology and Urodynamics

Urology is that branch of medicine which is concerned with the treatment of diseases of the urinary tract in men and women and of the reproductive tract in men (Rous, 1973). It will be clear that in urology, physical properties as flow, pressure, volume, and their relations are very important. A more or less separate discipline has therefore arisen which is called "urodynamics". Urodynamics concerns the knowledge gathered by the study of the physical events during transport of urine from the kidneys to the outside world. A description of urodynamical research is given by Melchior (1975). From the description it can be seen that urodynamics is a research field which demands interdisciplinary teamwork. Therefore, and since the actual structure of the urinary system is very complicated like that of all physiological systems, it is a very suitable field for a systems approach. The first aim in such an approach must be to describe quantitatively and in physical terms the properties of the urinary tract or parts of it. This thesis reports the results of such an approach to the passive properties of the urinary bladder in the collection phase.

B. Anatomy and physiology of the urinary tract

The urinary tract consists of the kidneys, the ureters, the urinary bladder, and the urethra. The kidneys produce a continuous flow of urine, which passes down two narrow tubes, the ureters, into the bladder. The flow in the ureter however, is not a continuous one but rather a bolus flow, encouraged by peristaltic contractions of the ureteric wall. The urine is collected in the urinary bladder and will be expelled after some time, via the urethra. The ureters enter, and the urethra leaves the urinary bladder in the distal part (in the part which is directed away from the head), a triangular structure which is called the trigonum. In the junction of the ureters with the bladder a sort of valve mechanism exists, which under normal conditions prevents the urine from flowing back into the ureters. Evacuation of the bladder is realized by the contraction of the muscle in the wall, the detrusor muscle. The urethra contains two closure mechanisms. One in the region of the outlet of the bladder and the first part of the urethra, and one more distal in the urethra. The musculature in the ureteric wall, the bladder and the proximal urethra are of the smooth type of muscle, which implies that they are beyond direct voluntary control. The distal closure mechanism consists of striated muscle and can be voluntarily controlled. Apart from muscle tissue, the wall of the urinary bladder, ureters and urethra also contain two other types of tissue, collagen and elastine (Remington, 1957). The way in which these tissues are interconnected is not yet known. In the working cycle of the urinary bladder, two phases can be distinguished: the collection phase in which the urine produced by the kidneys is collected in the urinary bladder, and the evacuation phase in which the collected urine is expelled via the urethra. Functionally coupled to these phases are two different types of properties of the urinary bladder, passive and active properties. Under passive properties we shall denote those properties which do not involve energy production, while active properties do. Once it was believed that the behaviour of the bladder in the collection phase depended upon active mechanisms only (Lippold and Winton, 1968). It is however now generally accepted that in this phase passive properties dominate (Hinman and Miller, 1964),

although active phenomena such as spontaneous contractions can be observed, and it might well be that active properties contribute to a behaviour, which is taken to be purely passive. In the evacuation phase, active properties play the most important role, although passive properties also have an influence. A survey of the physiology of the urinary system can be found in Coolsaet (1976), and Ruch and Patton (1966).

C. Purpose and justification of the investigation

The purpose of this investigation is to describe quantitatively, in physical terms, the passive properties of the urinary bladder in the collection phase.

Although the justification of such an investigation cannot be seen within the scope of the investigation itself and therefore should not be discussed here, some introductory remarks are made.

Since Mosso and Pellacani (1882) the functioning of the urinary bladder has been tested clinically by way of a method called "cystometry". Nowadays mostly a double lumen catheter (a catheter with two channels) is introduced into the bladder via the urethra or by means of puncture of the bladder through the abdominal wall (Nyström et al, 1973). Via one channel the bladder is filled slowly with a physiological solution or air (Bradley et al, 1968), using an infusion pump or the passive infusion from a bottle. The other channel is attached to a pressure measuring device. The inflow of fluid may be constant or intermittent, and a plot is made of pressure versus volume. An example of such a plot, Fig. 1, is derived from Simeone and Lampson (1937). It is clear, that the behaviour of the

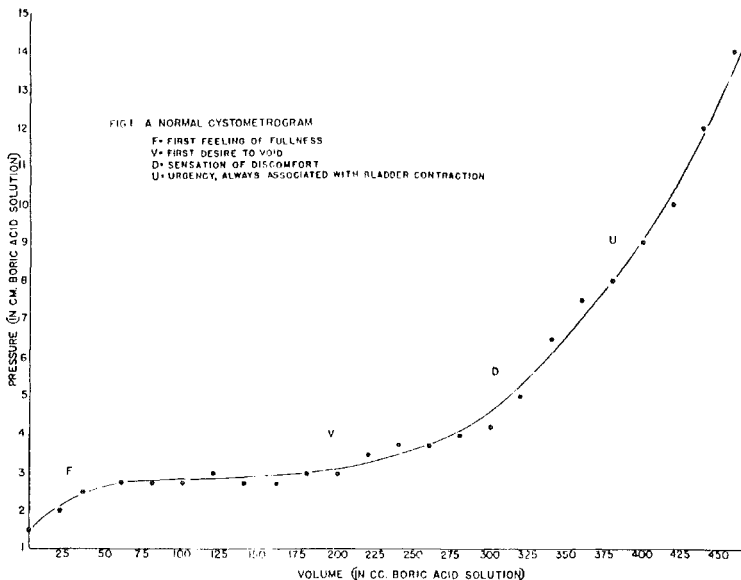


Fig. 1 - Normal cystometrogram from Simeone and Lampson (1937)

bladder in the collection phase is mainly tested in this way, though some indication about active properties, which dominate the evacuation phase, can be obtained from contractions observed as sudden pressure-rises in the curve.

There has been a great deal of speculation about the origin of the long flat portion of the cystometrogram, which enables the bladder to store a large amount of urine with only a small increase in pressure. By some authors this typical behaviour is ascribed to an active adaptation mechanism (Ausems, 1957). Others have shown that the shape of this part of the curve may be explained by purely passive mechanisms (Coolsaet et al, 1975; Langley and Whiteside, 1951). Through the years cystometry curves have turned out to be inconsistent, irreproducible and incomparable. In order to understand this it should be noted that the method used implies the assumption that the pressure-volume relationship is static, i.e. that only one pressure corresponds to one volume and that the "history" of the bladder has no influence.

Alexander (1971) however, showed that the pressure-volume relationship shows hysteresis, which implies a time dependent behaviour. This time dependency puts restrictions on the input flow rate, in order to be able to interpret the results of pressure-volume relationship studies as "static" (Coolsaet et al, 1973).

What has to be investigated is whether the behaviour of the urinary bladder can be described as being static or not under physiological conditions. Another thing is, that in clinical cystometry pressure is related to volume without taking into account that bladders with different unstrained (or initial) volumes are strained to a different level by filling both with the same volume. In the light of these facts more profound research is necessary. The present study, in which passive properties of the urinary bladder in the collection phase were investigated is a first effort in this direction. A large part of our work necessarily concerns the time dependency of the pressure-volume relationship because the supposed non-existence or non-importance of this dependency is the base on which clinical cystometry has been built.

D. Functional approach to the urinary bladder

In this work we shall use the black-box concept, i.e. we are not interested in how the urinary bladder is really constructed but only in how its behaviour can be described. This means that when we want to develop a detailed system flow chart later on in this paragraph, the different blocks in this system represent causal input-output relations which are not necessarily related to different parts of the bladder.

In approaching the urinary bladder in the collection phase from this point of view we first have to decide which variables are to be measured and/or controlled.

Obvious choices are the pressure p in the bladder in relation to barometric pressure and the volume V of fluid in the bladder. It will be shown that in order to describe the behaviour of the bladder, other quantities are also necessary, such as variables which describe the shape of the bladder, the wall thickness and so on.

These variables however, cannot be controlled externally. Depending on the geometry model, the variables which define the specific geometry of a certain bladder might be combined in such a way that they can be taken to be constants. For instance, if the bladder is considered as a thick walled sphere it can be fully described in terms of pressure p , volume V and wall thickness d during the collection phase. As it is very likely that the wall thickness d decreases when the bladder is filled, each of the three parameters has to be controlled or measured.

If on the other hand the volume V_t of the tissue of the wall (see chapter IV) is taken into consideration instead of wall thickness, only pressure and volume remain, because V_t may be assumed to be a constant for a given bladder. In that case the bladder in the collection phase can be defined in terms of a pressure-volume relationship. This relationship depends on the tissue volume V_t .

Differences between bladders may be corrected for differences in V_t , which, mathematically, is only of minor importance.

Next we have to decide whether to control volume and measure pressure, or vice versa. Though from a theoretical point of view the choice is rather arbitrary, control of the volume and measuring the pressure is the most logical approach as

in physiological conditions volume is the cause of pressure and not the other way around. Figure 2 characterizes this situation.

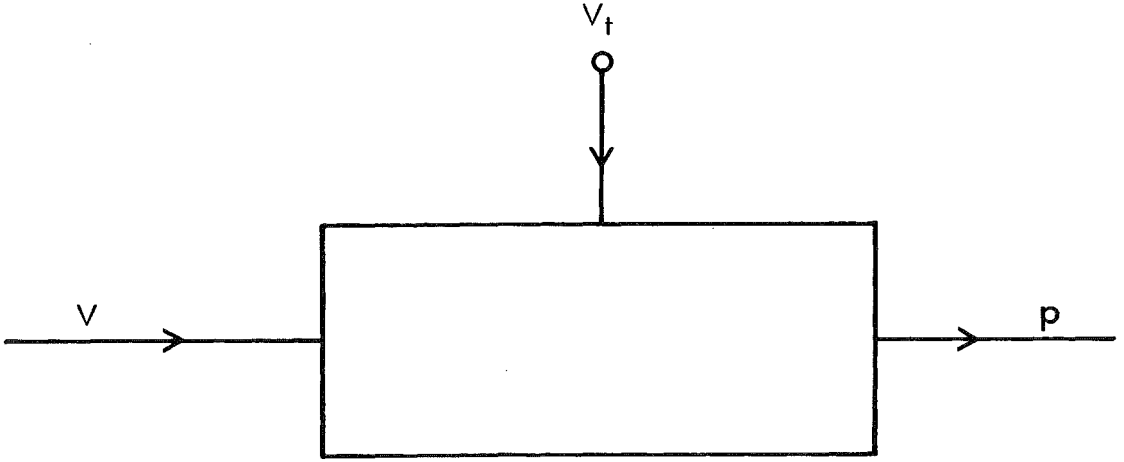


Fig. 2 - System flow chart of the urinary bladder in the collection phase

In order to simplify the approach it is useful at this point to philosophize about how the bladder actually "transforms" a volume signal into a pressure signal and to base a more detailed scheme on that approach. It is then clear that the interaction of volume and pressure takes place via the bladder wall. A certain volume V of fluid in the bladder, stretches the bladder wall to a certain degree. The strain ϵ is defined as:

$$\epsilon = \frac{l - l_0}{l_0} \quad \text{with } l_0 \text{ being the original length} \quad (1)$$

l being the stretched length

It should be noted that in our analysis we have always assumed that $l > l_0$. The peculiar things which happen when the bladder wall slackens are very difficult to describe. The straining of the wall causes a stress σ in the wall and this stress interacts with the geometry of the bladder to determine a pressure. This set of causal relations is illustrated in Fig. 3. Here, the block which gives the urinary bladder its specific properties is the "wall" block. The other two blocks

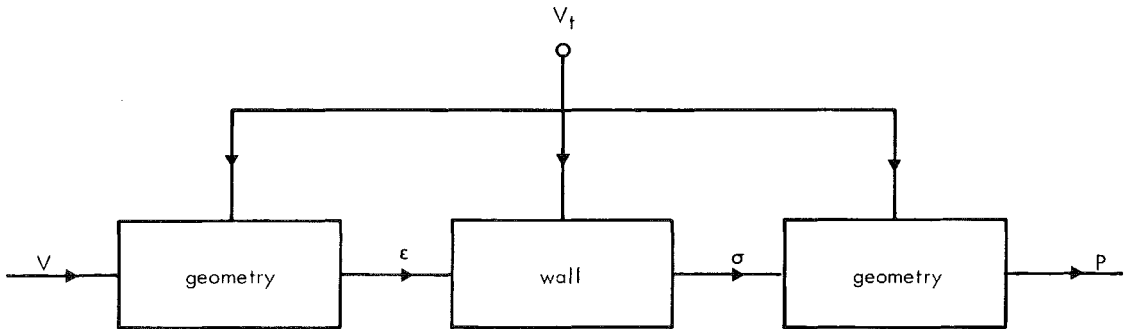


Fig. 3 - More detailed system flow chart of the urinary bladder
in the collection phase

can also be found, for instance, in system flow charts describing the behaviour of rubber balloons. We shall investigate the functions of the blocks separately. The two "geometry" blocks are treated in chapter IV. The "wall" block is split up into two sub-blocks. It will be shown, that bladder wall tissue is a non-linear visco-elastic material, which means that the output signal of the wall block depends on time as well as on strain or length (Jamison et al, 1968). These two dependencies are investigated separately in chapters II and III. Since at this point we do not know yet how time and length dependency are interrelated, we shall not introduce different blocks for these two dependencies in our system flow chart. Finally, in chapter V, the properties of all blocks will be combined in order to try to design a complete model of the urinary bladder in the collection phase. In all chapters experimental material concerning the specific causal relation described will be presented. Concerning the necessary experiments the following classifications can be made:

1. Experiments can be done on a living animal or man (in vivo), or with excised material (in vitro).
2. Experiments can be done on the total bladder (in toto), or on a strip of bladder wall (strip).

All experiments in chapter II and III are in vitro/strip experiments, while the experiments in chapter V are in vivo/in toto. The experiments of chapter IV are classified as in vitro/in toto, although these are not performed on biological material but on rubber balloons. Advantages of the various experimental methods will be given in the various chapters. Finally, all experiments were performed with material from pigs and dogs. According to Douglas (1972) the physiology of pigs shows a great deal of interesting similarities to that of humans. Dogs were used because their urinary bladder shows less spontaneous activity. From both types of animals sufficient data have been obtained in order that a comparison can be made.

Time dependent behaviour of the bladder wall

A. Theory

1. Introduction

The time dependent behaviour of the urinary bladder wall can be investigated by experimenting on isolated strips of bladder wall. This method has many advantages compared with measuring in vivo or in toto:

1. The geometry of a strip is easier to describe than the geometry of the total bladder. This means that less confusing effects caused by the geometry are added to the response.
2. Signals measured on strips are less contaminated with noise, for instance due to respiration, blood circulation, etc.
3. In vitro, it is easier to influence (for instance: eliminate) "active properties" of the tissue by the use of drugs.
4. Experiments on strips can be performed using waste material from other experiments or material from animals killed for consumption.
5. Measuring equipment can be made much simpler.

Arguments 2, 3 and 4 would also apply to in vitro/in toto experiments, arguments 1 and 5 would not. When measuring on strips of bladder wall, strain can be applied directly by stretching the strip, whereas the developed stress can be measured as force. The relationship between stress and force will be described in IIA3.

At this point we will discuss one of the reasons for separating the time and length dependency of the stress-strain relationship of the bladder wall. The relationship will be shown to be non-linear. In Fig. 1 it can be seen that the overall "static" behaviour of the urinary bladder in the collection phase is non-linear, but this non-linearity might of course have its origin only in the geometry blocks (in fact the first geometry block, which "translates" volume into strain is indeed non-linear, see chapter IV). On the other hand the wall block itself, which represents the behaviour of the urinary bladder wall, must be considered to be non-linear like all other biological materials (Ray, 1974). However, depending on the type of

non-linearity (see IIIA) it might be possible that the system can be linearized when measuring at only one fixed strain level. This would enable us to apply linear systems theory to the time dependent behaviour. Two strain signals are available which involve only one (or nearly one) strain level:

1. stepwise straining
2. infinitely small sinusoidal straining superimposed on a fixed strain level

Stepwise straining appears to be the most promising because the input signal contains all frequencies and especially the high frequencies, which are very relevant because the time dependent properties of the system under investigation show a high pass characteristic, with a high amplitude. This implies that time or frequency dependencies can be determined by one measurement only. We therefore used the stepwise straining method. The method using sinusoidal straining requires a scanning of the relevant frequency range and is therefore much more time-consuming. This method however is mathematically much more attractive. It is labeled "alternative" and treated in IIE.

2. Visco-elasticity

When stress is applied to material it will exhibit elastic and/or viscous properties. Elastic material will reach a deformation, or strain that remains constant as long as the stress is constant. The strain will disappear completely when the stress is removed. Viscous material will reach a constant deformation velocity under constant stress and when stress is no longer applied the deformation will remain constant. Material is said to be linear elastic or viscous when a linear relationship between stress and strain or strain velocity exists.

The urinary bladder wall has elastic as well as viscous properties (Hill, 1926; Axelsson, 1970; Alexander, 1971; Apter et al, 1972). Assume a construction of one discrete linear elastic element, represented mechanically by a spring, and one discrete viscous element, represented by a dashpot. These two elements can be combined in parallel (Fig. 4) or in series (Fig. 5).

The parallel model cannot be used as a model for the behaviour of the urinary

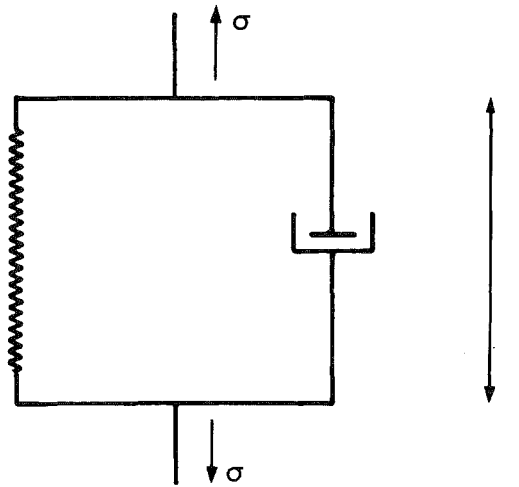


Fig. 4 - Parallel combination of one elastic and one viscous element

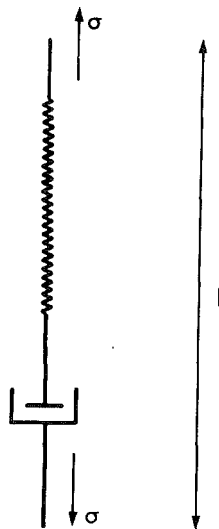


Fig. 5 - Series combination of one elastic and one viscous element

bladder wall, since it does not permit stepwise straining (the dashpot would generate an infinite stress) while the bladder wall does (see IIC). The series model can be strained stepwise. If we set for the elastic element:

$$F = E_s \cdot \epsilon \quad (2)$$

where F means force

E_s means apparent elastic modulus of a spring

and for the viscous element:

$$F = \eta_s \cdot \dot{\epsilon} \quad (3)$$

where η_s means apparent viscosity modulus of a dashpot

it can be shown (Coolsaet et al, 1975b) that the response to a unit step strain yields:

$$F(t) = E_s \cdot e^{-\frac{E_s}{\eta_s} t} \quad (4)$$

Usually we call $\frac{E_s}{\eta_s}$ the relaxation constant γ . If the amplitude of the stepwise straining does not equal one, formula 4 should be multiplied by the strain amplitude $|\epsilon|$. If we call $E_s \cdot |\epsilon|$ the coefficient a , we obtain:

$$F(t) = a e^{-\gamma t} \quad (5)$$

If we assume that the spring can be not only stretched but also compressed in a consistent way it is clear that the response to a negative step should also be exponential. In practice however it is not possible to stimulate a strip of bladder wall with negative steps. The distance between the ends of the strip can be decreased mechanically but this only causes the wall to wrinkle. In practice we always apply positive strain, compare ID.

When we try to describe the step response of a strip of bladder wall using equation (5) we shall find that one exponential term does not fit the measured curves adequately. The mechanical model can be expanded with extra series combinations

of viscous and elastic elements in parallel (Christensen, 1971). Furthermore it will be necessary to add a non-decaying component by adding a sole spring in parallel. The force developed on a step strain can then be described as:

$$F(t) = \sum_{n=1}^k a_n e^{-\gamma_n t} + a_0 \quad (6)$$

where k is the number of exponential terms.

As will be shown (IIC1) we will generally use a model generating three exponential terms and a constant as presented in Fig. 6.

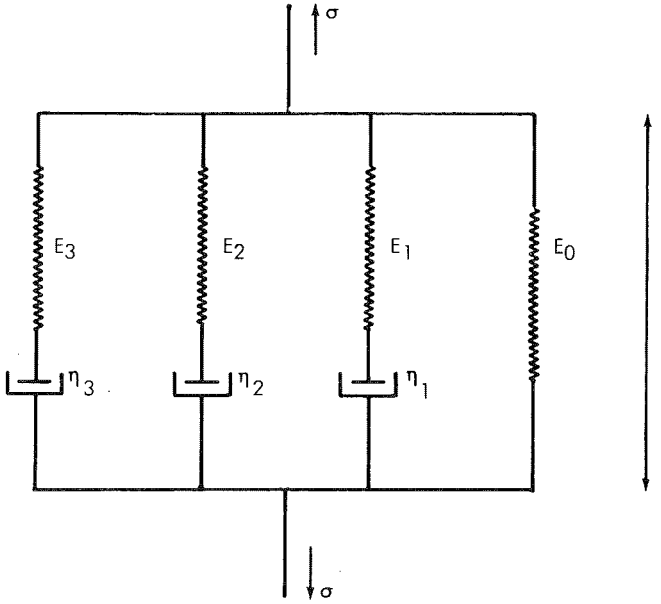


Fig. 6 - Mechanical model generating three exponential terms and a constant on a unit step strain

3. Geometry of a strip of bladder wall

Measuring the step response of a strip of bladder wall, and fitting the results with a sum of a number of exponential terms plus a constant, we obtain the coefficients a_n and relaxation constants γ_n as parameters. We want to relate these parameters to elastic and viscosity moduli of the bladder wall. Since in the bladder wall no discrete elastic and viscous elements are present but continuously distributed elastic and viscous properties the fundamental relations (2) and (3) should yield stress instead of force, so:

$$\sigma_n = E_n \cdot \epsilon \quad (7)$$

where σ_n is stress due to n^{th} spring-dashpot combination
 E_n is elastic modulus of n^{th} spring

The coefficients have the dimension of force, which can be related to stress as follows:

$$a_n = \sigma_n \cdot S \quad (8)$$

where S is cross-sectional area

From (7) and (8) we obtain:

$$E_n = \frac{a_n}{\epsilon \cdot S} \quad (9)$$

The cross-sectional area S cannot be considered as a constant and is very hard to determine in practice. Therefore, we introduce the volume of the tissue of the wall V_t :

$$V_t = l \cdot S \quad (10)$$

where l is length of the strip

From (9) and (10) we obtain:

$$E_n = \frac{a_n \cdot l}{\epsilon V_t} \quad (11)$$

and from equations (4) and (5):

$$\eta_n = \frac{E_n}{\gamma_n} \quad (12)$$

A crucial assumption is the constancy of the tissue volume so that it does not vary with strain. This can be formulated alternatively by saying that Poisson's ratio equals 0.5. This is a very common starting point in literature concerning the mechanical properties of rubber (King, 1946; King and Lawton, 1950; Frank, 1906). Rose et al (1973) use the same assumption for the ureteric wall (smooth muscle) and Harding (1952) and Goedhard (1971) for blood vessels, while King and Lawton (1971) state that soft body tissues behave like rubber. Anyway the assumption that tissue volume is constant seems to be more acceptable than assuming the cross-sectional area to be constant.

Now, using equations (11) and (12), and a procedure for fitting a sum of exponentials and constant to some signal, which will be described in IIB2, we obtain from our step response measurements elastic and viscosity moduli as fundamental parameters describing the properties of the wall. Although it is possible to describe the bladder wall in these terms, there are two reasons for a different approach:

1. By calculating viscosity moduli the variances of coefficients and relaxation constants are added, which yields standard deviations which are too large.
2. The relaxation constants turn out to be independent of strain, while elastic and viscosity moduli are not, see IIC2. This makes it possible to use separate parameters for describing time and length dependent properties.

For these reasons we shall describe the properties of the bladder wall in terms of elastic moduli and relaxation constants. In this chapter only the relaxation constants are relevant because these describe the fundamental time dependency of the stress-strain relationship.

4. Determination of tissue volume

In order to be able to calculate elastic moduli it is necessary to determine the tissue volume V_t . Since the density of the tissue is greater than the density of water, V_t can be determined accurately from the difference between the weight of

the strip of bladder wall in air and in water. When the strip is weighed in air (by using the force transducer and matching apparatus described in IIB1) we obtain:

$$F_a = V_t (\rho_t - \rho_a) \cdot g \quad (13)$$

where F_a is weight in air
 ρ_t is density of tissue
 ρ_a is density of air
 g is acceleration due to gravity

When the strip is submerged in distilled water we obtain:

$$F_w = V_t (\rho_t - \rho_w) \cdot g \quad (14)$$

where F_w is weight in water
 ρ_w is density of water

Combining (13) and (14) we obtain:

$$V_t = \frac{F_a - F_w}{g(\rho_w - \rho_a)} \quad (15)$$

Since ρ_a is small in relation to ρ_w (1 : 1000) it can be ignored in (15) yielding:

$$V_t = \frac{F_a - F_w}{g \cdot \rho_w} \quad (16)$$

B. Methods

1. Set-up of the experimental equipment

A block diagram of the set-up is represented in Fig. 7. A strip of about 10 x 20 mm

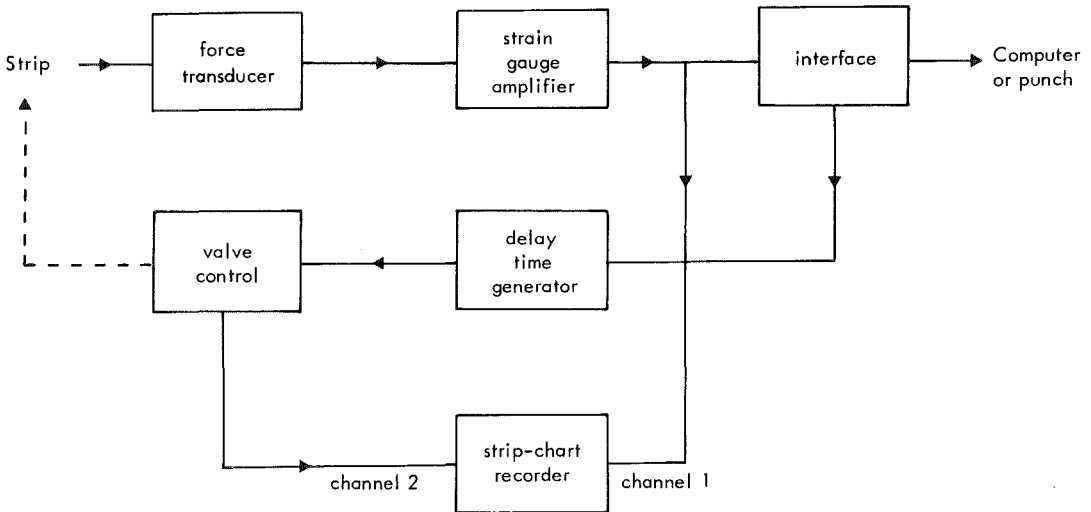


Fig. 7 - Block diagram of set-up of experimental equipment

is cut from the front wall in dogs or from the back wall in pigs of the urinary bladder. In the case of the pig bladders the back wall was used because the front wall showed an irregularity in the form of a ridge. Two clamps with penetrating pins constructed for this purpose are attached to ends of the strip. The upper clamp is connected to a Grass FT.03 force transducer (full range 10 Newton). The lower clamp is moved by means of a pneumatic cylinder. Initial length and the change in length are adjustable by means of microscrews (0 - 50 mm) with an accuracy of 0.1 mm. The strips are submerged in a physiological solution which is constantly perfused, aerated with 95% O₂ and 5% CO₂ and kept at 37°C. The signal from the force transducer is transmitted to a sampling interface via a standard strain gauge amplifier. The interface samples at a rate of 1 sample per second. In the first series of experiments the samples were then digitized and punched on papertape. The papertape was later converted into punch cards and these were fed

into an IBM 360/65. In later experiments the digitized samples were read directly into a Texas Instruments 980B mini-computer. The pneumatic cylinder is controlled by an electronic device called "Valve control". This unit is activated via a time delay generator by pulses generated by the interface at the sample rate. The importance of this triggering is to create a delay time that is fixed between the step-strain and the first sample (see IIB2). When the button "strain" on the valve control is pushed it only actually opens the pneumatic valve at the moment of the trigger pulse. The delay time generator delays the trigger pulses for 800 ms. This means that the first sample is taken 200 ms after the straining of the strip. This setting was experimentally obtained, see IIC3. Valve voltage and the measured force are recorded on a dual strip-chart recorder. The speed of the pneumatic cylinder will be discussed in IIC3.

The following physiological solutions were used (see Coolsaet, 1976):

1. The standard solution (called: natural) is a modified Krebs solution with the following composition in millimoles per liter: Na^+ 137.0; K^+ 5.9; Ca^{2+} 2.5; Mg^{2+} 1.2; Cl^- 134.0; HCO_3^- 15.5; H_2PO_4^- 1.2; glucose 11.5 (see Åberg and Axelsson, 1965).
2. A solution which should reduce the influence of the active properties of the tissue (called EGTA). The composition is the same as the solution under 1, however with addition of 0.5% EGTA and omission of calcium. EGTA "catches" the calcium which might still be present in the strip. In a calcium-free surrounding the contractile elements, whatever these are, should not be able to cause a contraction (Bülbring, 1970). The same result was aimed at using a D600 addition when measuring dog bladder strips (Mayer et al, 1972).
3. According to Axelsson (1970) it cannot be excluded that the cell membrane in a calcium-free EGTA solution is still depolarized by straining. By substitution of Na^+ by K^+ (148.1 mmol/liter), the membrane can be depolarized and can thus be checked to see whether this makes any difference. This solution is called "extra K^+ ".

4. In order to simulate "dead" tissue, glucose can be replaced by a dummy, in this case sorbitol (11.5 mmol/liter). The oxygen then has to be substituted by nitrogen. This group is called "sorbitol".

In all cases the time elapsed between the death of the animal and start of the experiments was about one hour. The strip was then submerged in the solution and allowed to "rest" for half an hour. Determination of the original length l_0 which was rather difficult to do (see chapter III) was accomplished by allowing the strip to stretch under the weight of the lower clamp (mass: 13 g) for about one second. Then the measurement cycle was started, which consisted of straining during 1000 seconds (so 1000 samples were taken) and a rest of 20 minutes. About ten measurements were taken from each strip. The applied strain level was 0.30. The tissue volume was determined according to the method described in IIA4, before the measurements. It was necessary to determine the absolute amplification factor of the entire measurement chain, which yields: 0.001055 N/mV. The digitizer is a BCD type one, the least significant digit represents millivolts, the full range is 1000 mV, which corresponds approximately to 1 Newton. At the strain gauge meter the amplification factor can be changed from 1.0 to 3.33 or 10.0 which yields a full range of 10 N.

2. Separation of multi-exponential signals

a. Statement of the problem

From our experiments, we obtain a set of experimental points (x_i, y_i) representing force as a function of time. From this data-set we want to obtain the parameters (a_n, γ_n) . Using a least squares criterion the problem can be stated as follows: find the parameters (a_n, γ_n) such that:

$$\sum_{i=1}^N \left(\sum_{n=1}^k a_n e^{-\gamma_n x_i} + a_0 - y_i \right)^2 = \text{minimum} \quad (17)$$

Because of the exponential terms, the equations to be solved in deriving the parameters (Gauss equations) are non-linear. Now it is generally

acknowledged that the solution of these equations is an awkward problem and that in practice it might even lead to a non-unique set of parameters (a_n, γ_n) (Lanczos, 1956). It is clear, on the other hand, that the "awkwardness" of the problem must be dependent on the properties of the set of experimental points (x_i, y_i) , since e.g. the separation of two exponentials with relaxation constants $\gamma_1 = 1; \gamma_2 = 1000$ should be a very simple matter. In this example the two exponential terms can almost be measured independently, one in the range from $x = 0$ to $x = 0.01$ (where the "faster" exponential is practically zero) and one in the range from $x = 0.01$ (where the slower exponential has in practice not yet shown any change) to $x = 10$. Thus the decision as to whether separation into the desired number of exponential terms is possible must be made on the merits of each individual case, for each set of experimental points (x_i, y_i) (or any similar set of data pairs).

b. Constant step approximation

Since the desired computer program had to be run on a mini-computer it had to be relatively short. Now we have already mentioned in IIB2a that the equations to be solved in order to determine the parameters are non-linear. They are however only non-linear in the exponents γ_n . This means that if these exponents are fixed, the optimum coefficients a_n can be obtained by simple matrix inversion, using the classical least squares method. We can therefore use an iterative method for the exponents only. The simplest method would be to perform iterative steps in the (exponent) parameter space, calculate the optimum coefficients and constant for each point, determine the sum of least squares and then choose the point with the lowest sum of least squares. Apart from its simplicity, this method has the advantage of giving a clear insight in the form of the minimum, thus supplying the user with an impression of the possibility of separation into exponentials. Of course it is impossible in practice to investigate the entire

parameter space, simply because it contains an infinite number of points. Therefore we need an initial estimate of the exponents. As the use of a certain sampling rate and number of experimental points (x_i, y_i) also implies a foreknowledge of the order of magnitude of the exponents (time constants), this is not a real limitation. The search can then be confined to evaluating a series of points in the vicinity of the initial estimate. Depending on the results, the "search area" can be displaced and the procedure repeated until a minimum is reached. It is clear that there will be an uncertainty in the parameters depending on the distance between the points investigated. This uncertainty is exactly defined and must be chosen on the basis of the accuracy required and the time available.

c. Operational interpretation

The procedure is very simple: Starting with the initial estimates of the exponents γ_n , take steps in a number of directions, calculate for each step the corresponding coefficients, constant and sum of least squares and choose the best direction. The procedure is then repeated. One problem is, how many and which directions should be attempted. The minimum number is $2k$, where k is the number of exponential terms. In this case one exponent is varied one step forward and one step backward, while the others are fixed. The search in the parameter space thus only takes place in the axial directions. It turned out that with our data the minimum could always be found in this way. In other applications it may be necessary to increase the number of directions by varying more exponents at a time. To accelerate the search procedure, the search is started with relatively large steps, which are halved every time the sum of least squares increases, until the defined minimum step is reached.

The rules for this procedure are contained in what we call "algorithm A". Although this algorithm gives a clear insight into the shape of the minimum, it is not very economical because it involves some unnecessary steps. One of

these is the step in the direction we just came from. Furthermore, if a lower sum of least squares can be obtained by increasing a particular exponent, there is then no need to investigate the decrease step because if this step were also to yield a lower sum of least squares (which implies that we are on a hill, with a minimum on both sides), there would be no way to tell which minimum is "better" or which is "the correct one". We might as well choose one at random by omitting the other step if a decrease is found in one direction. In practice the "hill situation" has never occurred in our data during work with algorithm A. Finally algorithm A also investigates the central point from which we make the steps. As this point was chosen as the best step in the previous iteration, the results for it are already known.

These three refinements, which almost halved the CPU time, are realized in algorithm B. Another approach which could be useful, especially when the initial estimates are far from the minimum, is laid down in algorithm C. This performs the same steps as algorithm B, except that when after one complete iteration the best direction has been decided on, it goes on with the same step size in this direction until the sum of least squares again begins to rise.

All the directions are then again investigated. This is repeated as many times as are necessary. Comparing the three algorithms from a theoretical point of view, we may state that A gives the clearest insight into the shape of the minimum, and is also the simplest, B works more or less the same as A and is about twice as fast but gives a less clear impression of the form of the minimum whereas C is faster than B when the initial estimates are very bad, but slower (because at least one extra step is tried in each iteration) when the initial estimates are good. In our case it turned out that the advantages of algorithm C were rarely used. We found therefore algorithm B to be the most convenient. For reference purposes we compared our algorithm to an algorithm as laid down in CACM 315 (Späth, 1966) which involves

a damped Newton-series iteration. The Fortran program consists of a Main program (see IIB3) and two subroutines, viz subroutine STEP which performs the iterations and subroutine LIN which performs the matrix inversion.

d. Test set-up

In order to test the algorithm under circumstances which as closely as possible approach the real measuring circumstances, a hardware exponential generator was build. It could generate a sum of three exponential terms and a constant, with or without additional white noise. The generator was sampled at constant intervals at a rate of 1 sample per second by the computer for a period of 1000 seconds, and the samples were put in an array to be computed by the subroutines STEP and LIN. For economic reasons only 400 samples were used in the fitting procedure, viz the first 200 samples and 200 equidistant samples chosen from the remainder. The trigger pulses for the sampling of the A/D converter were fed back to the exponential generator in order to trigger the start of the exponential signal generation (see Fig. 8).

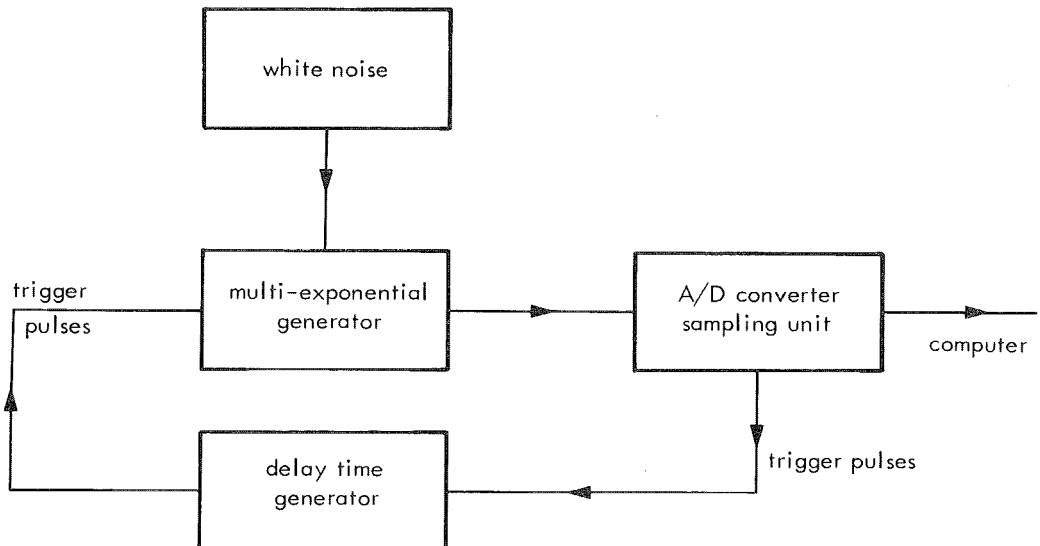


Fig. 8 - Block diagram of test set-up

This permitted investigation of the influence of the position of the first sample relative to the top of the signal (which is often random in practical measurements). In order to get a good estimate of the "real" values of the parameters the three exponential terms could also be generated separately. In designing the generator, we chose the relaxation constants from the region where the relaxation constants are found in real experiments on the strips of bladder wall (see IIC). In all cases the initial estimates of 0.40; 0.040 and 0.0040, were used with the minimum step-sizes 0.01; 0.001 and 0.0001, and a multiplication factor of 8. The coefficients and constant of the model were nearly equal. The amount of white noise added could be varied, and the frequency characteristic of the noise was flat, down to the frequency corresponding to the fastest relaxation constant.

In order to save time, "time scaling" was used, i.e. the experiments on the model generator were carried out at ten times the usual rate.

This scaling was of course incorporated in the computing of the results.

The delay time generator was adjustable between 0.1 and 0.9 Δt where Δt is the sample time (1 second). Two generated curves one with and one without added noise are presented in Figs. 9 and 10 respectively.

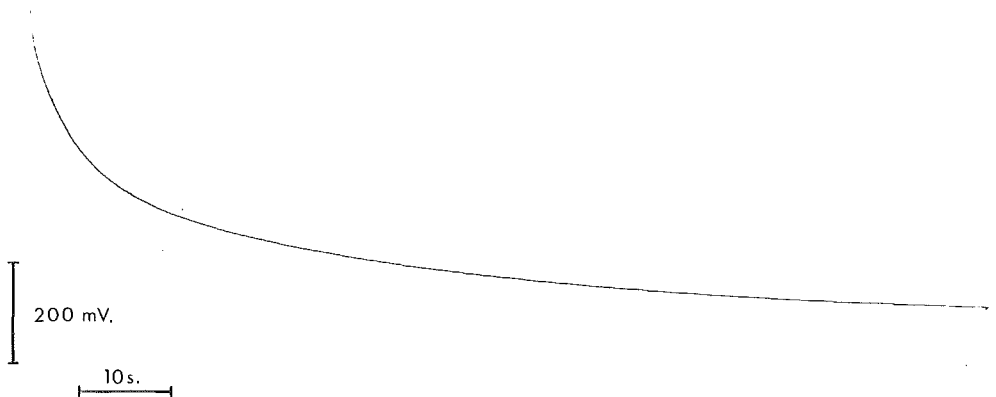


Fig. 9 - Three exponential curve generated without noise

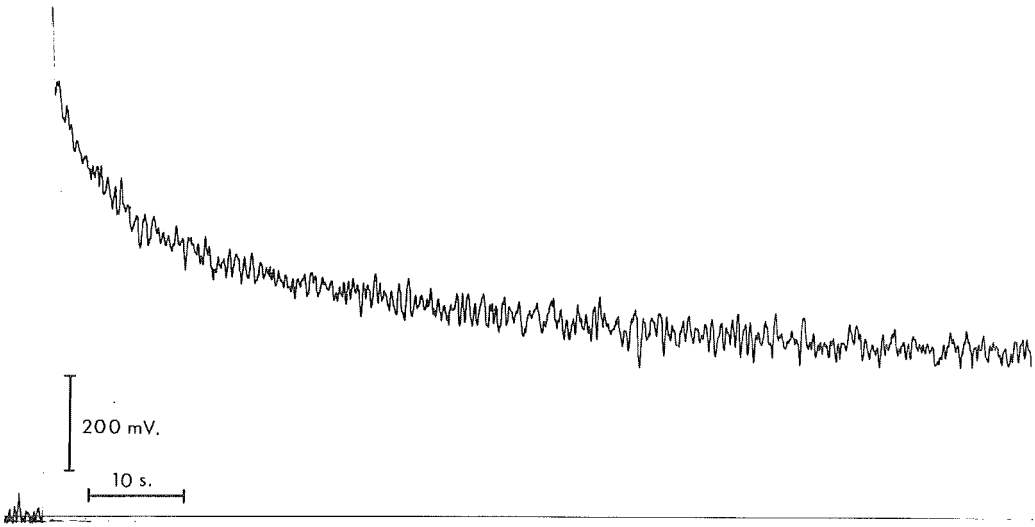


Fig. 10 - Three exponential curve generated with noise ($\sigma_{\text{noise}} = 20 \text{ mV}$)

e. Influence of the position of the first sample

By generating only one exponential term, and varying the delay time, we found that only the fastest exponential yielded a relaxation constant that depended on the delay time. The relaxation constant was found to vary between 0.35 s^{-1} and 0.45 s^{-1} , when the delay time varied between $0.1 \Delta t$ and $0.9 \Delta t$ (Table I). This dependence can easily be understood if we

Delay time	Relaxation constant (s^{-1})	Sum of least squares (mV^2)
$0.1 \Delta t$	0.44	98
$0.2 \Delta t$	0.44	16
$0.3 \Delta t$	0.45	6
$0.4 \Delta t$	0.45	5
$0.5 \Delta t$	0.35	1599
$0.6 \Delta t$	0.37	967
$0.7 \Delta t$	0.39	508
$0.8 \Delta t$	0.40	290
$0.9 \Delta t$	0.41	251

Table I

note that the signal generated has a rounded off top. As a consequence of the trigger configuration described in IIB2d, the computer has to start sampling before the exponential generator starts, therefore some samples have to be removed. The actual start of the signal is determined as the highest sample in the series. Let us now consider the situation shown in Fig. 11.

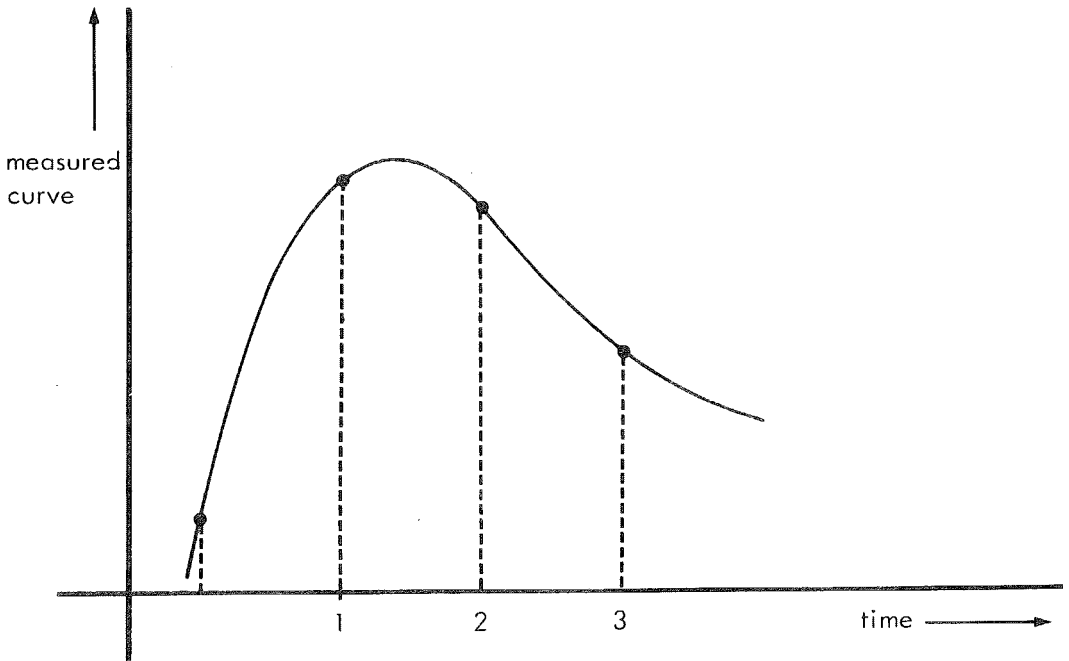


Fig. 11 - Hypothetical sample distribution on generated curve

In this situation the first sample will be chosen as the highest, which will result in a relaxation constant which will be too low. If this hypothesis reflects the real situation, then the "real" relaxation constant must be the highest one, and this one should give the lowest sum of least squares. This was found to be the case, see Table I. Furthermore, the actual shape of the curve can be reconstructed by carefully blending the samples from all experiments with a variable delay time which yields a curve sampled at

ten times the actual rate. This method also verified the hypothesis. Finally it should be possible to eliminate the dependence on the delay time by simply removing the first sample (if enough samples are available, this would have no influence on the relaxation constant); and indeed a relaxation constant of 0.45 s^{-1} was always found if the first sample was removed. Although the two "slower" relaxation constants did not vary as a function of delay time when measured separately (as in this case the falling edge of the exponential function is very flat compared to the rising edge the situation of Fig. 11 is unlikely to occur) a dependence was found when the three exponentials were measured simultaneously. The second relaxation constant then varied between 0.027 s^{-1} and 0.029 s^{-1} and the third between 0.0028 s^{-1} and 0.0029 s^{-1} . This must be due to correlation between the relaxation constants. In the following tests, the delay time was fixed as the value which yielded the smallest sum of least squares when fitting three exponentials simultaneously. In real experiments, where triggering of the system under measurement might not be possible artefacts of the type described above can be avoided by picking as the first sample not the highest, but the one with the lowest first derivative.

f. Influence of noise

A series of measurements was performed to test the influence of noise on the accuracy. First the exponentials were measured separately, which yielded very accurate values of the parameters. In fact (see Table II) no standard deviation could be determined for the exponents because they were all equal. It should be remembered in this connection, that the exponents are only determined with a limited accuracy equal to the step-size. For instance the step-size for the fastest exponent was 0.01. The result obtained (0.45) then means that an exponent of 0.44 or 0.46 would yield a higher sum of least squares. As the value found in eleven measurements was always 0.45, no standard deviation could be calculated. The coefficients (Table III) were

computed by solving a set of linear equations, which means that they can be determined to as many digits as desired. Standard deviations could therefore be given for all these values, with the exception of the constant a_0 which could be determined by simply switching off all exponentials and reading the value from the sampling interface display. It may be noted that the number of measurements, though large enough, varied considerably from run to run. The reason for this was that the test set-up was fully automatic except for switching on and off, so if the operator was interrupted then more measurements were taken. The average sum of least squares can be split up into two components representing:

1. the lack of fit between the signal and the model, and
2. the noise added to the signal

For the fastest exponent, when measured separately, the sum of least squares is very small. This is easily understood as here only a few experimental points really contribute to the sum of least squares. The relaxation constants could be determined with reasonable accuracy, as could the coefficients and constant (see Table III). Note that the coefficient of the fastest exponent is smaller than the others, which must reduce the accuracy with which the fastest exponent can be determined. Furthermore, the systematic error in the constant a_0 is equal to that in a_3 , which means that a part of the slowest exponential must have been interpreted as a constant level. Next, noise was added to the signal at different levels. The noise level could be checked from its contribution to the sum of least squares:

$$\begin{aligned} \phi(\text{noise}) &= \phi(\text{total}) - \phi(\text{systematic}) = N \times \sigma_{\text{noise}}^2 \\ \text{so: } \sigma_{\text{noise}} &= 5 \text{ should yield } \phi = 10150 \text{ mV}^2 \\ \sigma_{\text{noise}} &= 10 \text{ should yield } \phi = 40150 \text{ mV}^2 \\ \sigma_{\text{noise}} &= 20 \text{ should yield } \phi = 160150 \text{ mV}^2 \end{aligned}$$

This agrees reasonably with the measured values. The results of the fittings with noise can be seen in Tables II and III. It may clearly be seen, that

Parameter	Value (s ⁻¹)	Standard deviation	Systematic error	Details of determination*	Number of measurements	Average sum of least squares (mV) ²
Y ₁	0.45	-	-	s; $\sigma_{\text{noise}} = 0$	11	5
Y ₁	0.435	2%	3%	t; $\sigma_{\text{noise}} = 0$	12	150
Y ₁	0.37	10%	18%	t; $\sigma_{\text{noise}} = 5$	13	10 843
Y ₁	0.34	13%	24%	t; $\sigma_{\text{noise}} = 10$	22	41 540
Y ₁	0.41	37%	9%	t; $\sigma_{\text{noise}} = 20$	31	160 674
Y ₂	0.026	0	-	s; $\sigma_{\text{noise}} = 0$	15	2 100
Y ₂	0.029	2%	12%	t; $\sigma_{\text{noise}} = 0$	12	150
Y ₂	0.028	4%	8%	t; $\sigma_{\text{noise}} = 5$	13	10 843
Y ₂	0.028	9%	8%	t; $\sigma_{\text{noise}} = 10$	22	41 540
Y ₂	0.028	12%	8%	t; $\sigma_{\text{noise}} = 20$	31	160 674
Y ₃	0.0029	0	-	s; $\sigma_{\text{noise}} = 0$	12	540
Y ₃	0.0029	2%	0	t; $\sigma_{\text{noise}} = 0$	12	150
Y ₃	0.0029	3%	0	t; $\sigma_{\text{noise}} = 5$	13	10 843
Y ₃	0.0028	7%	3%	t; $\sigma_{\text{noise}} = 10$	22	41 540
Y ₃	0.0029	10%	0	t; $\sigma_{\text{noise}} = 20$	31	160 674

Table II *s = separately t = three exponentials simultaneously

Parameter	Value (mV)	Standard deviation	Systematic error	Details of determination*	Number of measurements	Average sum of least squares (mV) ²
a_0	260	-	-	$s; \sigma_{\text{noise}} = 0$	-	-
a_0	276	0.4%	6%	$t; \sigma_{\text{noise}} = 0$	12	150
a_0	274	0.8%	5%	$t; \sigma_{\text{noise}} = 5$	13	10 843
a_0	272	2%	5%	$t; \sigma_{\text{noise}} = 10$	22	41 540
a_0	271	4%	7%	$t; \sigma_{\text{noise}} = 20$	31	160 674
a_1	165	0.04%	-	$s; \sigma_{\text{noise}} = 0$	11	5
a_1	169	0.6%	2%	$t; \sigma_{\text{noise}} = 0$	12	150
a_1	166	6%	0.6%	$t; \sigma_{\text{noise}} = 5$	13	10 843
a_1	157	9%	5%	$t; \sigma_{\text{noise}} = 10$	22	41 540
a_1	174	10%	5%	$t; \sigma_{\text{noise}} = 20$	31	160 674
a_2	269	1%	-	$s; \sigma_{\text{noise}} = 0$	15	2 100
a_2	268	0.2%	0.4%	$t; \sigma_{\text{noise}} = 0$	12	150
a_2	265	2%	1%	$t; \sigma_{\text{noise}} = 5$	13	10 843
a_2	266	2%	1%	$t; \sigma_{\text{noise}} = 10$	22	41 540
a_2	265	5%	1%	$t; \sigma_{\text{noise}} = 20$	31	160 674
a_3	275	0.3%	-	$s; \sigma_{\text{noise}} = 0$	12	540
a_3	291	0.3%	6%	$t; \sigma_{\text{noise}} = 0$	12	150
a_3	290	1%	5%	$t; \sigma_{\text{noise}} = 5$	13	10 843
a_3	290	2%	5%	$t; \sigma_{\text{noise}} = 10$	22	41 540
a_3	291	3%	6%	$t; \sigma_{\text{noise}} = 20$	31	160 674

Table III *s = separately t = three exponentials simultaneously

the fastest exponent is influenced much more than the slowest. This would be expected as in practice fewer experimental points are available for the fastest exponent. In all cases the minimum was found. When the "real" parameters were used as initial estimates, they yielded a higher sum of least squares than that found at the actual minimum. It must therefore be concluded that all errors shown in Tables II and III are due to the difficulty of separating a signal into exponentials. The stepwise approximation method always yielded the real minimum, which did not always agree with "real" values of the parameters. It is therefore not possible to obtain better results by any other least squares method. The only possible way of obtaining a lower sum of least squares would be to determine the relaxation constants to a higher number of digits. However, there seems to be little reason for this in view of the low standard deviations obtained. Despite all the difficulties involved in separating signals into exponentials, we thus see that this is possible with a very reasonable accuracy under the given circumstances.

g. Rate of convergence of algorithm

The program was run on a Texas Instruments 980B mini-computer, with hardware multiply/divide, and software floating-point processing.

It was found that the evaluation of one point in the parameter space (one call to subroutine LIN) when fitting three exponentials to 400 experimental points took 10 seconds. (Experimental runs on a PDP 9 and Nova 2/10, both with hardware multiply/divide and software floating point both gave 10 seconds also.) The rate of convergence of algorithms can be compared by determining the number of parameter-point evaluations needed to reach the minimum. For a three exponential fit, one iteration using algorithm A involves 7 evaluations (central point + 2 steps in each of 3 directions). Algorithm B involves an average of 3.75 evaluations (viz 7 - the central point - the previous point - $1/4 \times$ the steps in the other directions if we

assume that in half of the cases the first, positive step in a certain direction yields a fall in ϕ , so that the step in the opposite direction can be omitted). Algorithm C involves either 4.75 evaluations (as for B plus the extra step) or 1 evaluation (when only the extra step is needed). It was found that when the initial estimates were reasonable, the optional extra step of algorithm C was rarely used, algorithm B must therefore be considered to be the fastest. Convergence from the initial estimates (0.40, 0.040 and 0.0040) to the results of Tables II and III (without noise) took an average of 22 iterations, using the minimum step-sizes 0.01, 0.001 and 0.0001 and a multiplication factor of 8. With algorithm B this means that 83 parameter points had to be evaluated which took 830 seconds or about 14 minutes. This may seem rather a lot, but it should be mentioned for the sake of comparison that the advanced iteration scheme according to CACM 315 involves the evaluation of 102 parameter points for convergence from the same initial estimates (Table IV). (It should be noted in this connection, that the derivative of the sum of least squares with respect to the parameters was estimated by making small steps in the axial direction of all parameters. This involves at least k evaluations per iteration, where k is the number of exponentials.) Furthermore, the algorithm of CACM 315 did not converge to the real minimum: Average sum of least squares = 462 for a three exponential fit to a curve without noise, while the constant step approximation method yields an average sum of least squares of 150. This means that the iteration was stopped too early. In all cases one of the three steps used to determine the first derivative of the sum of least squares actually yielded a lower sum of least squares than was finally reached. This could not be improved by varying the damping factor λ . The iteration seemed to be almost totally insensitive to variations in λ : varying this parameter between 0.1 and 0.99 did not influence the results, though $\lambda = 1$ did yield a significantly worse result.

Parameter	Value (s ⁻¹ /mV)	Standard deviation	Systematic error	Details of determination*	Number of measurements	Sum of least squares (mV) ²
γ_1	0.44	10%	2%	$t; \sigma_{\text{noise}} = 0$	11	462
γ_2	0.029	4%	12%	$t; \sigma_{\text{noise}} = 0$	11	462
γ_3	0.0030	3%	3%	$t; \sigma_{\text{noise}} = 0$	11	462
a_0	290	1%	11%	$t; \sigma_{\text{noise}} = 0$	11	462
a_1	174	2%	5%	$t; \sigma_{\text{noise}} = 0$	11	462
a_2	275	2%	2%	$t; \sigma_{\text{noise}} = 0$	11	462
a_3	303	1%	10%	$t; \sigma_{\text{noise}} = 0$	11	462

Table IV *t = three exponentials simultaneously

h. Conclusion and discussion

It is generally acknowledged that fitting exponentials to measured data is a troublesome task. Two types of difficulties can be distinguished:

1. The minimum in the quality function (in this case the sum of least squares) may be hard to detect.
2. The minimum may not agree with the "real" values of the parameters.

It will be clear that difficulties of the second type can be detected (by testing with models as described in IIB2d) but cannot be resolved, unless we use another type of quality function. However difficulties of the first type can be resolved, because if a minimum did exist, however shallow, it should be possible to work out refined methods to detect it.

Our constant-step approximation method was designed on the assumption that the minimum in the quality function does agree with the real values of the parameters but may be hard to detect. It follows that this method has the following features:

1. The procedure is very simple. This means that little can go wrong.
2. The procedure yields a clear insight into the form of the minimum, i.e. in the intractability of the given set of data.
3. With a flat minimum, the procedure ensures that steps are continued until the quality function starts rising again, thus ensuring that the minimum is reached.

Of course our method does involve a lot of computation, but with a mini-computer at one's disposal one can afford the time taken to explore a considerable part of the parameter space. Besides, a method which would be expected to be much more efficient such as the CACM 315 actually turns out to need more time to converge to a worse approximation of the minimum, when the initial estimates supplied are reasonable. Concerning the accuracy which can be reached, we may state that when the relaxation constants involved are about one order of magnitude apart, they can be determined with satisfying accuracy even if much white noise is added to the signal.

Initially, another computer program, which implied a Marquardt iteration-method was used (Kirkegaard, 1970). The constant step approximation method was developed mainly for testing purposes. It turned out however (Coolsaet et al, 1976) that this method always yielded a lower sum of least squares. Later it was found that the Kirkegaard program could reach the same minimum when it was used in double precision (Kuik, 1976). However because it needs less memory space, and for its simplicity we continued to use the constant step method. The fundamentally achievable accuracy when separating a signal into exponentials was investigated at Delft Technical University (Kuik, 1975).

From the fact that the theoretically achievable accuracy of the parameters estimated from a signal contaminated with normally distributed white noise is determined by the Cramér-Rao inequality, he concluded among others that:

1. The theoretical minimal standard deviations (TMS) in the parameters are proportional to the standard deviation of the noise added to the signal.
2. Non-whiteness of the noise causes a decrease in achievable accuracy, as less effective (independent) samples are then available.
3. The TMS decrease with the total observation time, or the number of samples over the sample rate.
4. The TMS decrease with the number of samples per inverse relaxation constant.
5. When more than one relaxation constant is estimated, the TMS increase when the "distance" between the relaxation constants decreases.

All conclusions confirm the expectation that the achievable standard deviations should decrease with the total number of available independent samples per exponential. Concerning the absolute values, for instance when three exponentials are estimated with: $\gamma_1 = 0.36 \text{ s}^{-1}$; $\gamma_2 = 0.028 \text{ s}^{-1}$; $\gamma_3 = 0.0036 \text{ s}^{-1}$; $a_1 = 210$; $a_2 = 74$; $a_3 = 67$; $a_0 = 78$; sample rate is 1 per second, number of samples is 900; standard deviation of white noise

is 1; and the frequency spectrum of the noise is flat, he obtained:

$$\frac{\sigma(\gamma_1)}{\gamma_1} = 1.4\% ; \quad \frac{\sigma(\gamma_2)}{\gamma_2} = 1.9\% ; \quad \frac{\sigma(\gamma_3)}{\gamma_3} = 1.2\%$$

The standard deviations in the coefficients and constant are in the same order of magnitude. It can be stated that these achievable accuracies are in the same order of magnitude as the experimentally determined accuracies (see Table II). Furthermore the experimentally determined standard deviations are indeed roughly proportional to the standard deviation in the noise as stated in conclusion 1. Therefore we conclude that the method of separating exponential signals is (for the given set of signals) an adequate method of parameter estimation. This must at least partly be due to the "pleasant" properties of these signals, as for instance the fact that the relaxation constants differ about a factor of ten.

3. On-line computer analysis

During the experiments, the results are analysed on-line by means of a Texas Instruments 980B mini-computer. The entire installation consists of a 24k CPU with hardware multiply/divide, a Silent 700 thermal printer/keyboard with two cassette units, a high speed papertape reader, high speed papertape punch, Diablo moving head disc and digital inputs and outputs connected to the A/D interface. The subroutines STEP and LIN, which are described in the previous paragraph and perform the actual separation into exponentials, are called from a Main program which rules the data-flow in the experiments. It is therefore necessary to give a short global description of the working of the Main program. The program consists of ten phases, which are normally executed in numerical order. A flow chart is presented in Fig. 12.

At the start of the program we enter phase one. Here we enter the information as to whether we are performing an experiment on strips or total bladders, and whether we wish to handle the data off-line or on-line. We shall assume that we

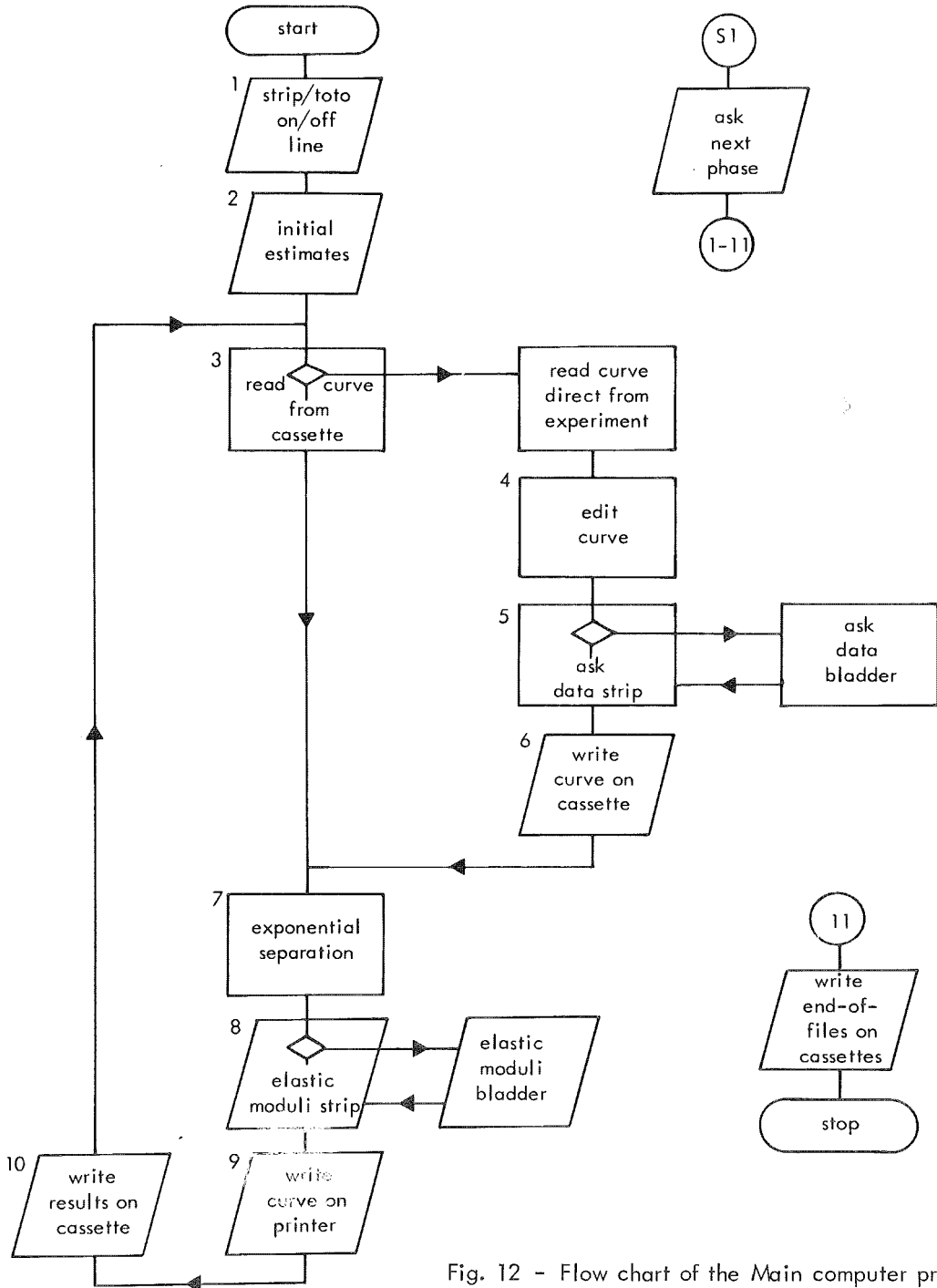


Fig. 12 - Flow chart of the Main computer program

are doing a strip experiment on-line. In phase two we should then type in the initial estimates for the relaxation constants, minimal step-sizes etc. In phase three a thousand samples are read in via the sampling interface. We have then to determine which sample corresponds to the start of the experiment since the sampling has to be started before the actual straining (see IIB1). The computer therefore picks the highest from the first hundred samples, and then from the ten succeeding samples, starting with the highest one, the one with the lowest first derivative. A number of samples is printed. The sample chosen is indicated and a correction for this choice is requested. In strip experiments this correction is not usually necessary, because then the beginning of the experiment is well defined by a sharp peak. In phase five details about the experiment should be entered, such as experiment number, strain, tissue volume, etc. In phase six these data and the measured data are written on a cassette-unit for computation later on. In phase seven the actual exponential separation is started by calling subroutine STEP. Then, in phase eight elastic and viscosity moduli are computed according to the formulas (11) and (12) after multiplication with the amplification factor described in IIB1.

In phase nine the measured curve is printed out and in phase ten the resulting parameters are written on another cassette. The process then begins again with phase three.

When we ask for off-line computing, in phase one, measurements are taken from the cassettes written in phase six instead of from the on-line samples in phase three, and phases four, five and six are omitted. When performing experiments on total bladders, the phases five and eight are changed in order to handle the different geometry (see chapter IV).

There are two possibilities of intervention in the normal order of execution, realized by two sense switches on the CPU. When setting sense switch one, the machine will ask at the end of a phase with which phase to continue. By setting sense switch two, some phases which take a long time can be aborted (only phases three, seven and nine) and execution continues with the next phase. By setting

sense switch one and asking for phase eleven the program is terminated. Finally, two other sense switches can be used, in order to punch or print samples as soon as they are read.

Another program can be used to read the results written on the cassette in phase ten, add them to a large file containing the results of all measurements, and compute averages and standard deviations.

C. Results

1. Order of investigated system

What we first want to determine experimentally is the order of the system under investigation, i.e. the number of exponentials which should be used, or the value of k in equation (6).

If the measured force decay can be described by a mono-exponential function ($k = 1$) a semi-logarithmic plot will reveal a straight line, provided the final value of the signal (caused by the constant in equation (6)) is first subtracted. The curve obtained however is far from a straight line (Coolsaet et al, 1975a).

Using the method for analysis described in IIB2 the measured curves were then fitted with two and three exponential functions. An example of the results can be seen in Figs. 13 and 14. At first sight the three exponential function seems to fit the measured points very well. A better criterion of course is the sum of least

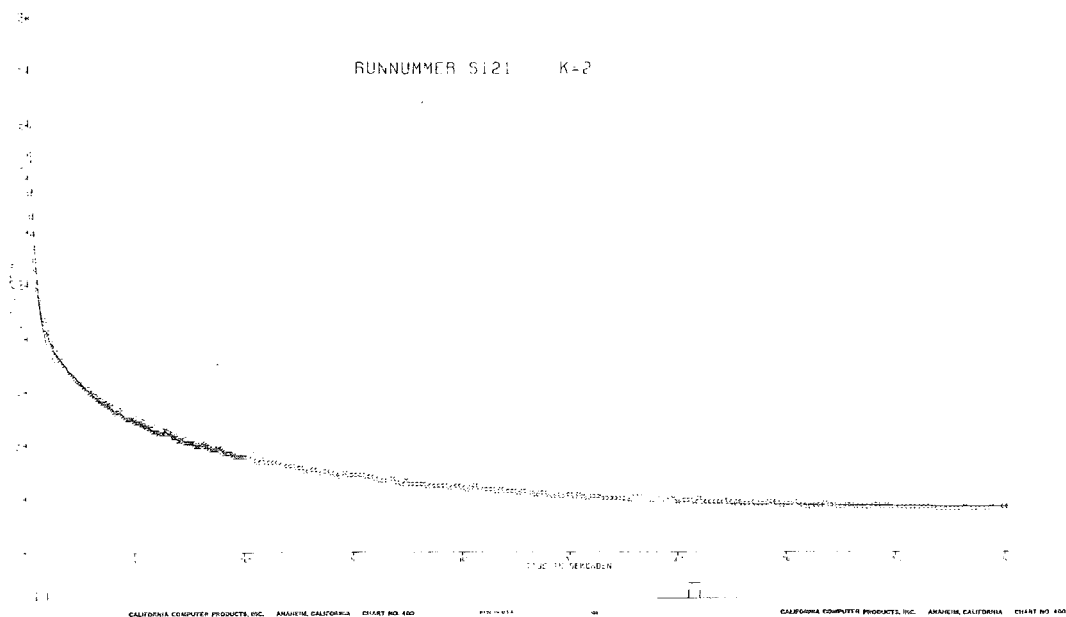


Fig. 13 - Measured points (crosses) and fitted force decay curve (line)
for the two exponential model

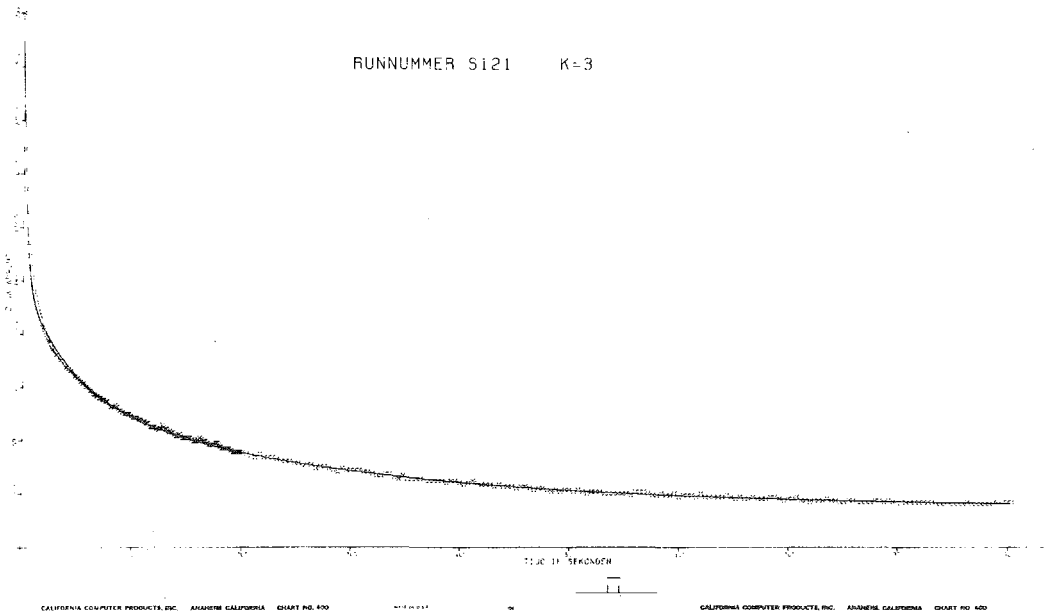


Fig. 14 - Measured points (crosses) and fitted force decay curve (line)
for the three exponential model

squares. The program described in IIB2 was modified in order to be able to fit more than three exponential terms, and a representative group of curves (the EGTA group, see IIC2) was fitted with an increasing number of exponential terms. The results can be seen in Fig. 15 and Table V. It should be noted that Fig. 15 is a semi-logarithmic plot. This was done because we are not interested in the absolute amount of decrease of the sum of least squares when increasing the number of fitted exponentials, but rather in the improvement factor. From the flattening of the average sum of least squares at $k = 4$ we can conclude that the order of the system is four. In trying to confirm this in a more objective way we noted the following: according to Draper and Smith (1967) the sum of least squares can be split up into two components:

1. The bias error due to misfitting of the curve.

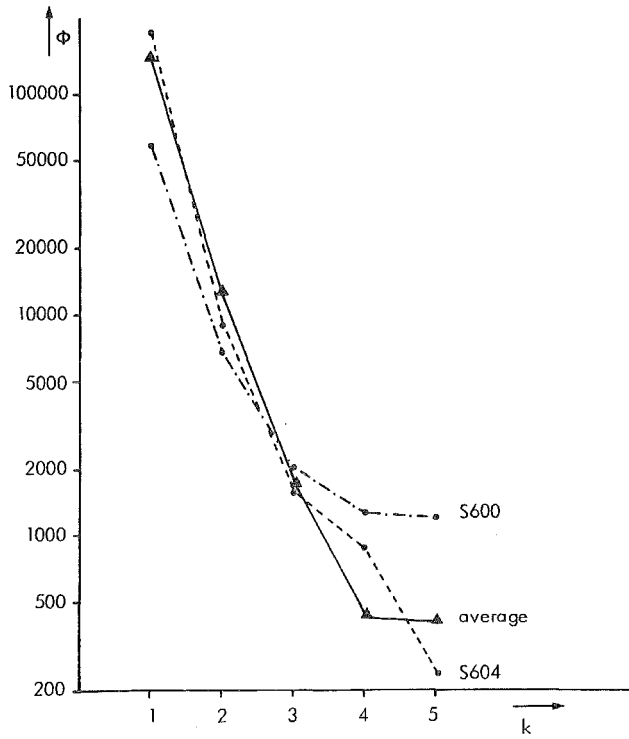


Fig. 15 - Average sum of least squares as a function of number of fitted exponential terms

Number of fitted exponentials	Average sum of least squares (mV) ²	Relative standard deviation	Number of experiments
1	146081	114%	105
2	12226	105%	105
3	1692	145%	104
4	424	175%	103
5	402	302%	103

Table V - Average sum of least squares as a function of number of fitted exponential terms

2. The random error due to noise on the signal.

When the number of fitted exponentials equals the order of the system, the bias error equals zero. The sum of least squares only reflects the random error then. By increasing the number of fitted exponentials the sum of least squares may still decrease somewhat, because we are then fitting the random noise with exponentials. It would be convenient to have an estimate of the random error which can be expected in the experiments. In in vitro experiments four possible causes for the random error can be expected:

1. Spontaneous activity of the tissue.
2. Artefacts caused by movement of the tissue, e.g. that caused by oxygen bubbles.
3. Electrical noise caused by the instrumentation etc.
4. Quantization noise in the digitizer.

Possibility 1. is eliminated as far as possible by examining curves from the EGTA group (see IIB1). The value of the standard deviation caused by 4. can be very easily estimated. The least significant digit equals 1 mV. According to Rabiner and Gold (1975) the standard deviation in the quantization noise then equals $1/\sqrt{12} = 0.29$ mV.

The random error caused by 2., 3. and 4. together can be estimated by hanging a piece of rubber freely in the solution, turning on the oxygen, and reading a great number of samples. This yields a standard deviation of 0.27 mV. Evidently 2. and 3. are not important. As in practice 400 samples are fitted (see IIB2) we would expect the average sum of least squares to be about $400 \times (0.29)^2 = 33$ when no bias error is present. We see in Fig. 15 however that this minimum is not reached by the average sum of least squares which indicates that some extra noise caused by spontaneous activity might be present.

Another interesting observation is that the standard deviation in the sum of least squares is much larger when fitting five exponentials in comparison to the four exponential fittings. This is at least partly due to the fact that some curves can obviously adequately be fitted with three exponentials (see Fig. 15, curve S600)

and others require at least five exponentials (ditto, curve S604). We can only conclude therefore that not all measurements reveal the same order of the system, but that the average order is four.

There are several reasons for describing the system under investigation with a lower order model:

1. We should not have any illusions about the significance of the obtained parameters when fitting four exponentials to the signal.
2. The bias error due to fitting a three exponential model instead of a four exponential model is relatively small. In this case the standard deviation per data point would yield:

$$\sqrt{\frac{1692 - 424}{400}} = 1.78 \text{ mV}$$

As the average value of the signal equals 500 mV (half of full scale) this gives an average relative standard deviation of $\frac{1.78}{500} \times 100\% = 0.4\%$.

3. For some curves the four exponential fit is not significantly better than the three exponential fit. These would be "overfitted" when using a four exponential model.

We will therefore describe the step response of urinary bladder wall tissue in terms of a model, consisting of three exponential terms and a constant.

2. Relaxation constants as functions of the chemical environment

When measuring force as a function of time in response to a step-wise straining on a strip of urinary bladder wall the basic shape of the curve obtained resembles that in Fig. 16. Pig bladder strips and sometimes also dog bladder strips when measured in the "natural" solution show a spontaneous activity which appears to be simply added to the curve (see Fig. 17). It was in fact shown that by electrical stimulation similar contractions can be evoked which do not alter the measured response but are indeed only superimposed (Coolsaet et al, 1975a). The spontaneous activity can be increased by adding extra calcium to the solution. Furthermore the activity is seriously affected by the temperature of the solution.

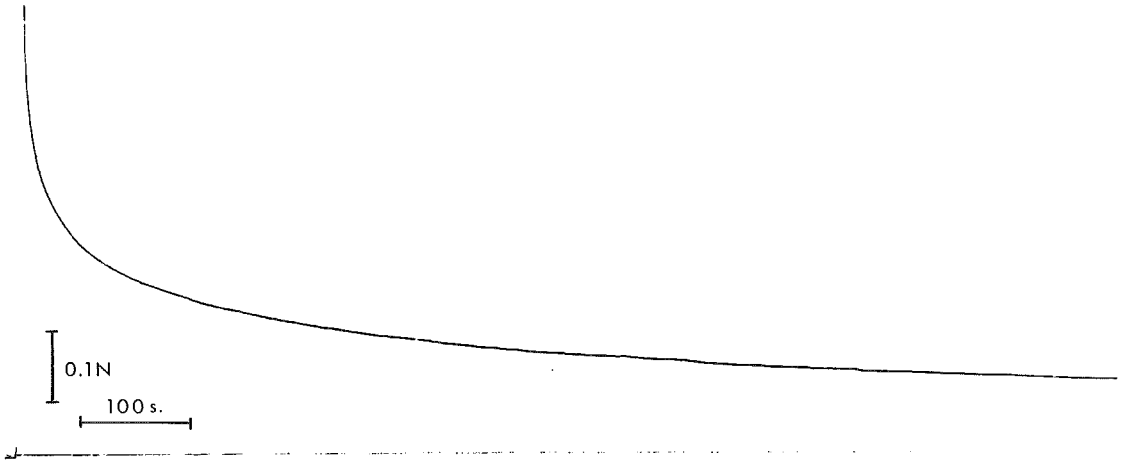


Fig. 16 - Force as a function of time in response to a step-wise straining

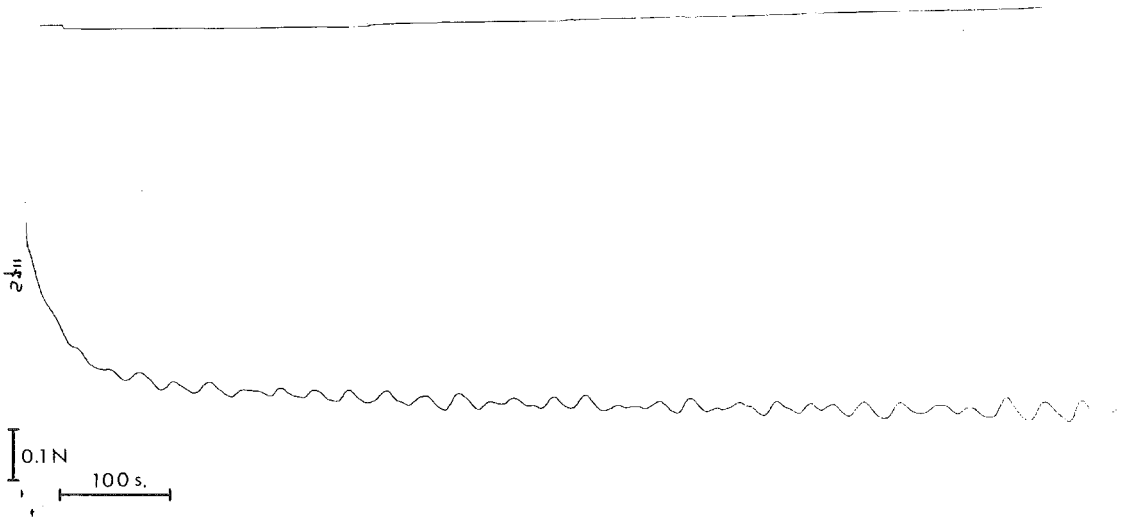


Fig. 17 - Curve with spontaneous activity

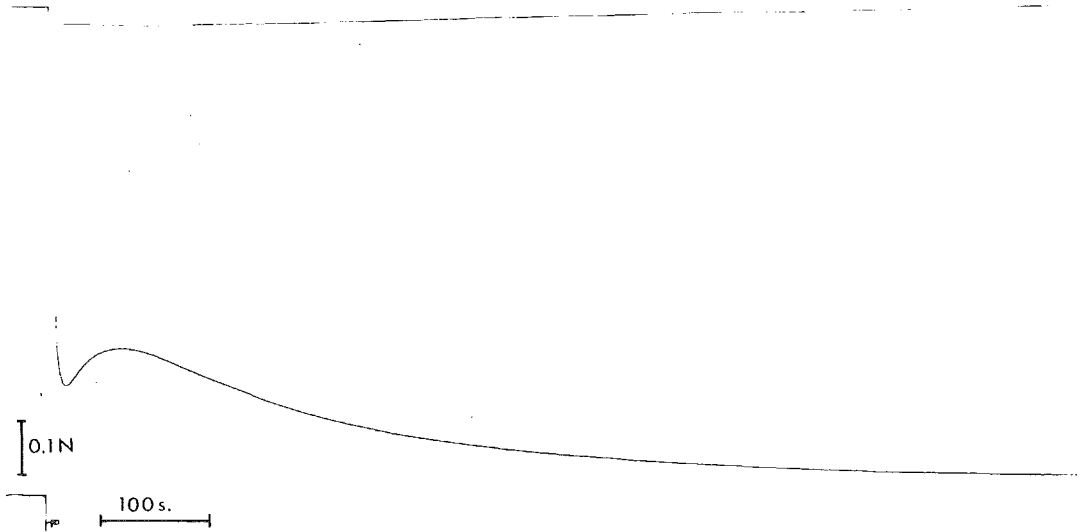


Fig. 18 - Curve measured at 22°C instead of 37°C

Figure 18 shows a curve measured at 22°C instead of 37°C. When using the solutions called D600, EGTA, extra K or Sorbitol spontaneous activity was not observed. As for the present we only want to consider the passive properties of the urinary bladder, we are only interested in the measurements of these groups. The other groups are included for reference. Table VI shows the average relaxation constants and standard deviations for a number of measurements from each group. As mentioned in IIB1, about ten measurements were taken from one strip. For instance the group "pigs; EGTA" contains measurements from ten different strips or bladders. By means of variance-analysis it was possible to split the variance of the relaxation constants into two components. The first component is related to differences between measurements on one strip and is called physiological spread. The second component concerns differences between strips and is called biological spread. The corresponding standard deviations are shown in Table VI for the groups "dogs; natural" and "pigs; EGTA". Notice that the lower standard deviations in the latter group are clearly caused by a lower biological spread. By means of the

Group	$\gamma_1 (s^{-1})$	$\sigma(\gamma_1)$	$\gamma_2 (s^{-1})$	$\sigma(\gamma_2)$	$\gamma_3 (s^{-1})$	$\sigma(\gamma_3)$	number of measurements
Dogs; natural -physiological spread -biological spread	0.47	66% 50% 46%	0.045	71% 59% 40%	0.0050	50% 46% 14%	118
Dogs; D600	0.82	33%	0.062	37%	0.0037	30%	26
Pigs; natural	0.23 (5.32)	66% (99%)	0.033 0.14	45% 28%	0.0044 0.0090	64% 46%	19 99
Pigs; EGTA -physiological spread -biological spread	1.05	23% 21% 8%	0.077	51% 49% 13%	0.0061	62% 60% 16%	104
Pigs; EGTA; increasing strain	0.96	27%	0.069	52%	0.0052	56%	98
Pigs; extra K	1.00	21%	0.054	18%	0.0038	21%	131
Pigs; Sorbitol	0.82	35%	0.047	40%	0.0036	47%	26

Table VI - Relaxation constants of the various groups of measurements

F-test it is possible to test whether differences between strips are significant in comparison to differences within the strips. It appeared that in the group "dogs; natural" two relaxation constants showed significant biological spread ($p < 0.05$) and in the group "pigs; EGTA" only one relaxation constant did. From this we can tentatively conclude that it is probable that large differences between strips are merely caused by active properties.

Concerning the group "pigs; natural" it should be noted that this was a group with a great deal of spontaneous activity. The effect on the fitting procedure was disastrous. It turned out that the resulting relaxation constants fell apart in two widely differing groups. From the largest group the relaxation constants can theoretically not even be determined with reasonable accuracy (see IIC3).

For the bad results in this group we give two possible causes:

1. The properties of the curves themselves (apart from the spontaneous activity) might show a large spread.
2. The spontaneous activity might influence the fitting procedure.

Concerning the last point it should be noted that the frequency range of the "noise" (spontaneous activity) here is obviously very close to the observed relaxation constants. This can cause serious trouble (see IIB2). As dog bladder strips show much less spontaneous activity, in the group "dogs; natural" no problems occurred, though the standard deviations are rather large. It can be stated that the accuracy attained in the other groups is quite satisfactory. Again we are led to the conclusion that large standard deviations in the relaxation constants are only caused by active properties. It is interesting to observe that the standard deviations in the group "pigs; extra K" are still somewhat smaller than in the EGTA group which supports the argument of Axelsson (1970), mentioned in IIB1. Furthermore, concerning the relaxation constants all groups differ significantly though the groups with activity suppressing drugs (dogs; D600, pigs; EGTA, extra K and Sorbitol) show greater mutual resemblance than towards the other two groups. Apter and Mason (1971) also noted that a contracted muscle shows properties different from a relaxed one. We shall consider the relaxation

constants of the groups "dogs; D600" and "pigs; EGTA" as representative for the time dependent behaviour of the passive properties of the urinary bladder wall. The group "pigs; EGTA; increasing strain" contains measurements at increasing strains between 0.2 and 1.6. From the fact that the standard deviations in this group are not significantly larger than in the corresponding group measured at constant strain, we conclude that the relaxation constants are independent of strain. This was also concluded by Coolsaet et al, 1975b. The validity therefore of the values displayed in Table VI is not restricted to a strain level of 0.30. Concerning the elastic moduli, which were of course also obtained by these measurements, no statistically significant average could be obtained because these parameters showed a generally decreasing trend as a function of time despite the constant strain level.

Implications of this phenomenon and separate measurements in order to determine these parameters will be discussed in chapter III.

3. Check of conditions

The described measurements imply a number of assumptions. Objective criteria can be used in order to test the validity of some of these assumptions. Such criteria can be applied to the speed of the pneumatic cylinder, the sampling rate and the total measurement time. Furthermore the measured parameters allow us to make some remarks with regard to the fundamental achievable accuracy. The setting of the delay time generator will also be discussed here, since it depends on experimental material. Assumptions which were not checked but are nevertheless more or less important, are discussed in IIC4.

Our first assumption concerns the speed of the pneumatic cylinder. In our mathematical analysis we assume a straining which is infinitely fast. This of course cannot be realized, and is also not necessary. The only thing we should require is that the straining is fast in comparison to the time constants of the system under test. In Fig. 19 distance versus time of the pneumatic cylinder is plotted. We see that at the maximum strain (50 mm) the movement of the cylinder takes about 60 ms.

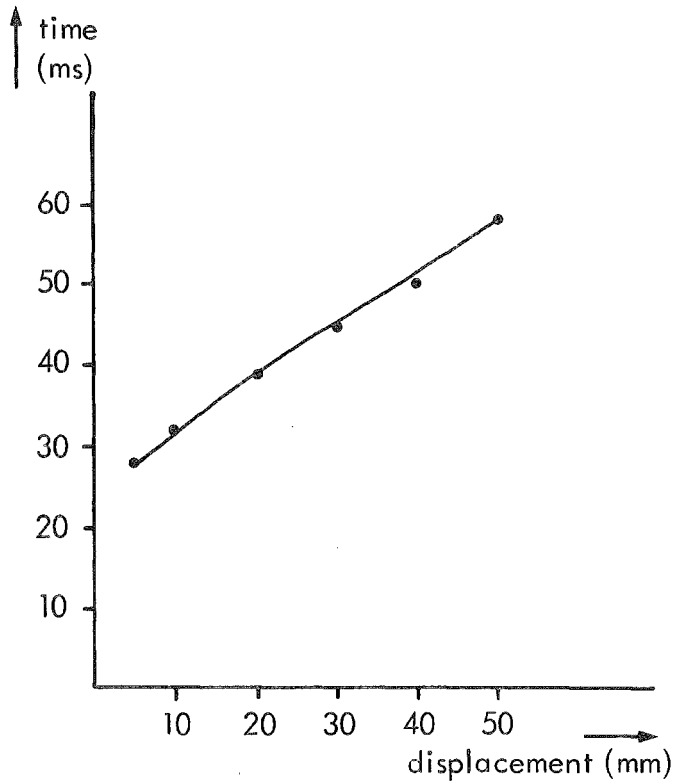


Fig. 19 - Displacement versus time of the pneumatic strain device

This is approximately 16 times as fast as the fastest time constant, see Table VI, which equals $\frac{1}{1.05} = 0.95$ s. Here we do not consider the extreme relaxation constant 5.32 as a relevant value. With regard to the sampling rate it can be stated that at least two samples per exponential must be available. As an exponential only differs significantly from zero during a time lasting three times the time constant ($e^{-3} = 0.05$) it follows that the sample interval should be smaller than approximately 1.5 times the fastest time constant. According to the data of Kuik (1975) the achievable accuracy is still acceptable when the fastest time constant and sample interval are about equal. According to these criteria and keeping in mind that the sample interval is one second, the fastest relaxation

constant of Table VI in the order of 1.0 s^{-1} is reliable but not the higher value of 5.32 s^{-1} . That is why this value is placed between parentheses.

A related problem is that of the total amount of samples. Again assuming, that an exponential "lasts" about three time constants we can state that the total sample time should be in the order of three times the slowest time constant which yields in our case (see Table VI) $\frac{3}{0.0036} = 833$ seconds. In practice we sampled for about 1000 seconds. As stated in IIB2 not all samples were considered, but only the first 200 and then one out of four, in total 400 samples. As however the fastest time constant "lasts" only about three seconds, and the next is at least a factor ten slower this slowing down of the sample rate with a factor four implies that the second fastest exponential is relatively sampled about 2.5 times as fast as the fastest exponential. That is why this reduction will not have a significant influence on the accuracy.

It is important to mention here again that the relaxation constants are at least a factor ten apart. As stated in IIB2 this has a very positive influence on the achievable accuracy, and must partly cause the successful separation into exponentials which is generally recognized as a very awkward problem.

The delay time generator (see IIB1) must be set in such a way that the first sample is taken after the "rounded-off" part of the signal (see IIB2), otherwise the fastest relaxation constant will be too small, that is unless the first derivative of the signal is checked in order to find the steepest part of the curve. This was in fact done. Nevertheless the influence of the delay time was checked because no triggering would cause an unnecessary high random fluctuation of the parameters, and a wrong triggering (or delay time) would force the computer program to systematically drop the first sample which yields a coefficient which is too low. The easiest way of finding the obviously best delay time, is to temporarily drop the first derivative criterium in the computer, and then to use the delay time setting which yields the largest of the fastest relaxation constants. It turned out that this relaxation constant could be varied by a factor two in this way. Finally $0.8 \Delta t$ was chosen as the best delay time.

4. Conclusion and discussion

The time dependent behaviour of the passive properties of the urinary bladder wall can be described in terms of the mechanical model presented in Fig. 6. The average required number of spring-dashpot combinations is four, but the behaviour of the wall can adequately be described by using only three combinations.

In "reality" of course it is most likely that not a discrete number of spring-dashpot combinations is "present" in the bladder wall strip, but a distribution as described in IID3. In that case using four or any amount of discrete combinations is always an approximation. The average relaxation constants (inverse of the time constants) for the three combinations are presented in Table VI, for dogs in the row "dogs; D600", for pigs in the row "pigs; EGTA". The differences between these two sets of relaxation constants are not very large. The accuracy of the relaxation constants is quite satisfactory.

In drawing these conclusions from the experimental material presented in IIC1 and IIC2 two assumptions have implicitly been made:

1. The relaxation constants are independent of strain.
2. The relaxation constants are independent of the place and direction in which the strip is cut (homogeneity and isotropy).

With regard to the first assumption some evidence in this direction is presented by Coolsaet et al (1975b). Although here a method of analysis was used in a way which yielded a systematic error, namely the Marquardt iteration, see IIB2, we can at least conclude that the relaxation constants remain in the same order of magnitude when the strain is varied. Furthermore, Table VI also contains a group of measurements made at increasing strains. The standard deviations of this group are not significantly larger than the standard deviations of the corresponding group measured at constant strain.

For the second assumption no direct proof is available. Conclusions however, can be drawn from the fact that the average relaxation constants measured on dog strips can be compared favourably to those measured on dog bladders in vivo/
in toto. We will discuss this matter in more detail in chapter V.

D. Alternative analysis methods

1. Introduction

In the previous paragraphs the step response of the urinary bladder wall was described in terms of a model consisting of three exponential terms and a constant. Here we shall criticize this model in more detail.

In modelling there are two features which should be fulfilled:

1. The signal generated by the model with adequate parameter settings should fit the measured data. This enables us to just store the parameters instead of the original data. As the number of parameters is smaller than the number of fitted data points we can call this "data reduction".
2. The parameters abstracted from the signal should be significant in two ways:
 - 2.1. They should be unique.
 - 2.2. They should be significant by being related to distinct elementary structures in, or fundamental properties of the system.

Applying these criteria to the exponential model presented here, we note that although the model conforms to condition 1. and 2.2., the exponentials that are used are non-orthogonal functions. This means that they are not mutually "independent" as demanded by condition 2.1. An exact definition of orthogonality will be given in IID2. Here it is sufficient to mention some of the awkward problems which arise when using non-orthogonal functions. For instance when a signal consisting of four exponentials is described using three exponentials, the parameters obtained do not display information concerning the parameters of the four exponential system. Furthermore the same signal can often be described by different sets of parameters (Lanczos, 1956; Van Duyl, 1974), so that there is a lack of uniqueness. Finally, even when separation into exponentials is possible, it remains a time-consuming and very difficult procedure. That is the reason that a number of alternative models have also been tried out.

2. Orthonormal exponential functions

A set of functions $u_n(t)$ is said to be orthonormal if:

$$\int_{-\infty}^{+\infty} u_i(t) u_j(t) dt = \delta_{ij} \quad (18)$$

where δ_{ij} is the Kronecker delta
 $\delta_{ij} = 0$ for $i \neq j$
 $\delta_{ij} = 1$ for $i = j$

If the functions are orthogonal instead of orthonormal equation (18) is the same, except for the δ_{ij} which is replaced by $c_{ij} \cdot \delta_{ij}$ where c_{ij} is an arbitrary constant. In order to avoid the problems mentioned in IID1, the first idea that comes to mind is to describe the measured force $F(t)$ using a set of orthonormal functions as follows:

$$\begin{aligned} F(t) &= \sum_{n=1}^{\infty} b_n u_n(t) \quad \text{for } 0 < t < \infty \\ F(t) &= 0 \quad \text{for } -\infty < t \leq 0 \end{aligned} \quad (19)$$

$$\text{where } b_n = \int_0^{\infty} F(t) \cdot u_n(t) dt \quad (20)$$

Here we have changed the lower limit of the integral, which should be $-\infty$ by analogy to equation (18), to 0 because $F(t)$ equals 0 for $t < 0$. In practice we hope to be able to describe the signal adequately by only a limited number of terms in (19) and we can integrate only over a limited time in (20). Lee (1960) described a set of exponential orthonormal functions u_n which may be applicable in our situation. The fact that the exponent varies proportionally to the ordinal number (n), however, makes these functions less universal than desired. A lot of terms therefore have to be contained in formula (19) when describing a signal which contains very fast and very slow exponential terms.

A new set of orthonormal functions was therefore developed, featuring a variable "distance" between the exponents. The general form of the functions is:

$$u_1(t) = C_{11} e^{-a_1 t} \quad (21)$$

$$u_2(t) = C_{21}e^{-a_1 t} + C_{22}e^{-a_2 t} \quad (22)$$

or generally:

$$\begin{aligned} u_n(t) &= C_{n1}e^{-a_1 t} + C_{n2}e^{-a_2 t} + \dots + C_{nn}e^{-a_n t} \\ &= \sum_{i=1}^n C_{ni}e^{-a_i t} \end{aligned} \quad (23)$$

For the set of functions that Lee generated, it can be stated that:

$$a_i = i \times a_1 \quad (24)$$

And in our case we want to avoid any fixed relation between:

$$a_i \text{ and } a_1$$

The functions defined in this way can be made orthonormal by inserting equation (23) into (18), and then generating a set of equations by choosing all possible combinations of i and j .

This yields a set of $\sum_{i=1}^n i$ equations with the same number of unknown variables,

the C_{ni} . When solving these equations (which can be done very fast by mathematical insight) it turns out that:

$$C_{11} = \sqrt{2a_1} \quad (25)$$

$$C_{21} = \sqrt{2a_2} \cdot \frac{-2a_1}{a_1 - a_2} \quad C_{22} = \sqrt{2a_2} \cdot \frac{a_1 + a_2}{a_1 - a_2} \quad (26)$$

or generally:

$$C_{ni} = \sqrt{2a_n} \frac{\prod_{i=1}^{n-1} (a_i + a_1)}{\prod_{\substack{i=1 \\ i \neq j}}^n (a_i - a_1)} \quad (27)$$

Inserting (27) into (23) yields the functions $u_n(t)$:

$$u_n(t) = \sum_{i=1}^n \sqrt{2a_n} \frac{\prod_{i=1}^{n-1} (a_i + a_i)}{\prod_{i=1}^n (a_i - a_i)} e^{-a_i t} \quad (28)$$

Lee's functions can be obtained from these by simply inserting (24) into (28). Using these functions a computer program was written to calculate the coefficients b_n according to (20) for measured data. A numerical integration according to the Simpson rule was used. An extra problem was formed by the fact that $F(t)$ does not tend to zero, as already mentioned in IIA2. This would mean firstly that the integration has to be done over an infinite number of data points, and secondly that the coefficients b_n are biased because a constant is not orthonormal to the set of functions (28). Therefore, a constant was subtracted from the $F(t)$ signal before applying the numerical integration. It is important to realize the essential difference between this method and any least squares approximation method. The latter improves the fit of a generated curve by changing the parameters while the first one only determines parameters in a direct way. Consequently a least squares method will always yield a very good fit, except when too few parameters are fitted. A "goodness-of-fit" criterion therefore cannot be used here to state the significance of the parameters. Using the orthonormal function method, however, the whole method can be controlled by generating a curve according to (19) and comparing it to the original curve. The parameters will always be unique. The average relative difference between real and regenerated data points was used as a criterion. Curves were generated, using an RC circuit generator according to the formula:

$$F(t) = 200e^{-0.37t} + 270e^{-0.027t} + 295e^{-0.0027t} + 295 \quad (29)$$

The parameter values are approximately the same as those used in testing the least squares constant step approximation method, described in IIB2.

No noise was added to the signal which was sampled at a rate of 1 sample per

second during 1000 seconds. In order to control the proper working of the numerical integrator, it was first tested on the signal (29) with three functions u_n , using the exponents:

$$\begin{aligned}a_1 &= 0.37 \\a_2 &= 0.027 \\a_3 &= 0.0027\end{aligned}$$

The average fit error, calculated as the average difference between sampled data points and computed data points according to equation (19) then yielded 1.1%.

The signal was then fitted using six functions u_n (the same number of parameters as used in the least squares analysis, which fits three coefficients and three exponents, apart from the constant for which a value of 295 was subtracted here)

using: $a_1 = 0.001$; $a_2 = 0.003$; $a_3 = 0.01$; $a_4 = 0.03$; $a_5 = 0.1$; $a_6 = 0.3$.

The average fit error yielded 8.7% and using $a_1 = 0.003$; $a_2 = 0.01$; $a_3 = 0.03$; $a_4 = 0.1$; $a_5 = 0.3$; $a_6 = 1.0$ the error yielded 5.3%. The difference between these errors is in the same range as the error introduced by limiting the signal to 1000 samples which is caused by the very slow exponent 0.001.

This relative break-off error, which equals:

$$e = \frac{-(a_n + \gamma_i) \times 1000}{\quad} \quad (30)$$

where

a_n = the smallest exponent in the used u_n functions

γ_i = the smallest exponent in the generated $F(t)$ function

yields 2.5% when $a_n = 0.001$ and $\gamma_i = 0.0027$.

For the greater exponents this break-off error is negligible.

There is no large error caused by the numerical integration, as proved by the 1.1% fit when the "real" exponents are fitted.

Also the number of fitted orthonormal functions is not too small because by adding the sixth function it showed no significant improvement (with the five exponents $a_1 = 0.003$; $a_2 = 0.01$; $a_3 = 0.03$; $a_4 = 0.1$; $a_5 = 0.3$ the average fit error still yields 5.3%). From the remaining errors (5%) it must be concluded that the signal $F(t)$ cannot be described adequately in terms of such orthonormal functions. In

terms of the conditions mentioned in IID1 this method is very strong in condition 2.1. but it does not obey condition 1.

3. Continuous relaxation spectrum

Fung et al (1972) stated that any discrete model for describing the visco-elastic behaviour of tissue is artificial and that in fact a continuous model should be used.

This would mean that a logical extension of the discrete model:

$$F(t) = \sum_{n=1}^k a_n e^{-\gamma_n t} + a_0$$

is the continuous one:

$$F(t) = \int_0^{\infty} a(\gamma) e^{-\gamma t} d\gamma + a_0 \quad (31)$$

Two possibilities are now available:

1. A relaxation spectrum $a(\gamma)$ can be stated.

Insertion of $a(\gamma)$ into (31) will yield the characteristic stress relaxation then, and the parameters which define the shape of $a(\gamma)$ must be obtained from comparison with actual measured data. For instance:

When:

$$a(\gamma) = a_1 \delta(\gamma - \gamma_1) + a_2 \delta(\gamma - \gamma_2) + a_3 \delta(\gamma - \gamma_3) \quad (32)$$

where δ is the Dirac delta function

is inserted, the former exponential model is regained. The parameters to be determined are the heights of the peaks, and their positions, which in fact are the coefficients a_n and exponents γ_n , see Fig. 20.

Of course any shape for $a(\gamma)$ can be stated, so the real approach must be to determine which shape must be used experimentally.

Before we do this (section 2) one particular interesting relaxation spectrum must be checked. Van Liew (1967) proposed a normal distribution for the inverse of the relaxation spectrum, i.e. the time constant spectrum of some biological processes as, for instance, clearance in kidneys and lungs.

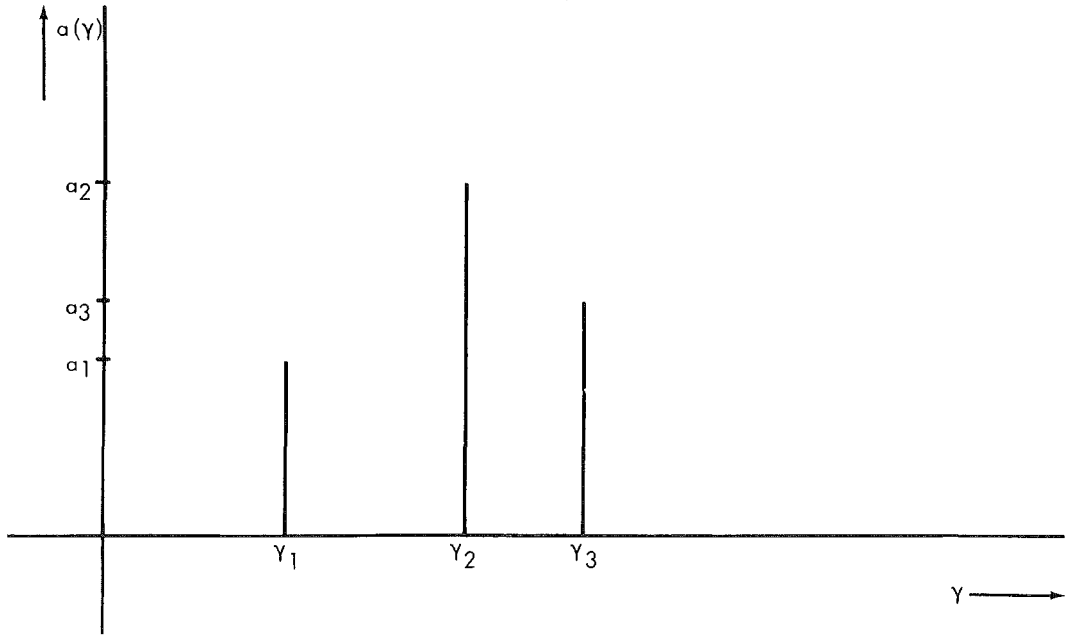


Fig. 20 - A relaxation spectrum which yields a discrete three exponential model

The interesting feature from this concept is that the two parameters $\bar{\tau}$ (average time constant) and $\sigma(\tau)$ (standard deviation) can be obtained from the results of a discrete exponential analysis, as follows:

$$\bar{\tau} = \frac{\sum_{n=1}^k \frac{a_n}{\gamma_n}}{\sum_{n=1}^k a_n} \quad (33)$$

$$\sigma(\tau) = \sqrt{\frac{\sum_{n=1}^k a_n \left(\frac{1}{\gamma_n} - \bar{\tau} \right)^2}{\sum_{n=1}^k a_n}} \quad (34)$$

Another favourable aspect of this concept is that the average time constant can also be obtained simply without a discrete exponential analysis, by means of the "height over area method" (Van Duyl, 1974). Referring to Van Liew the two parameters $\bar{\tau}$, $\sigma(\tau)$ should be more reproducible than the original (a_n, γ_n) . In order to test this for 17 series of approximately 9 measurements the parameters $\bar{\tau}$ and $\sigma(\tau)$ were computed from the relaxation constants and coefficients obtained by a least squares method for every measurement, and then averaged per series (one series represents all measurements made on one strip of urinary bladder wall material, see Coolsaet et al, 1975b). It turned out that in 50% of the tested parameters the relative standard deviations in the $\bar{\tau}$, $\sigma(\tau)$ were worse than in the (a_n, γ_n) , and 20% were better. This was definitely no improvement. A reason for this might be that the relaxation constants γ_n are approximately a factor ten, thus very far, apart in our data (compare IIC2).

This makes it very unlikely that one Gaussian distribution can be used to describe it. An alternative approach is to presume three normal distributions. This however does not yield a reduction in the number of parameters, and the calculations used in order to obtain the new parameters are rather complicated.

2. The determination of the shape of the $a(\gamma)$ function would seem very easy.

Apart from the constant a_0 formula (31) which governs the transformation from the relaxation distribution $a(\gamma)$ to the time signal $F(t)$ is exactly equal to the Laplace transform, with the Laplace parameter s replaced by time t , and t (in the Laplace transform) replaced by γ . This would mean that the $a(\gamma)$ distribution can be obtained from the measured $F(t)$ curve by applying an inverse Laplace transform. A method for numerical inverse Laplace transformation has been proposed by Gardner et al (1959). A critical evaluation of this method showed that it is seriously affected by a number of factors thus making it useless (Sparreboom et al, 1976). Although this method seems very attractive at first sight, and it obeys all our conditions mentioned in IID1, it is not applicable because of the practical problems involved in an inverse Laplace transformation on numerical data.

4. Analogue simulation

Van Duyl et al (1976) proposed an electronic device for a quick analysis of exponential decay curves. It was shown that with this instrument it is very feasible to fit two exponentials and a constant to measured data. Principally, the method consists of projecting the measured signal $F(t)$ on an oscilloscope screen, together with a generated multi-exponential decay curve. The parameters of the generated curve can be changed manually in order to make the curves coincide. The fitted parameters can then be read from the control settings. An interesting feature is, that spontaneous activity, which causes the computer analysis used here a great deal of problems, can be very easily "interpolated", as the activity seems to be simply added to the signal (see IIC2). A prototype of the device was tested on our application, which demanded fitting of three exponentials and a constant. Forty measurements were fitted, and the parameters obtained were compared to those obtained by least squares analysis. The average difference was 40%. The reason for this huge error is that there is very little improvement in fit when the parameters are changed significantly in the vicinity of the minimum of the sum of least squares. Obviously such small changes cannot be detected by the human eye. The simulator was therefore extended with a small calculating device which displays a criterion of fit. In that case, however, our argument concerning the spontaneous activity mentioned above does not apply any more. In fact, what we are performing when using a criterion of fit, is the same method of analysis that is used by the computer (see IIB2). Because we cannot change all parameters (if three exponentials and a constant are fitted we need to vary seven parameters!) at the same time in a consistent way, we must vary them one at a time and then observe the criterion of fit. The same is done by the computer, only faster and with the extra advantage that the coefficients and constant do not have to be optimized in this way, but can be found by simple matrix inversion (see IIB2).

We must conclude therefore that although this device may be useful clinically, where the fitting of two exponential terms and a constant might suffice (see VA3), it does not obey condition 2.1. within the scope of the work described by this

thesis, where fitting of three exponential terms and a constant is required.

5. Power series

It is often suggested that a single power series might fit the data reasonably well, using a small number of terms. Keeping in mind that the data can be described adequately by a sum of three exponential terms and a constant, we reason as follows:

The series expansion of one exponential term yields:

$$e^{-\gamma t} = \sum_{n=0}^{\infty} \frac{(-\gamma t)^n}{n!} \quad (35)$$

When describing one exponential term, the maximum value of γt for which the exponential differs significantly from zero is about three. We can then estimate the number of terms necessary to describe this exponential adequately as follows: When substituting three for γt in equation (35) we can observe that the n^{th} term follows from the $n-1^{\text{th}}$ by multiplying with a factor $\frac{-3}{n}$. This means that the terms increase until $n = 3$ and then they start to decrease. We can then state that in this case at least six terms will be necessary. In our real signals at least three exponential terms can be found. When the greatest relaxation constant is combined with the maximum value of t , the maximum value of γt which can be expected is about 1000. This means that in order to obtain a reasonable fit at least 2000 terms have to be considered. We see that this method fails to obey condition 1 (mentioned in IID1) which requires a data reduction.

6. Other models

A great number of special models has been proposed in the past in order to describe the behaviour of smooth muscle or, more specifically, the urinary bladder. Two have been discussed elsewhere (Coolsaet et al, 1976). The first model was proposed by Apter et al (1970) for describing the behaviour of muscle. It includes active properties but also predicts step responses. A computer program was

developed which simulates Apter's model. It turned out that under certain conditions behaviour was predicted which has never been observed in muscle. When the model is strained stepwise and is then kept at constant length for some time before being finally released, it jumps back to an unstretched length. This length is shorter than the original unstretched length.

Another model, published by Glantz (1974) describes only passive properties. Using the model a computer program was developed in order to fit measured curves to the curves predicted by the model. It turned out that our data could not be fitted.

A model based on thermodynamics is proposed by King and Lawton (1950). It describes the static behaviour of the bladder very accurately, but cannot deal with dynamic properties like stress relaxation because of the fundamental restriction to quasi-static processes. For the same reason Stacy et al (1955), who also applied thermodynamics to describe the behaviour of elastomers used a simple multi-exponential model to describe stress-relaxation.

7. Conclusion and discussion

A number of alternative models has been tested with respect to the conditions mentioned in IID1. None of them turned out to be better than the discrete visco-elastic model which was originally used. When this model is forced with a stepwise straining a stress results which can be described by a number of exponential terms. The fitting of this multi-exponential signal is an awkward problem as mentioned in IIB2. However, this problem arises from the fact that we force the model with step responses, and not from the model itself. We have therefore tried some alternative measurements with another input signal.

E. Alternative measurements

1. Theory

In order to avoid problems which occurred when fitting step responses we would like to test our system with orthogonal input signals. The most natural of these is sinusoidal straining.

In this section we want to check the response of our model to sinusoidal straining and find out how we must apply this in order to be able to determine the model-parameters from the responses. From the mechanical model presented in Fig. 6 and equations (2) and (3) a third order differential equation can be obtained which describes the relationship between stress and strain in the time domain. Instead of inserting a sinusoidal input signal and formally solving the equation it is easier to calculate the response of one spring-dashpot combination at a time and subsequently add up the results. This yields an amplitude and phase characteristic of the type shown in Fig. 21 (Bode diagram). Note that the higher of each pair of "bending points" (points where the amplitude plot changes direction) reflects the frequency $\frac{E_n}{\eta_n}$ which we called the "relaxation constant" in the step response measurements. Notice furthermore that this system displays a high-pass characteristic. This leads to a complication. As will be shown, the system under test is non-linear (IIIA3, IIE2). Very often in this case a method called "describing function" can be used. This implies that the higher order harmonics generated by the non-linearities of the system are neglected, because they are usually weakened by a low pass characteristic of the system. It is clear in this case that this would not do. We tried therefore to measure the time dependent properties of a strip of urinary bladder wall using a very small strain which varied sinusoidally with time (compare IIA1). In order to reduce the influence of the non-linearities we should keep the amplitude of the forcing sinus as small as possible. Furthermore, because of the impossibility of applying a negative strain to a piece of wall (see IIA2) it is necessary to apply a prestrain which is large enough to prevent the sinusoidal strain to become negative. An example of the resulting strain signal is shown in Fig. 22. The prestrain level ϵ_p should equal the strain level applied when

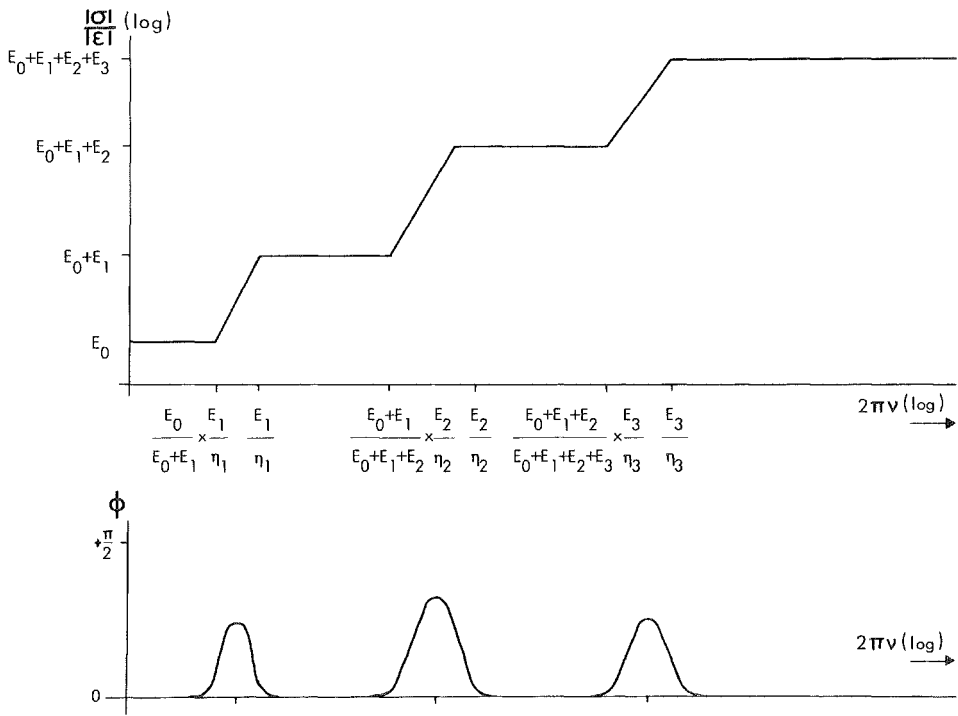


Fig. 21 - Theoretical amplitude and phase characteristic according to the mechanical model

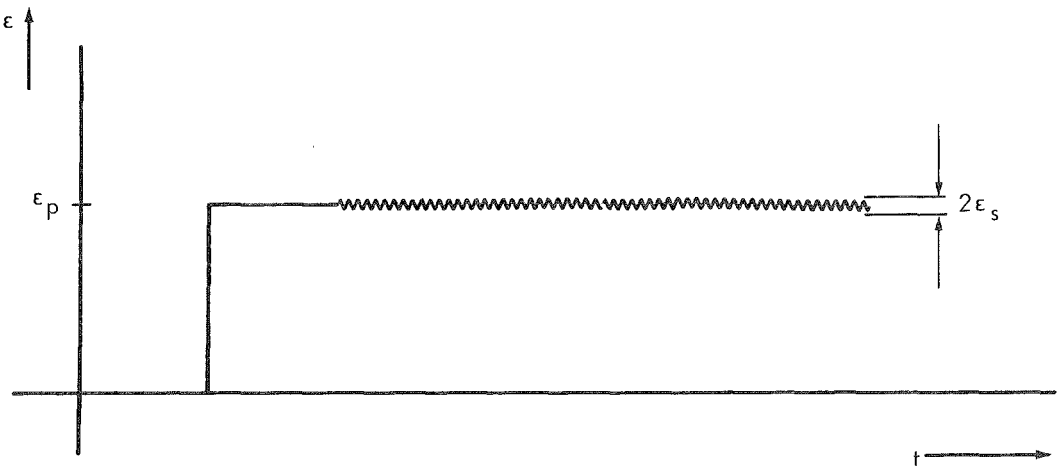


Fig. 22 - Applied strain as a function of time

measuring step responses (0.30, see IIB1).

2. Experimental equipment set-up

Strips of urinary bladder wall from pigs were used in an EGTA solution as described in IIB1. The strips were attached to two clamps with penetrating pins; one was attached to the bottom of the container, while the other was attached to a Grass Force transducer which was moved by an eccentric mechanism via a rigid rod. A frequency range of 0 - 2 Hz could be reached. Discontinuities in the strain signal, caused by the fact that a step motor was used, were reduced adequately by a mechanical reduction.

The amplitude of the strain sine wave was approximately 2 mm, which means a relative strain of about 0.08. The average strain level (ϵ_p) used was 0.30 (see Fig. 22). It was not possible to make the input signal smaller because at low frequencies the output signal would then be so small, that it was impossible to detect. Strain and stress could be recorded on a dual strip-chart recorder or on an X-Y recorder which enabled a better judgment to be made of the stability of the signal. By inserting a steel spring instead of a piece of bladder wall, the hysteresis present in the set-up itself could be tested. This, however, proved to be negligible (Fig. 23). This pattern turned out to be independent of the frequency.

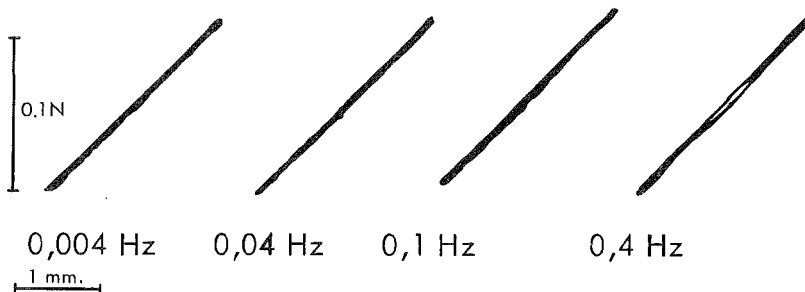


Fig. 23 - Stress-strain plot of a steel spring; strain is plotted horizontally, and stress vertically

3. Results

In Fig. 24 a characteristic measurement is shown. The upper trace represents strain, the lower trace stress. In Fig. 25 stress-strain plots are shown. It is clear,

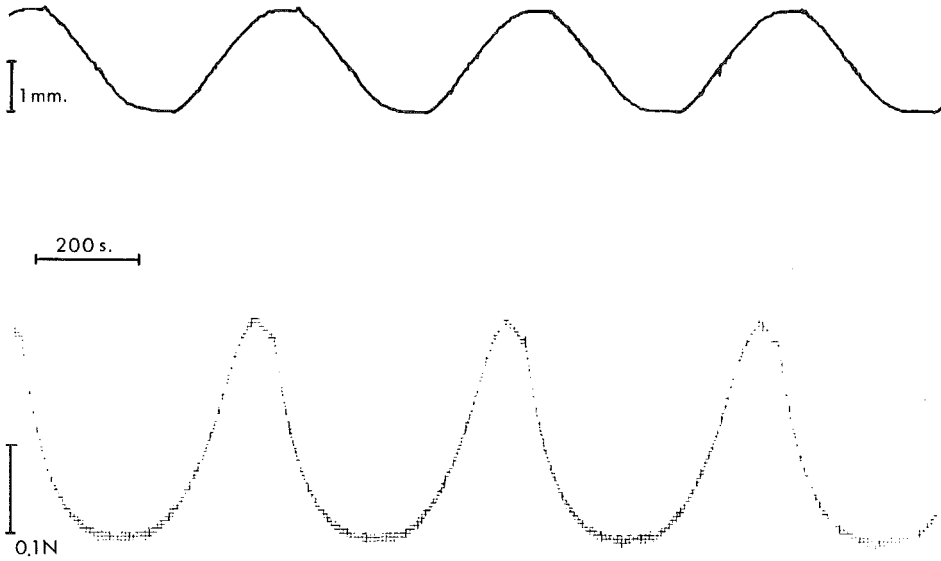


Fig. 24 - Stress and strain recorded during sinusoidal forcing; upper trace represents movement of upper clamp (strain); lower trace represents force on force transducer (stress)

that the input signal is in fact too large because the output obviously deviates from a sine wave. Another mechanism, however, could also be responsible for this deviation (see IIIA1). We decided to try to experiment in spite of the non-linearities in order to test the entire concept. From four bladder strips the amplitude ratio (stress amplitude over strain amplitude) and phase were measured as a function of frequency. The Bode diagram of the best result (strip 3) is represented in Figs. 26 and 27. The amplitude characteristic shows a significant increase with increasing frequency in three of the four measurements. It did not

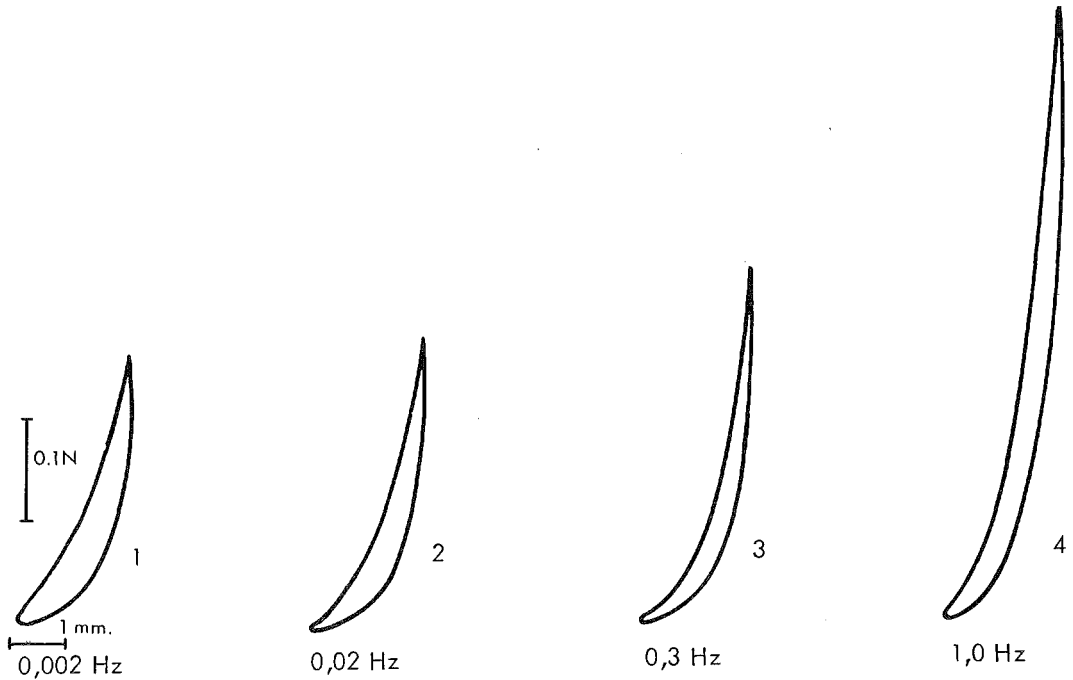


Fig. 25 - Stress-strain plot of a piece of bladder wall; strain is plotted horizontally and stress vertically

turn out to be possible to obtain significant figures concerning the position of the supposed "bending points" in the amplitude characteristic.

However, when Fig. 26 is compared to the average relaxation constants presented in Table VI, slight agreement can be noticed.

A feature that easily could be checked is the total increase ratio of the amplitude, i.e. the amplitude ratio at the highest frequency, over the amplitude ratio at the lowest frequency. These are shown in Table VII. It follows that this total increase ratio equals the inverse of the relative elastic modulus e_0 which yields 5.9 (compare with chapter III). Because measurement 3 has the highest total increase ratio it also shows the most pronounced "bending points" and was therefore presented as being "the best". Another observation is that whether a high or low increase ratio is found depends on the sequence of the measurements (from high to

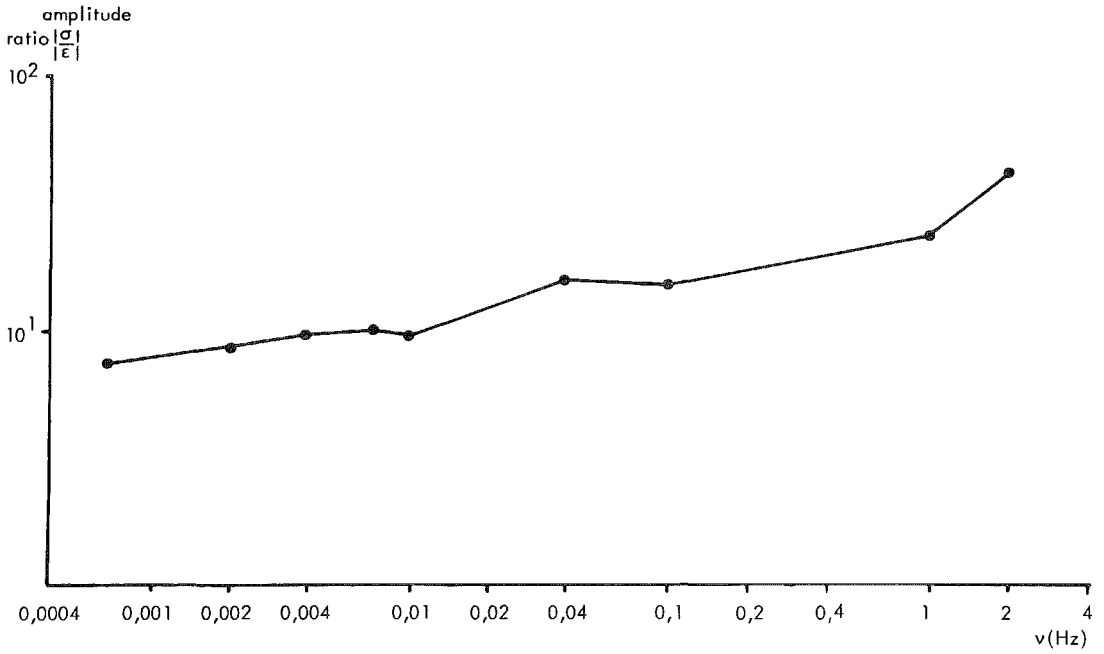


Fig. 26 - Amplitude characteristic of bladder strip 3

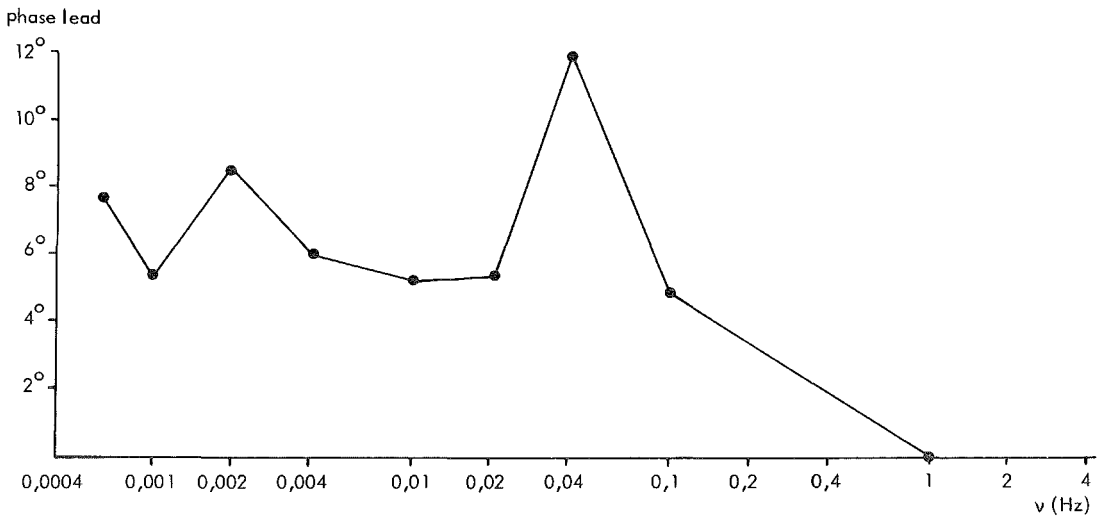


Fig. 27 - Phase characteristic of bladder strip 3

Measurement	Total increase ratio
1	2.0
2	3.0
3	6.0
4	1.2

Table VII - Amplitude ratio at the highest frequency over the amplitude ratio at the lowest frequency

low frequencies or from low to high) because the stress response to sinusoidal straining with constant amplitude and frequency decreases as a function of time. This behaviour, which is not predicted by the model, led among others to the extension of the model presented in chapter III.

We performed the measurements in an alternating sequence, that is, we started with the highest frequency, then measured the lowest, then the highest minus one etc. By repeating the highest frequency measurement later on, an entirely different result was occasionally obtained. A significant result concerns the phase characteristic. We found that stress always led strain, as the model predicted, which we call a positive phase shift. Apter and Graessley (1969) called this a negative phase angle and sometimes observed a positive phase angle at low frequencies, when measuring on smooth muscle. It should be noted that they explained this by means of the activity of the muscle while in our experiments activity was suppressed. Again only slight agreement can be noticed between peaks in the phase characteristic and the relaxation constants in Table VI.

4. Conclusion and discussion

It turned out that the results obtained with small sinusoidal signals were not very reliable, which may partly be due to the simple approach.

On the other hand, these results demonstrate some fundamental difficulties, which are characteristic of this type of measurement. One of these is the fact that

the large frequency range that has to be examined (for comparison to step response results at least 0.001 - 10 Hz) combined with the necessity of observing at least a few periods of the low frequency components in order to obtain significant results, causes a very long measuring time. During this time the properties of bladder wall strips may change, especially the elastic moduli (Coolsaet et al, 1975b). As all measurements made on one strip during an experiment should be combined in order to obtain a full insight into the time dependent behaviour, there is no way to observe the changes in this behaviour during the experiment. Furthermore, although the time dependent behaviour in isolation (as characterized by relaxation constants, compare IIC2) can be shown to be reproducible, even if measurements are taken at long intervals, the elastic moduli are not, but decrease during the day the measurements are made. In terms of the Bode plots this means that the "bending points" are reproducible, but the slope of the amplitude characteristic is influenced by the sequence in which the frequencies are scanned. The crucial point of course, is whether the "bending points" are recognizable in the Bode plots, but this turns out not to be the case even in the best measurement that was taken. As this best measurement shows a slope as definitive as could be expected according to the step response measurements we conclude that no improvement can be expected from a better set-up. Sinusoidal measurements do not offer a good possibility of measuring the time dependency of the stress-strain relationship of the urinary bladder wall. From the results obtained it can be stated that the sinusoidal measurements at least confirm the observation that the system under investigation acts as a high-pass filter. It is also from this point of view advisable to use stepwise straining as the input function as a step contains a great deal of high frequency energy.

III. Length dependent behaviour of the bladder wall

A. Theory

1. Conclusions from time dependent behaviour

The step response measurements on bladder wall strips, as described in chapter II, yield relaxation constants and elastic moduli. As stated in IIC4 we assume that the relaxation constants do not depend on the amplitude of the stepwise straining. The elastic moduli do however depend on the amplitude of the stepwise straining. This strain or length dependency in combination with the geometry blocks described in chapter IV determines the length-or the volume-amplitude dependency of the pressure-volume relationship of the urinary bladder. In this chapter therefore investigations are described on the dependency of the elastic moduli on the amplitude of the strain:

$$E_n = E_n(|\epsilon|) \quad (37)$$

where $|\epsilon|$ is the amplitude of the applied strain

Initially we tried to determine these functions simply by performing a number of step response measurements on strips with increasing strain. It turned out, however, that the functions measured in this way were not reproducible. Sometimes the elastic moduli increased with the strain, sometimes they decreased, and occasionally a combination of increase and decrease was seen (Coolsaet et al, 1975b). An interesting feature was that the trends in the four elastic moduli (three from the three exponentials and one from the constant) were generally alike. Next the series of measurements at constant strain level, described in IIC2, were performed. It turned out that the elastic moduli were not constant in spite of the fact that the applied strain amplitude was constant. A generally decreasing trend as a function of time was observed. Again the trends in the four elastic moduli were alike. We concluded that two mechanisms were active in the previous measurements, viz the strain dependency (37) which probably tends to increase the elastic modulus at increasing strain, and the fact that the elastic moduli decrease as a function of time. The result is obviously that all possible combinations of

increasing and decreasing trends can be seen.

Concerning the cause of the decrease of the elastic moduli we note the following.

It was observed that during the "rest period" between the strains (see IIB1) the strip tended to hang more and more limply as the experiment continued. Related to this phenomenon is the problem of the initial length l_0 . This length has to be determined in order to be able to calculate the length l to which a strip has to be stretched to realize a strain according to relationship (1). Furthermore the l_0 length has to be determined when the strip is already attached to the clamps because we are interested in the length of strip which is actually strained and not in that part which serves as a grip for the clamps. It appeared that when we slowly increased the initial length by adjusting the appropriate microscrew on the pneumatic strain device no sharp edge on the force as a function of time curve can be observed at the point where the strip is fully tautened. Furthermore, as the strip is rather thick (3 - 5 mm) it is difficult to see whether the strip is fully tautened.

Finally, the strip already begins to show relaxation phenomena when it is definitely not fully tautened. This must mean that parts of the strip start being strained (and thus relax) while other parts are not yet tautened. The problem is generally referred to as being very awkward and elaborate solutions have been proposed (Åberg and Axelsson, 1965). Various methods were attempted in order to obtain a reliable estimation of the length l_0 . Experiments were done in which the length l_0 was adjusted before every measurement in an attempt to obtain reproducible elastic moduli. It turned out, however, that no method was entirely successful. We finally decided to determine the initial length l_0 by allowing the strip to stretch for about one second under the weight of the lower clamp, which is about 13 g, and then keeping it constant during the experiment. This method is still unreliable, and the errors involved are in the order of magnitude of 20%.

Concerning our problem of the observed decrease of the elastic moduli we note that this may be caused by the strip hanging limp, which is in fact an increase of the length l_0 . This increase then causes an effective strain which is lower than the calculated strain, and as a consequence causes an under-estimation of the

elastic moduli.

Our mechanical model, as presented in Fig. 6, does not feature a variable rest length. In order to include this in the model we added an extra dashpot in serie with the model, which is assumed to have a very high viscosity modulus, so that it does not give a significant contribution to the stress-relaxation measurement. The problem now is, that the length l_0 of the model thus modified can only increase. In fact an increasing l_0 is what we observed in most strips, however obviously with an in vivo bladder it is not probable that the rest length always increases. To enable us to reset the extra dashpot we therefore add an active element to our model. As in our measurements active properties were suppressed (by EGTA) the active element is assumed here to have no influence. In Fig. 28

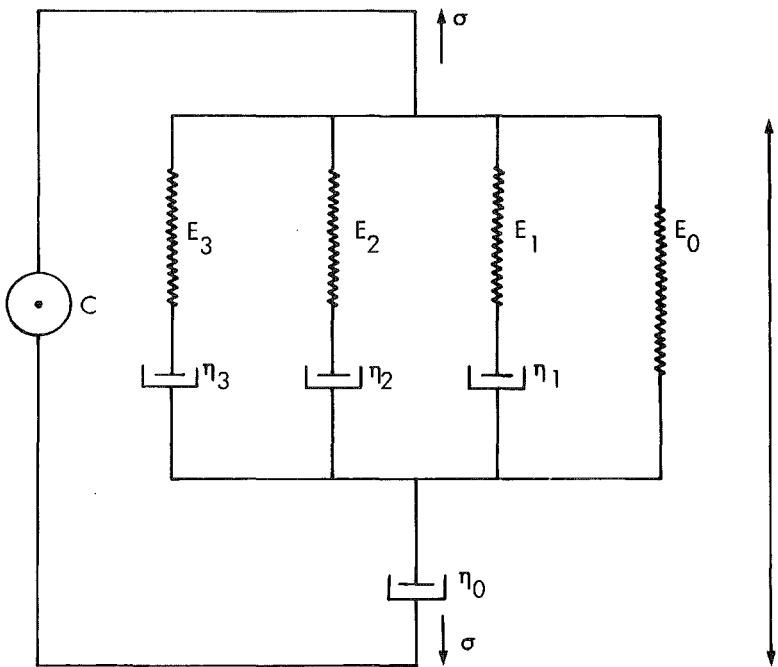


Fig. 28 - Modified mechanical model with initial length dashpot and active element

the modified model is shown. If measurements are performed at increasing strain the elastic moduli increase or decrease depending on which mechanism "wins", that is the η_0 dashpot or the strain dependency. In the case of decreasing elastic moduli (in model-terms: caused by η_0) the trends should be similar for all moduli. In the case of the increasing moduli the trends might be different, because every elastic modulus might have its own strain dependency. However, we observed that in this case also the trends were similar. Therefore our basic assumption in this chapter is that the trends in all elastic moduli are the same, which means that the elastic moduli relative to their sum should be constant.

We define:

$$E_n(|\epsilon|) = E(|\epsilon|) \cdot e_n \quad (38)$$

where

$$E(|\epsilon|) = \sum_{n=0}^k E_n(|\epsilon|) \quad (39)$$

and

$$e_n = \frac{E_n(|\epsilon|)}{E(|\epsilon|)} \quad (40)$$

We will call e_n the relative elastic moduli and $E(|\epsilon|)$ the elastic modulus function. In terms of the diagram, represented in Fig. 3, this means that the "wall" block is split up into a time dependence block, and a length dependence block (elastic modulus function). The outputs of these blocks are multiplied to yield the stress signal (see Fig. 29). Since our basic assumption is that the relative elastic moduli are independent of strain, they should also be insensitive to errors in l_0 and they can be calculated from the step response measurements. Table VIII contains averages and standard deviations of the relative elastic moduli for the series of measurements denoted as "pigs; EGTA; increasing strain" in Table VI. Strain varied between 0.2 and 1.6. Notice that the relative standard deviations in the relative elastic moduli are smaller than those in the relaxation constants displayed in Table VI. This means that the relative elastic moduli in fact are more reproducible parameters. Concerning the elastic modulus function, this function cannot be calculated from the step response measurements, since here errors in l_0

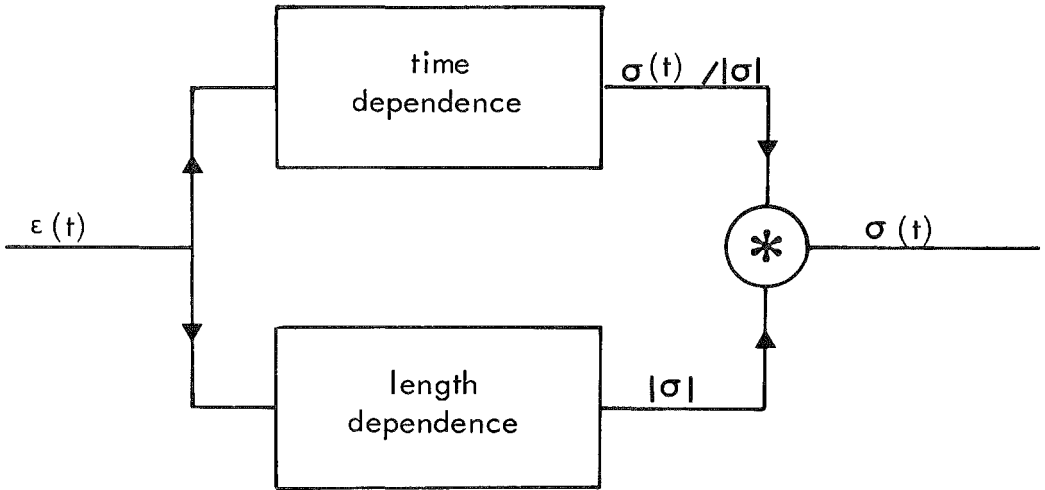


Fig. 29 - Detailed system flow chart for the "wall" block

Relative elastic modulus	Value	Relative standard deviation	Number of measurements
e_0	0.17	32%	98
e_1	0.50	19%	98
e_2	0.20	15%	98
e_3	0.14	22%	98

Table VIII - Relative elastic moduli and standard deviations

affect the results. Another measurement method will be discussed in IIIA2.

2. Introduction to pulse measurements

The problem in determining the elastic modulus function from step responses consists of the increase of the length l_0 caused by the force working on the initial length dashpot η_0 see Fig. 28. The increase in l_0 is considerable since the strips are strained for a very long time (fifteen minutes per measurement).

Analogously to the method followed in chapter II, where we measured the time

dependence of the bladder wall at constant length, we should here determine the length dependence at constant time. Strictly speaking this is not possible, but we can approach this ideal situation by keeping the straining periods as short as possible. Remember that here we only want to determine the elastic modulus function, which is the sum of all elastic moduli, and not the moduli separately. In order to determine this sum we only need to know the original height of the step responses. We therefore can restrict our straining time to the time necessary to register the initial height. As the straining lasts only a short time, we expect that the influence of the η_0 dashpot will be small. As our input signal is no longer a step but a pulse, we refer to these measurements as pulse measurements. Due to the necessary fast input signals we are obliged to perform these experiments on bladder wall strips. The same advantages for strip measurements as mentioned in IIA1 also apply here.

3. Non-linearities

By stating that the elastic moduli depend on the strain amplitude (relation (37)) the first non-linearity in our system is introduced. From Fig. 1 it is clear that the static behaviour of the total urinary bladder is non-linear, and in chapter IV we will show that the first geometry block is also non-linear. It is therefore that some remarks concerning non-linearities have to be made here.

An important feature in this context is the fact that we found the relaxation constants to be independent of strain. From relations (4) and (5) we see that this implies that the viscosity moduli must show exactly the same strain dependence as the elastic moduli. Notice that the moduli depend on the total strain, related to the total length of the model, presented in Fig. 6, which is a combination in series of a spring and a dashpot. This means that we could write:

$$\sigma = E(|\epsilon|) \cdot \epsilon_1 \quad (41)$$

where ϵ_1 represents the strain working on the spring, and is not equal to ϵ , which is the strain working on the series combination.

In a mechanical model it would seem almost impossible to construct a non-linear

spring with a non-linearity which is not connected to the length of the spring alone, but connected to the length of the spring and a series element. Of course in the bladder wall no discrete elastic and viscous elements are present and our mechanical model is only a simplified representation by way of discrete elements. Nauta Lemke et al (1972) list a number of characteristics of non-linearities. According to their classification the elastic modulus function shows a static, univalent, hard non-linearity. Although the urinary bladder wall is obviously a dynamic system, the non-linearity is called static because the elastic modulus function does not depend on time. It is univalent because at one strain level we only find one value for the elastic modulus function, and hard because - as we will see in IIIC - the first derivative of the elastic modulus function increases with strain. Other classification criteria with regard to the explicit or implicit nature of the non-linearity and its symmetry or asymmetry are not applicable in our case because negative strain cannot be applied. An interesting question is whether the non-linearity might be of the type "saturation". Although this generally causes a sharp edge in the characteristic which is not seen in our case (compare IIIC) we might argue that the increase of the elastic modulus function at high strain is obviously due to the fact that the material cannot be strained any further and that it indeed must be saturation. In fact what our non-linearity is called is quite arbitrary as long as we know the consequences of its characteristics. We conclude that as long as one strain amplitude is applied to the urinary bladder wall, which is the case when stepwise strainings are applied, the material behaves linearly, because the strain dependence appears in the numerator as well as in the denominator of the relaxation constants. The amplitude of the response, however, depends in a non-linear way on the strain amplitude. The consequence concerning our mechanical model is that the elements must have rather artificial properties.

B. Methods

A system flow chart of the set-up is presented in Fig. 30.

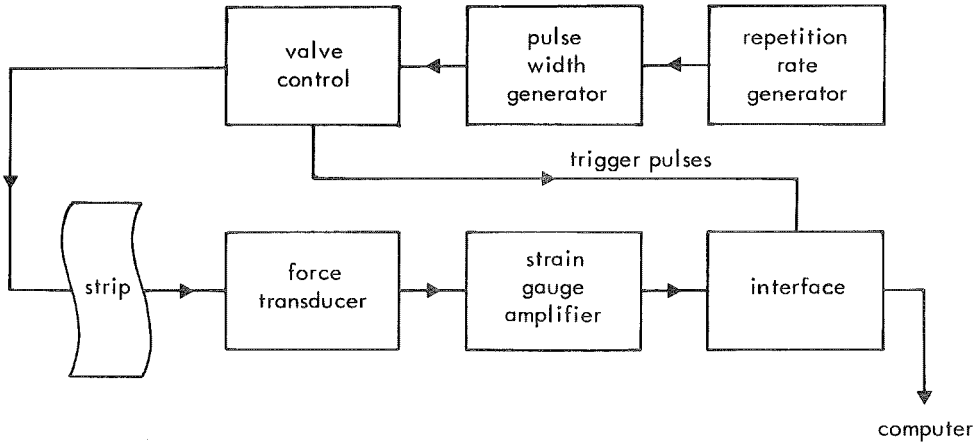


Fig. 30 - System flow chart of set-up of experimental equipment for pulse measurements

The same pneumatic strain device was used as described in IIB1. A series of pulses is generated by two generators controlling the repetition rate and the pulse duration respectively. Unless otherwise specified the repetition rate was 0.016 Hz (or one pulse every 62.5 s) and the pulse duration was 625 ms. The valve control unit was altered in such a way that it could follow a logical (0 - 1) input signal, which means that the straining of the strip followed the same time schedule as the electrical input pulses (see Fig. 31). A fixed delay time after the start of the straining (540 ms) four trigger pulses with intervals of 38 ms were sent to the interface. At each trigger pulse a sample was read. The four samples were read into the computer which calculated the average value and the standard deviation. The average was chosen as a measure of the response to a certain strain level and will be called from now on the average peak force. The amplification in the total set-up is identical to the value described in IIB1. In most cases the strain gauge amplifier was set to an amplification factor of 3.33. For other settings adequate corrections were used. Strips from the posterior (back) wall of pig bladders were

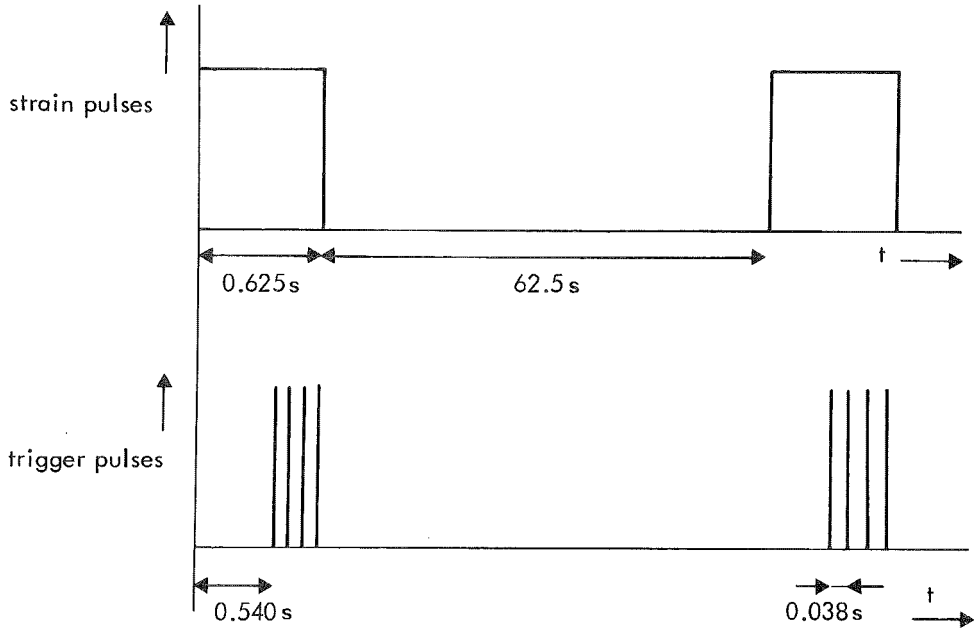


Fig. 31 - Relationship between strain and trigger pulses

used. The solution used was the one with the EGTA added. Initial length and tissue volume were determined as described in IIB1. Remarks should be made with regard to the "time-dimensioning" of the set-up. The interval between the samples read by the interface was the maximum sample rate of the interface. We used four samples in order to obtain a reliable impression of the standard deviation. The value of the delay time between the "start of straining" and the first trigger pulse was determined by inserting a steel spring at the place of the strip, and by increasing the delay time from zero to the lowest value for which no transients in the four samples could be observed. When the spring was stretched maximally (50 mm, see IIB1), the relative standard deviation in the samples was about 0.2%. The large delay time that was necessary in comparison to the high speed of the pneumatic cylinder (see IIC3) gave rise to the conclusion that the observed transients must be caused by vibrations in the set-up. The strain pulse duration was made as short as possible by increasing it until no more transients in

the fourth sample could be seen when using the steel spring dummy. With regard to the pulse repetition rate, an interval of about one minute was used in order to be able to adjust the microscrews between two measurements. The results of measurements with longer intervals between the pulses will be discussed in IIIC.

C. Results

The reproducibility of our method was tested by applying a series of strain pulses with amplitude 0.30. It turned out that the relative standard deviation of the four samples was small (usually less than 2%). This standard deviation actually reflects the visco-elastic relaxation during the pulse straining. The relative standard deviation in the average peak force of the responses to different pulses, however, yielded up to 56% for 30 measurements on one strip.

Increasing the intervals between pulses to five minutes did not result in a smaller standard deviation.

Since succeeding measurements tended to yield lower responses, we concluded that the influence of the η_0 dashpot was still too large. We therefore tried to find a method which allowed corrections depending upon the lengthening of the η_0 dashpot. Pulses at two different strain levels were alternated. Though the reproducibility of the average peak forces of the responses to pulses of equal strain level was still bad, it turned out that the absolute differences between these peak forces for two strain levels were very reproducible as long as the two strain levels were not too far apart. In Table IX the results of these reproducibility tests are shown. For instance, for the strain levels 0.3 - 0.6, measurements were taken from 10 strips, with at each strain level 15 alternated pulses. The fact that the difference between the average peak forces is very reproducible corresponds to our

Strain levels	Average relative standard deviation of difference between peak forces	Number of pulses per measurement	Number of measurements
0.3 - 0.6	10%	15 + 15	10
0.6 - 0.9	14%	15 + 15	4
0.9 - 1.2	13%	15 + 15	4

Table IX - Reproducibility of the difference between average peak forces of pulse responses at two different strain levels

conclusion concerning the influence of the η_0 dashpot. The restriction to strain levels which are "not too far apart", means in practice that the difference between the strains must not be larger than 0.4. This can be understood from the observation that the very large extension of the η_0 dashpot at very large strains would cause no effective strain at all at the smaller of the two pulses.

Using this information a measurement series of increasing strain pulses with added correction pulses was designed. The series was measured as follows:

0.1 - 0.2 - 0.1 - 0.3 - 0.1 - 0.4
0.3 - 0.5 - 0.3 - 0.6 - 0.3 - 0.7
0.6 - 0.8 - 0.6 - 0.9 - 0.6 - 1.0
0.9 - 1.1 - 0.9 - 1.2 - 0.9 - 1.3
1.2 - 1.4 - 1.2 - 1.5 - 1.2 - 1.6 (see Fig. 32)

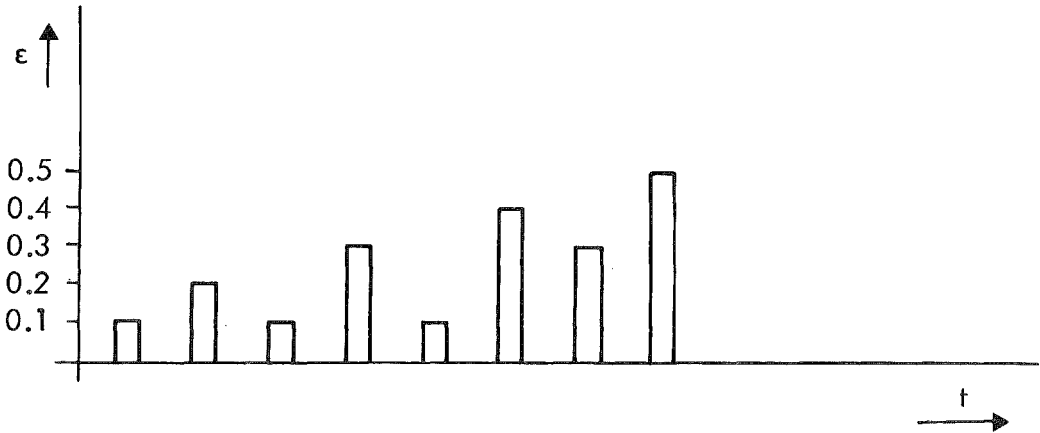


Fig. 32 - Strain pulses arranged so that correction is possible

Here the 0.1; 0.3; 0.6; 0.9 and 1.2 strain level pulses serve as correction pulses.

The correction is performed by computing the difference between the response to a strain pulse and the preceding correction strain pulse, and adding to this difference the "true" value of the response to the correction strain pulse.

Corrections using lower correction strain pulses are included in this "true value" so that in fact the whole series is corrected to the level of the first 0.1 strain measurement. A plot of these corrected values versus strain is seen in Fig. 33. The

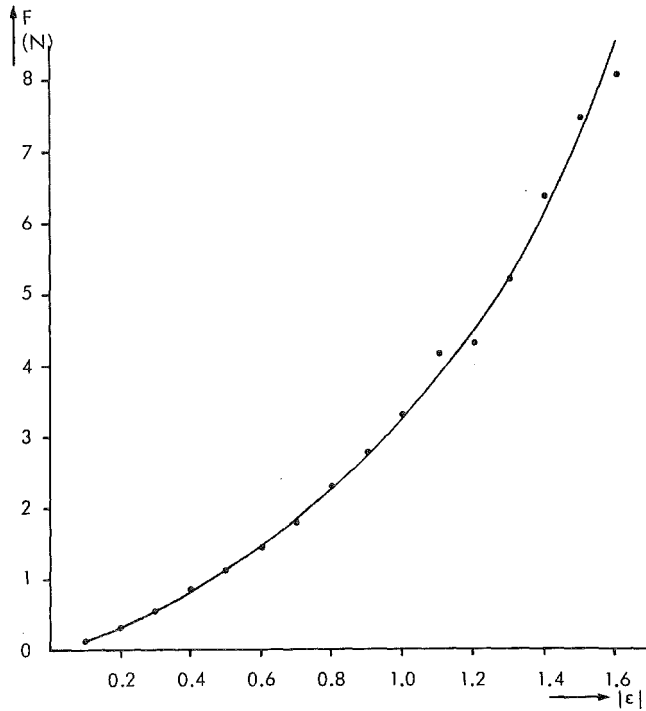


Fig. 33 - Corrected average peak force as a function of strain

values are multiplied by the amplification factor mentioned in IIB1.

Using a small computer program containing an implementation of formula (11) the elastic modulus function as a function of strain was computed. In Fig. 34 the dots represent the values thus calculated. The plotted curve has resemblance to the ones measured by Fung (1968). As in the literature it is commonly assumed that the elastic modulus or moduli from smooth muscle depend exponentially on strain (see for instance Glantz, 1974), a mono-exponential function was fitted to the data by performing a semi-logarithmic transformation and calculating a regression line. The result can be seen in Fig. 34 (line). In mathematical terms, we thus describe the elastic modulus function as follows:

$$E(|\epsilon|) = |E| e^{\beta |\epsilon|} \quad (42)$$

We shall call $|E|$ the elastic coefficient, and β the elastic exponent.

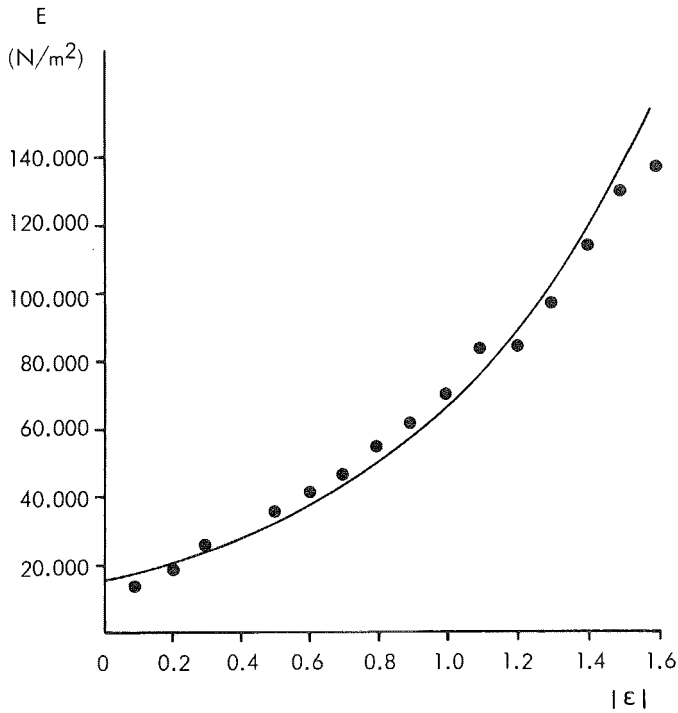


Fig. 34 - Measured elastic modulus function (dots) and fitted mono-exponential function (line)

Ten measurements were performed on strips of bladder wall from seven different bladders. The parameters determined are shown in Table X.

Parameter	Average value	Relative standard deviation	Number of measurements
β	1.28	19%	10
$ \epsilon $	16 084 N/m ²	43%	10

Table X - Average and standard deviation for the parameters defining the elastic modulus function

The average standard deviation of the data about the regression line yielded 5740 N/m^2 , whereas the standard deviation of the data plotted in Fig. 34 yielded 6816 N/m^2 so that we may call the fit in Fig. 34 representative for the average fit.

D. Conclusion and discussion

We conclude that the length dependent properties of the urinary bladder wall can be adequately described by adding an η_0 dashpot which reflects changes in initial length of the tissue to the mechanical model. The four elastic moduli of the model show a mono-exponential trend as a function of the strain, which is identical for all moduli. The average exponent and coefficient of this exponential trend are shown in Table X for pig bladder wall. The three dashpots η_1 , η_2 and η_3 show exactly the same strain dependence as the elastic moduli, so that the relaxation constants are independent of strain.

The reproducibility of the exponent in the exponential model which is called elastic exponent is good (relative standard deviation 19%), whereas the reproducibility of the coefficient called the elastic coefficient is less good (relative standard deviation 43%).

In drawing these conclusions the following assumptions have been made:

1. The tissue volume is independent of strain.
2. The length dependent properties are independent of the place and the direction in which the strip is cut (homogeneity and isotropy).
3. The elastic moduli relative to their sum are independent of strain.

Assumption 1. has already been discussed elsewhere, and assumption 2. has not been verified. In fact in chapter II we assumed the same about the time dependent properties so that in combination with this assumption we assume that all passive properties of the urinary bladder wall are homogeneous and isotropic. Concerning assumption 3., this is supported by the fact that the relative elastic moduli are quite reproducible (Table VIII).

Finally it should be noted that the mechanical model now has rather artificial properties, so that it would be very difficult to construct from mechanical parts. However, as long as the model serves as an aid to thought enabling us to talk about the urinary bladder wall in an easy way, it may be quite useful.

IV. Geometry of the urinary bladder

A. Theory

In this chapter we will develop descriptions of the two geometry blocks in Fig. 3.

Our basic assumption will be that the urinary bladder is a thick walled sphere (Osborne and Sutherland, 1909, and Matsumoto and La Grange, 1973).

In that case, the first geometry block, which relates strain to volume, can be described as follows:

$$\varepsilon = \frac{l - l_0}{l_0} = \frac{l}{l_0} - 1 = \left(\frac{V}{V_0} \right)^{1/3} - 1 \quad (43)$$

Two things should be noted, first the fact that the tissue volume is not used in this equation, which means that the line from V_t to the first block can be deleted in Fig. 3, and second the fact that (43) is a non-linear relationship. This means among others that a sinusoidal volume signal does not generate a sinusoidal strain, so that it is highly unlikely that the bladder will yield a sinusoidal pressure from a sinusoidal volume signal. However, this non-linearity has no influence on the measurements with stepwise input signals since here only one volume level is steadily applied.

The second geometry block, relating pressure to stress, causes much more trouble. From Lamé (1852) page 212, we obtain the following relationship for a thick walled sphere:

$$\sigma(r) = \frac{p_0 r_0^3 - p_1 r_1^3}{r_1^3 - r_0^3} + \frac{r_0^3 r_1^3}{2r^3} \frac{(p_0 - p_1)}{r_1^3 - r_0^3} \quad (44)$$

where

$\sigma(r)$ is tangential stress in the wall at radius r

p_0 is pressure in the sphere

p_1 is pressure outside the sphere

r_0 is inner radius

r_1 is outer radius

Regrouping the terms of (44) gives the relationship presented by Love (1927) page 142, with the exception of the symbols 0 and 1 for outer and inner which are reversed:

$$\sigma(r) = \frac{p_0 r_0^3}{2r^3} \frac{r_1^3 + 2r^3}{r_1^3 - r_0^3} - \frac{p_1 r_1^3}{2r^3} \frac{r_0^3 + 2r^3}{r_1^3 - r_0^3} \quad (45)$$

A similar formula can be found in Vocke (1969).

Inserting:

$$V_t = \frac{4}{3}\pi (r_1^3 - r_0^3) \text{ so that } (r_1^3 - r_0^3) = \frac{3V_t}{4\pi} \quad (46)$$

and:

$$V = \frac{4}{3}\pi r_0^3 \text{ so that } r_0^3 = \frac{3V}{4\pi} \quad (47)$$

in formula (45) yields:

$$\sigma(r_0) = \frac{3p_0}{2V_t} (V + \frac{V_t}{3}) - \frac{3p_1}{2V_t} (V + V_t) \quad (48)$$

for $r = r_0$ and:

$$\sigma(r_1) = \frac{3p_0}{2V_t} (V) - \frac{3p_1}{2V_t} (V + \frac{2}{3} V_t) \quad (49)$$

for $r = r_1$.

To get only one expression for the stress in the wall as a function of pressure and volume, we take the average of equations (48) and (49):

$$\sigma(\bar{r}) = \frac{3p_0}{2V_t} (V + \frac{1}{6} V_t) - \frac{3p_1}{2V_t} (V + \frac{5}{6} V_t) \quad (50)$$

where \bar{r} means mean radius

The relative difference between (48) and (49) has a magnitude of $\frac{1}{3} V_t$ relative to V . Assuming that $V_t < 0.1 \times V$ this will be less than 4%, which means that taking

the average of (48) and (49) introduces an error of about 2%.

Equation (50) can be approximated by:

$$\sigma(\bar{r}) = \frac{3}{2V_t} (p_0 - p_1) \left(V + \frac{1}{6} V_t \right) \quad (51)$$

The error introduced by neglecting $\frac{4}{6} V_t$ with respect to V will be about 7% again assuming that $V_t < 0.1 \times V$. The deleting of $\frac{V_t}{6}$ in equation (51) simplifies the equation. Furthermore $p_0 - p_1$, which is the pressure difference across the wall, is the pressure p in the bladder with respect to barometric pressure, and we refer to the average stress $\sigma(\bar{r})$ as the stress σ in the wall. We then obtain:

$$\sigma = \frac{3pV}{2V_t} \quad (52)$$

This relationship can also be obtained by calculating a simple balance of force over two half spheres (Matsumoto and La Grange, 1973, and Coolsaet et al, 1975a). Hinman and Miller (1964) use the relation $S = pV$ where S means stress. The method used here is preferred because it clearly shows the assumptions and errors involved. When $V_t < 0.1 \times V$, which in normal practice is a rather realistic assumption, the total error which is introduced by replacing equations (48) and (49) by equation (52) is about 10%. The simpler method, however, can be used in order to get an impression of the importance of the assumption that the urinary bladder is spherical. This can be very easily done by applying the method to a cube, which yields the same relation as equation (52), or to a rectangular parallelepiped with 2 sides of length l_a and one of length l_b , which yields:

$$\begin{aligned} \sigma_a &= \frac{pV}{2V_t} \left(2 + \frac{2l_b}{l_a + l_b} \right) \\ \sigma_b &= \frac{pV}{2V_t} \left(2 + \frac{l_a}{l_b} \right) \end{aligned} \quad (53)$$

where σ_a is stress parallel to side with length l_a
 σ_b is stress parallel to side with length l_b

It is remarkable, that the essential form of equation (53) equals that of equation

(52), and that the only difference between (52) and (53) is the constant factor.

The same results are even found on a regular pyramid. As during our step response measurements only one strain level is applied for each measurement, we can expect that when the bladder deviates from a sphere, small quantitative errors in computed data are introduced. The qualitative shape of the measured curves, however, is not affected.

B. Methods

In IVA we developed models for the two geometry blocks in Fig. 3.

In this section we will describe a method of testing the validity of these models. Since both relations (43) - for the first geometry block - and (52) - for the second geometry block - are independent of time we do not have to involve time in our test. What we should investigate is the length dependency of our geometry blocks. This can be done by measuring the pressure-volume relationship of a bladder, calculating the stress-strain relationship of the "wall" block from the results, and then measuring this stress-strain relationship directly on a strip of bladder wall. In order to delete the time dependency from the properties of the bladder, we should take quasi-static measurements. These, however, are very time consuming. Furthermore we then have to deal with the problem of the initial length of the tissue and the bad reproducibility of measurements on the length dependency (see chapter III). The measurements therefore were performed on a rubber balloon which showed negligible viscosity. Here the initial length could be observed as a sharp edge in the pressure-volume or stress-strain relationship. The balloon was connected to the catheter and to the apparatus as described in VB. In order to avoid the influence of gravity the balloon was submerged in water. It was filled by increments of fluid, and pressure readings were taken after waiting about one minute. From the volume and pressure values we then calculated the stress and strain for every measurement and from them the elastic modulus, using the relationship:

$$\sigma = 2\varepsilon E \quad (54)$$

The reason for the factor 2 here is the fact that we strain the material in all directions and not only in one as is the case with strips. It can easily be shown (see Frank, 1906, or Brody and Quigley, 1948) that this yields a multiplicative factor of $\frac{1}{1-\mu}$, where μ equals Poisson's ratio which we assume to be 0.5 (V_t is constant). The elastic modulus is also obtained from measurements on a strip from the wall of the balloon. The equipment described in IIB1 is used, except that the strip is strained by simply adjusting the "initial length" microscrew. In both cases

(total balloon and strip) measurements were first taken by an incremental increase in strain and then by a similar decrease, and the average of these two measurements was used.

Since the density of the rubber may be assumed to be constant, we could confine ourselves to determining the weight of the material instead of the tissue volume (which was easier to do) and then multiplying this value by the density.

C. Results

Measurements were taken from three balloons. Typical results are shown in Fig. 35, Fig. 36 and Fig. 37.

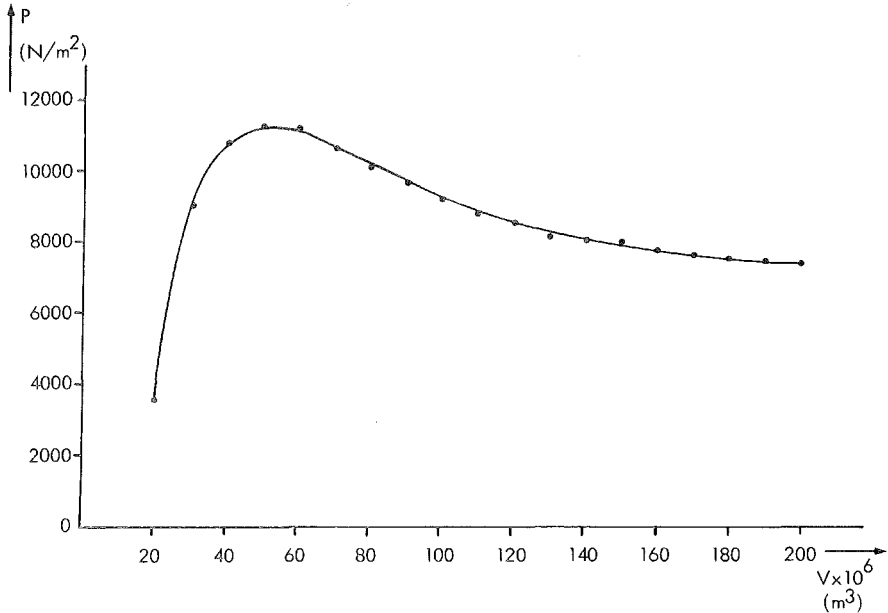


Fig. 35 - Pressure as a function of volume for a rubber balloon

Figure 35 displays pressure as a function of volume for the total balloon, while Fig. 36 displays force as a function of length for a strip from this balloon. In Fig. 37 we plotted the elastic modulus as a function of strain, computed from the total balloon measurement and from the strip measurement. In Table XI the average elastic modulus is tabulated for all measurements. Some remarks should be made. First of all, concerning the difference between the elastic moduli at low strains the following explanation can be given: As the wall of the balloon is curved, the strip cut from it will also be curved. The curvature in the direction in which we strain the strip did not cause the trouble, but the curvature perpendicular to the strain direction causes the sides of the strip to be strained first, while only at higher strains is the middle of the strip strained. The result is an apparently lower elastic modulus at low strain. For the observation that at high

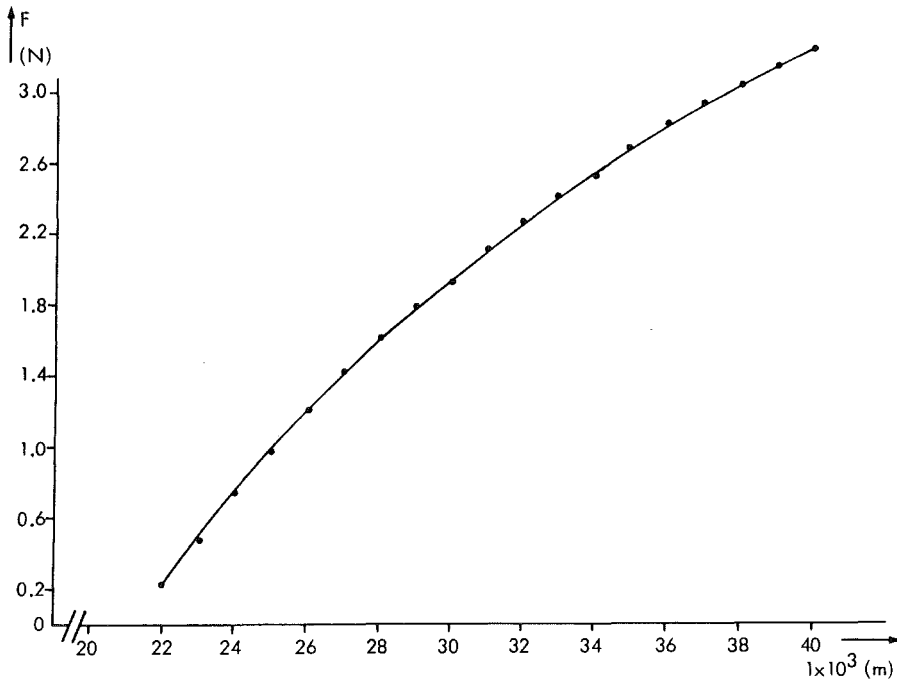


Fig. 36 - Force as a function of length for a strip of rubber

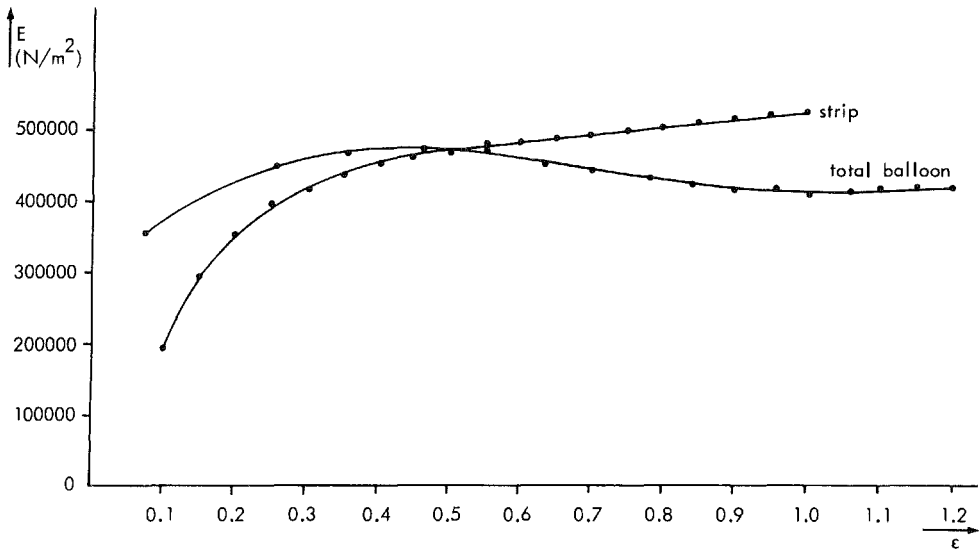


Fig. 37 - Elastic modulus as a function of strain, determined from measurements on a rubber balloon and a strip of rubber

Measurement number	Result from measurement on total balloon			Result from measurement on strip			Difference between average elastic moduli
	elastic modulus (N/m ²)	relative standard deviation	number of measured points	elastic modulus (N/m ²)	relative standard deviation	number of measured points	
1	517 662	3%	7	520 284	10%	22	1%
2	427 375	6%	20	434 841	22%	20	2%
3	507 359	5%	19	455 733	23%	20	11%

Table XI - Average elastic moduli, relative standard deviation and difference for measurements on rubber balloons and strips of rubber

strains the elastic modulus measured on strips is higher than the one measured on a total balloon, another explanation may hold: In this case the strip of wall constricts. The consequence of this is, that now there is also a strain component perpendicular to the original strain, which causes an apparently higher elastic modulus. In Table XI we see that the standard deviation in the elastic moduli is significantly larger for the measurements on strips in comparison to the measurements on the total balloon, which means that here the measured curve has a greater deviation from the average.

D. Conclusion and discussion

From the tests performed on rubber balloons we can conclude that: if the geometry under investigation is spherical and if the volume of the wall material is constant, then the model is reasonably accurate. References supporting these two assumptions are given in IVA and IIA3. The test shows furthermore that the numerical values for amplification factors etc. of the experimental equipment are correct, and the factor two used in equation (54) is also applicable. The measurements presented provide us with new material which forces us to reexamine our reasoning in IIA1 concerning the advantages of measurements on strips. From our results in IVC we see that in the case of experiments on strips, more artefacts are observed than in experiments on whole balloons. This means that although the geometry of strips is easier to describe, in practice however measurements on strips are also afflicted with problems. Kunov et al (1975) even prefer to measure flat objects in a spherical geometry. In our case, however, enough reasons remain to prefer measurements on strips, as for instance the fact that fast straining is much easier than fast filling. Another point of discussion is the shape of the pressure-volume relationship in Fig. 35. At first sight it is amazing that pressure decreases when volume increases. The effect is displayed by all rubber balloons (Frank, 1910, and Frank, 1928). This decrease cannot be explained by a decrease in elastic modulus. There may be two reasons. In the first place, when the balloon is inflated and the volume of the wall remains constant, the wall becomes thinner. In the case of the limit, when volume approaches infinity, the wall is infinitely thin and therefore no pressure difference across the wall can exist. In the second place, when the sphere is inflated, the curvature of the wall decreases which means that the resultant, inwardly directed force (which yields pressure) is a decreasing fraction of the increasing stress. The result is a decreasing pressure (Winton and Bayliss, 1968).

Concerning the urinary bladder the following should now be noted. We see that a sphere with constant elastic modulus yields a decreasing pressure at increasing volume (after a certain maximum volume). This means that it is the rise in pressure

at the greatest volume that should surprise us rather than the "long flat portion" in the static pressure-volume relationship of the bladder (see Fig. 1). This must be caused by an increasing elastic modulus (compare chapter III). We can conclude by stating that no active mechanisms are necessary to explain the fact that an urinary bladder can store a great deal of urine without a significant rise in pressure. A rubber balloon would do even better in this case.

V. Evaluation of total bladder model

A. Theory

1. Introduction

In the previous chapters models for the various blocks in our block diagram of Fig. 3 are proposed and tested. Furthermore, the "wall" block was divided into two blocks. This results in a block diagram as shown in Fig. 38.

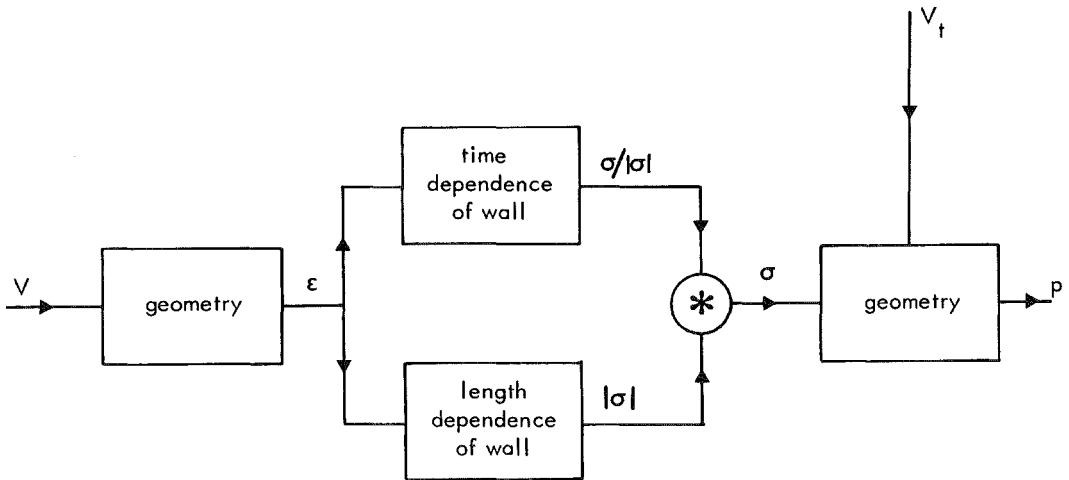


Fig. 38 - Total systems flow chart of the passive properties of the urinary bladder in the collection phase

For the first geometry block, the length dependent wall block, and the second geometry block the formulas (43), (42) in combination with (54) and (52) hold. The time dependent wall block is described by the mechanical model presented in Fig. 28. We can see that in the above mentioned relations V_t only influences the second geometry block. The connections from V_t to the other blocks could, therefore, be omitted in this block diagram.

In order to evaluate the total bladder model thus formed, we could combine all mathematical descriptions of the blocks into one differential equation. Because of the non-linearities involved, this equation would be very difficult to solve. For

certain input signals, however, such as a very slow ramp, where all the derivatives can be neglected, the equation reduces to a very simple one. That is how we will calculate the response to a "quasi-static" input signal as applied during clinical "quasi-static cystometry" in VA2. For dynamic input signals such as the stepwise volume changes described in VA3, we will use another approach viz the "following" of the signal through the block diagram by calculating the response to its specific input signal for every block.

Some problems involved in measurements on whole bladders should be mentioned here. One problem is that of the initial or unstrained volume of the bladder, related to the problem of the initial length of bladder wall strips (see chapter III). Because of relationship (43) we should first know the initial volume of the bladder in order to be able to calculate the strain involved. The initial volume, however, is very hard to determine, especially in vivo, because when the abdominal wall is not open, there is no way to tell whether the urinary bladder wall is hanging limp, just tautened or already strained. In practice we used a syringe to very slowly fill the bladder until there was a significant rise in pressure. This is a very unreliable method which undoubtedly introduces errors. However, many of the parameters of our model are independent of strain (the relaxation constants and the relative elastic moduli) and are thus not influenced by V_0 errors. For the other parameters the standard deviation will show how important this and other errors can be.

Another problem is that we have described the passive properties of the urinary bladder here. In a living animal there is no good way to eliminate active properties. In fact a great deal of spread in the amount of activity can be expected, depending upon whether anesthesia is given and how much (see VB). Two solutions are possible. We can either consider the measured responses as dominated by passive properties, or try to differentiate between phenomena caused by active and by passive properties. The latter method, however, demands a knowledge of active properties which we do not have. Therefore only the former method remains. In IIC2 we concluded that dog bladder strips showed little

spontaneous activity. Therefore we expect that the behaviour of dog bladders in vivo can be described adequately by using only passive mechanisms.

Finally formula (52) shows that we must know the value of the tissue volume of the bladder, in order to evaluate the response of the geometry block to some input signal. This value cannot be determined without opening the abdominal wall which is not always possible (for instance when performing measurements on patients). In that case an average value will have to be used (see VC) or we will have to correlate V_t to another parameter which can be determined. We will examine an example of this procedure in VC.

2. Cystometry

For a very slow ramp as input (strain) signal the mechanical urinary bladder wall model (see Fig. 28) reduces to the E_0 spring in combination with the η_0 dashpot. Assuming that the η_0 dashpot has a viscosity modulus which is too high to follow the ramp at the low stress caused by the sole E_0 spring, then only this spring remains.

We can write for the time dependent properties of the wall then:

$$\sigma = 2\epsilon E_0 \quad (55)$$

The factor 2 has its origin in the straining of the material in all directions, see relation (54). Insertion of formulas (38) and (42) yields:

$$\sigma = 2\epsilon e_0 |E| e^{\beta|E|} \quad (56)$$

From relation (52) we obtain:

$$p = \frac{2V_t}{3V} \sigma \quad (57)$$

Combining (56) and (57) with (43) finally yields:

$$p = \frac{4V_t e_0 |E|}{3} \cdot \frac{(V/V_0)^{1/3} - 1}{V} e^{\beta|(V/V_0)^{1/3} - 1|} \quad (58)$$

If therefore a cystometrogram is really quasi-statically measured, our models describe the bladder adequately, and active properties have no influence, it should

be possible to fit a curve to it according to formula (58). In Fig. 39 the dots

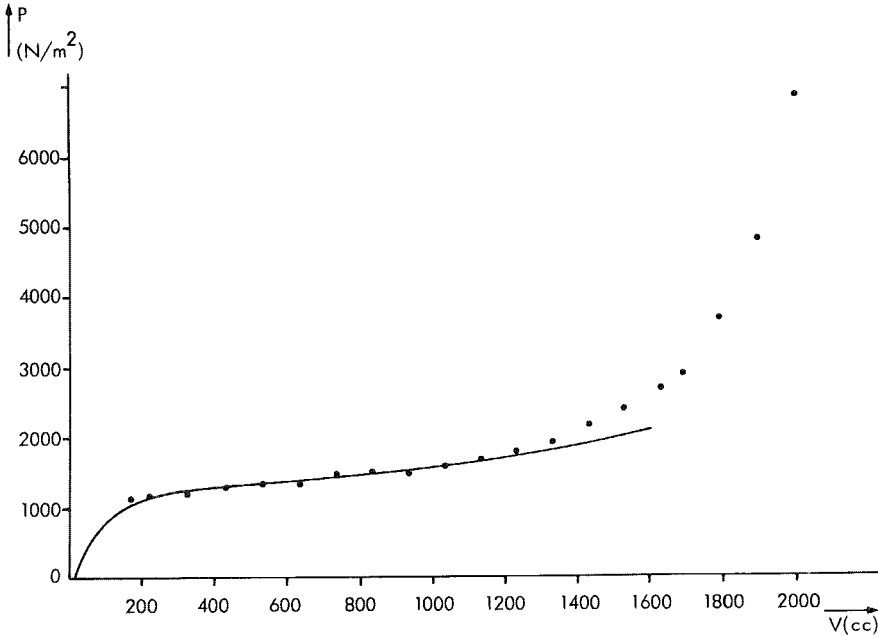


Fig. 39 - Pseudo-static cystometrogram measured on a pig bladder in vitro (dots) and fitted function (line)

represent measured data on a pig bladder in vitro. Readings were taken fifteen minutes after incremental volume increase. The line in Fig. 39 represents the pressure function derived from relation (58) with:

$$\frac{4V_0 e_0 |E|}{3} = 0.1 \text{ Nm}$$

$\beta = 0.733$ and $V_0 = 23 \text{ cm}^3$. It turned out that it was not possible to "fit" the sharply rising part of the cystometrogram. This can be ascribed to an elastic modulus function which is at high strain not mono-exponential. In Fig. 40 the dots represent the elastic modulus calculated from the cystometrogram in Fig. 39. We indeed see a deflection from a straight line at strains above 2.8 which agrees with the volume of 1227 cm^3 , up to which our fitting of the cystometrogram succeeded, in this semi-logarithmic plot. This finding is compatible with our measurements of the elastic modulus function in chapter III where, because we only measured up to

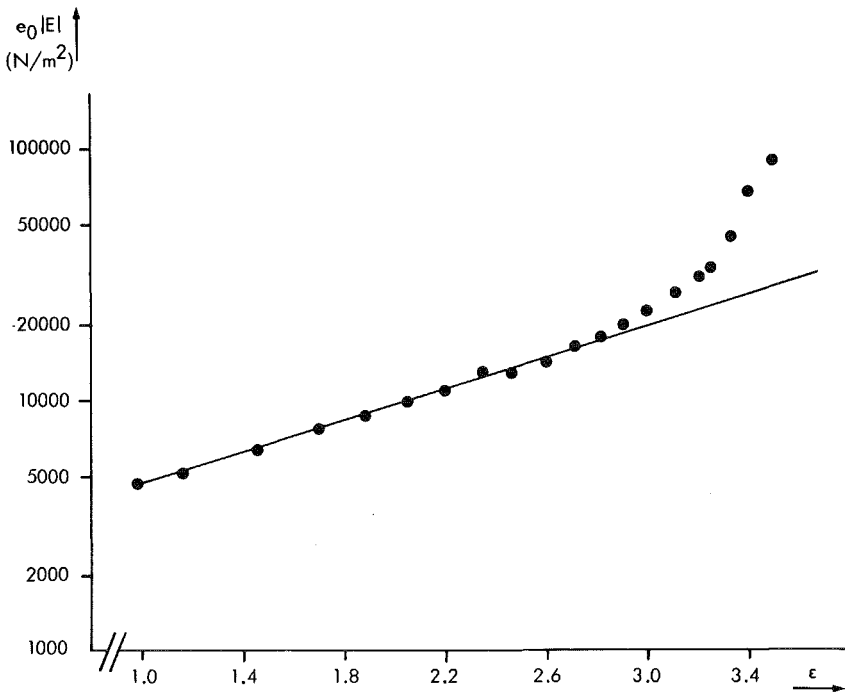


Fig. 40 - Semi-logarithmic plot of elastic modulus function derived from pseudo-static cystometrogram of pig bladder

$\epsilon = 1.6$, we were always able to fit a mono-exponential function. It should be noted that higher strains, above 1.6, were not possible in these measurements because the measurements being dynamic included all elastic moduli, and therefore would yield forces which were too high. From our cystometrogram-fitting we conclude that relation (58) describes the data adequately up to the strain where the elastic modulus function is no longer mono-exponential. It should be noted that these high strains are never reached under physiological circumstances because unless general anaesthesia is applied micturition has then already taken place.

A far more important conclusion is that we obtain from the usual clinical cystometrogram only the parameters V_0 and β and a combination of $|EI|$, V_t and e_0 from the twelve parameters which define our bladder wall model (viz V_0 ; V_t ; e_0 ; e_1 ;

$e_2, e_3, \eta_0, \gamma_1, \gamma_2, \gamma_3, |E|, \beta$). This means that such a cystometrogram displays very little information about the passive properties of the urinary bladder.

In the next section we describe a method which yields more information.

3. Step response measurements

If we apply a stepwise volume change to the urinary bladder the strain in the wall will also change stepwise. The stress in the wall will then follow the characteristic multi-exponential decay curve which has already been measured in chapter II. From formula (52) we see that at a constant volume (which we now have after the stepwise change) pressure is proportional to stress.

We can therefore expect a multi-exponential pressure decay, characterized by the same relaxation constants as measured on strips.

Concerning the information stepwise measurements display, we note the following. From one step response measurement we obtain the relaxation constants $\gamma_1, \gamma_2, \gamma_3$ (providing that we also fit these curves with three exponentials) and the relative elastic moduli e_0, e_1, e_2, e_3 . In order to evaluate these values we have to know the initial volume V_0 . If we have a measurement for the tissue volume V_t and if we do more measurements on one bladder at convenient strain levels, a correction as was used in chapter IV for pulse measurements is possible. We then also obtain the elastic coefficient $|E|$ and the elastic exponent β . In this way all the parameters except η_0 can be determined.

In practice we cannot apply a stepwise volume change, as displacement of a volume of fluid always takes time. It turned out that the volume (or strain) signal could not be considered as stepwise even at very high filling rates. Two consequences will be discussed here. The first is that the coefficients of our multi-exponential decay formula (6) will no longer reflect the elastic moduli, but will yield lower values. If we assume that the straining is performed at a constant speed we can correct the measured coefficients by calculating the response to a ramp of our model. We of course only have to do this for one spring-dashpot combination, because the others will behave similarly. Formula (5) displays the

response of one spring-dashpot combination to a stepwise straining. From the step we obtain a ramp by dividing through the step amplitude $|\epsilon|$ (thus obtaining a unit step) multiplying by the straining rate v and then integrating with respect to time.

This yields:

$$\epsilon(t) = vt \quad (59)$$

The response to this input signal is obtained by performing the same operations on formula (5):

$$F(t) = \frac{av}{\gamma|\epsilon|} (1 - e^{-\gamma t}) \quad (60)$$

At a time t_1 the ramp passes into a constant level, thus producing a "physical step". The response at time t_1 to the ramp yields the height of the mono-exponential decay or the apparent coefficient a_a . In formula:

$$a_a = \frac{av}{\gamma|\epsilon|} (1 - e^{-\gamma t_1}) \quad (61)$$

The amplitude of the physical step, or the "strain level" is determined by inserting t_1 in (59):

$$|\epsilon| = vt_1 \quad (62)$$

Combining (61) and (62) yields:

$$a_a = \frac{av}{\gamma|\epsilon|} \left(1 - e^{-\frac{\gamma|\epsilon|}{v}}\right) \quad (63)$$

From the measured or apparent coefficient a_a we therefore obtain the "real" coefficient a according to:

$$a = a_a \frac{\gamma|\epsilon|}{v} \frac{1}{1 - e^{-\frac{\gamma|\epsilon|}{v}}} \quad (64)$$

We should note, that in practice not the straining but the volume change is performed at constant speed and that we here implicitly assumed the elastic moduli to be constant, which is not the case (see chapter III), so that relation (64) yields only an approximate correction.

The second consequence from the non-stepwise character of our input signal can be

read from equation (64). If we fill a bladder with a V_0 of 20 cm^3 to 160 cm^3 at a constant rate of $10 \text{ cm}^3/\text{s}$, the strain yields:

$$\left(\frac{160}{20}\right)^{1/3} - 1 = 1$$

The volume is filled in $\frac{160 - 20}{10}$ seconds = 14 seconds, so that we can approximate the straining with a constant speed of $1/14 \text{ s}^{-1}$. The correction factor for the coefficient connected to the fastest exponential term then yields, when we insert $\gamma_1 = 1.05 \text{ s}^{-1}$:

$$\frac{14.7}{1 - e^{-14.7}} \quad \text{or almost } 15$$

The correction factor for the second coefficient will yield when inserting $\gamma_2 = 0.077 \text{ s}^{-1}$:

$$\frac{1.08}{1 - e^{-1.08}} \quad \text{or almost } 1.6$$

This means that our fastest exponential term is diminished with approximately a factor 10 more than the slower term. From Table VIII we can see that the ratio between e_1 and e_2 equals 2.5 in step response measurements on strips. In the experiment described above the ratio of the uncorrected coefficients would yield about 0.26, which means that the parameters of the fastest exponential term can hardly be determined. We conclude that with the data mentioned above at high strain levels the fastest exponential term can be neglected in which case a two-exponential model is sufficient.

B. Methods

All experiments were performed on female mongrel dogs under continuous intravenous pentobarbital anaesthesia. Dogs were used because dog bladders show less spontaneous activity (see IIC).

Most experiments were performed with open abdomen in order to avoid the influence of the abdominal wall. According to Coolsaet et al (1975a) the influence of the abdominal wall on the relaxation constants of a two-exponential model is small, but an influence exists.

A double lumen catheter was introduced into the bladder. Via one channel the bladder was filled with a physiological solution (saline) at a temperature of 37°C. The pump used was specially developed at the Technical University of Delft, Department of Medical Electronics (report nr. M110). The pump can follow an arbitrary electrical input signal up to a certain maximum flow. In fact it transforms an electrical signal into an identical volume signal at a rate of 200 cm³/volt. The maximum volume is 1000 cm³ and the maximum flow is 9.16 cm³/s. The input applied to the pump during these measurements was simply a constant voltage. Starting the pump then would cause it to fill the bladder with the maximum flow to the desired volume.

The pressure in the bladder is measured via the other channel of the catheter using a Statham pressure transducer. This means that the pressure is "transported" to the transducer by a water column. Wesseling and Van Vollenhoven (1969) investigated the accuracy, and especially the frequency response, of these catheter-manometer systems. They conclude that in the frequency range in which we are interested (up to 1 Hz, compare to sample rate) no problems occur. The transducer-amplifier system yields a total amplification factor of 20.92 mm Hg/V which means 2.791 N/m²/mV. At the pressure amplifier the amplification factor can be changed from 1.0 to 3.0 or 10.0. Using the same interface as described in IIB1 the electrical pressure signal was punched on papertape at intervals of one second during 15 minutes. Volume (as an electrical output signal from the pump) and pressure were also recorded on a two-channel strip-chart recorder. The initial

volume of the bladder was determined by slowly filling it by using a syringe, see VA1. About ten measurements were taken from each animal at intervals of fifteen minutes. The punched papertapes were converted to punch cards which were fed to an IBM 360/65 for analysis. The IBM machine was used because these measurements were performed before the in vitro experiments described in chapter II, and at that time our own mini-computer was not yet in use. The analysis method was the same as described in IIB2. After measurement the bladder was extirpated in order to determine the tissue volume. Since this volume is larger than the tissue volume of the strips (see chapter II) we could simply submerge the bladder in a measuring glass filled with water.

C. Results

It turned out, indeed, that the dog bladders showed very little spontaneous activity. Table XII shows averages and standard deviations of the relaxation constants. The averages are calculated from the measurements on seven dogs, but many measurements had to be omitted because of errors in the experimental procedure. The relaxation constants shown in Table XII are in very good agreement with the relaxation constants measured on strips, which are shown in Table VI, first row. From this agreement we conclude that our reasoning in VA3 concerning the proportionality of stress and pressure was correct and that in this case our geometry model can be applied. It should be noted that all measurements were made at a rather low strain, so that three exponentials could be fitted. With regard to isotropy it can be noted that the parameters measured on strips are representative of the parameters averaged over the total bladder (which is what we measure in vivo). Obviously anisotropy does not appear to be a serious problem.

Concerning the elastic moduli, we noted that it was not possible to draw any conclusions concerning the elastic modulus function, as these measurements were not performed in a manner which allowed correction for the increase in the initial length. In fact, as long as the experiment lasted, all kinds of trends were seen in the elastic moduli as a function of time. It should be remembered that in these experiments the influence of the active element C could not be eliminated so that even a rising trend is possible according to our model. However, the relative elastic moduli should still yield reproducible values. These are shown in Table XIII. A good comparison is again obtained with the values measured in vitro, see Table VIII. Apparently the largest difference between the values in Table VIII and XIII is found in e_1 . This parameter is the one most sensitive for the "weakening" effect due to the non-stepwise filling, as mentioned in VA3. Again we see, as in the case of strips, that the relative elastic moduli are more reproducible parameters than the relaxation constants. The average initial volume yielded 30 cm^3 with a relative standard deviation of 67% and the average tissue

$\gamma_1(s^{-1})$	$\sigma(\gamma_1)$	$\gamma_2(s^{-1})$	$\sigma(\gamma_2)$	$\gamma_3(s^{-1})$	$\sigma(\gamma_3)$	Number of measurements
0.45	69%	0.059	54%	0.0043	42%	44

Table XII - Average relaxation constants and standard deviations measured on dog bladders in vivo

$e_0(-)$	$\sigma(e_0)$	$e_1(-)$	$\sigma(e_1)$	$e_2(-)$	$\sigma(e_2)$	$e_3(-)$	$\sigma(e_3)$	Number of measurements
0.17	65%	0.36	33%	0.29	28%	0.18	28%	44

Table XIII - Average relative elastic moduli and standard deviations measured on dog bladders in vivo

volume yielded 26 cm^3 , with a relative standard deviation of 54% for the seven bladders. The ratio between initial volume and tissue volume, averages 1.1. As there is a correlation between these values (correlation coefficient: 0.87) in practice the measuring of only one of the values might be sufficient. Kondo and Susset (1973) attempted to find a relationship between V_t and the body weight without success, so that in order to obtain our parameters we still have to determine either V_t or V_0 .

VI. Conclusion

It can be concluded that dog urinary bladders in the collection phase are dominated by passive properties. Pig bladders show more active properties but the passive properties are similar to those of dog bladders. These passive properties can be described adequately in terms of the model represented by Figs. 38 and 28, and relations (43), (42), (54) and (52) in the physiological range. The following assumptions are made:

1. All parameters which reflect properties of the bladder wall in our model are independent of the place from which, and the direction in which they are measured (homogeneity and isotropy).
2. The relaxation constants and the elastic moduli relative to their sum are constant.
3. The tissue volume of the bladder wall is constant.
4. The urinary bladder is spherical.

The model involves twelve parameters viz the following:

1. The tissue volume V_t .
2. The initial volume V_0 .
3. Three relaxation constants $\gamma_1; \gamma_2; \gamma_3$.
4. The initial length viscosity η_0 .
5. Four relative elastic moduli $e_0; e_1; e_2; e_3$.
6. The elastic coefficient $|E|$.
7. The elastic exponent β .

For all parameters except η_0 averages and standard deviations have been given for dog and pig bladders. The values were obtained by various measurement techniques. The model describes adequately a "pseudo-static cystometrogram" in the physiological range. However, the sharply rising part of the cystometrogram at high volumes cannot be fitted, since here the elastic moduli do not depend mono-exponentially on strain. It might be possible to extend the model by describing the elastic modulus function with a multi-exponential function. In the

range in which the urinary bladder normally works, however, the mono-exponential function gives a satisfactory fit. As in the case of a static cystometrogram only two or three of the twelve parameters can be obtained, this method should be regarded as a poor choice for testing the passive properties of the urinary bladder. Furthermore in order to be able to measure a pseudo-static cystometrogram we have to fill the bladder at such a slow speed that the dynamical properties can be neglected. From the ramp response which we have already used in VA3 we calculate an approximation of the error in the measured pressure due to the spring-dashpot combination with the smallest relaxation constant when straining at a speed v .

This yields:

$$\text{relative error} = \frac{e_3}{e_0} \cdot \frac{v}{l e l \gamma_3} \left(1 - e^{-\frac{l e l \gamma_3}{v}} \right) \quad (65)$$

Inserting a straining speed of 0.0001 s^{-1} , a strain of 0.5 and some values from the tables we find an error of about 8%. This seems quite reasonable until we realize, that measuring the cystometrograms up to a strain of 2 would then take about six hours.

When measuring a cystometrogram up to a strain of 2 in about half an hour, the error at a strain of 0.5 yields 65%. At lower strains the error is larger, at higher strains smaller, as can be seen from formula (65).

An alternative is to measure step responses on the urinary bladder. The model describes these responses adequately. One step response measurement (which takes fifteen minutes) yields eight parameters (supposing we have been able to estimate the initial volume V_0) and more measurements on one bladder yield ten parameters.

We conclude therefore that this is a superior way of testing the passive properties of the urinary bladder.

Finally, of the twelve parameters, nine describe properties of the bladder wall.

Values for these parameters can be measured on isolated strips of bladder wall and

can be compared with the values measured in vivo.

Concerning future developments, two directions can be seen. First the model can be extended with active properties, which may be measured in the evacuation phase. Secondly the model must be tested on human bladders. If applicable, which seems likely (one human bladder strip was tested and the results could be adequately described by our model), the parameters of the model determined by step response measurements would display more information than a cystometrogram does. We could therefore expect it to be a better diagnostic tool. Pattern recognition techniques can be applied to obtain "normal" values for the parameters and test for significant deviations.

Summary

In the working cycle of the urinary bladder two phases can be distinguished, the collection phase in which the urine produced by the kidneys is collected in the urinary bladder, and the evacuation phase in which the collected urine is expelled. In the collection phase, passive properties (i.e. properties which do not involve an energy production) are important. In this thesis a model is presented describing the passive properties of the urinary bladder in the collection phase. A systems approach is used. The system under investigation, which is defined in terms of a pressure-volume relationship, is divided into four subsystems or blocks, viz two geometry blocks, a block describing the time dependent properties of the bladder wall, and a block describing the length dependent properties of it. Models are developed and tested for each block separately. The geometry is described as a thick-walled sphere with a constant tissue volume. The time dependence of the properties of the wall can be explained using a visco-elastic model, and the length dependence of the wall properties is shown to yield elastic moduli which depend mono-exponentially on strain. Estimates for the parameters involved are obtained merely from experiments on strips of urinary bladder, obtained from the local slaughterhouse.

By assembling the blocks, a total model of the passive properties of the urinary bladder in the collection phase is obtained. The model contains twelve parameters. The classical way of investigating the urinary bladder by filling it slowly and measuring the pressure produced, yields a pseudo-static pressure-volume relationship which is called a cystometrogram. The model predicts the form of the cystometrogram in the physiological range.

An extension could be made in order to be able to describe cystometrograms at higher volumes, but this, however, did not seem very useful.

A classical cystometrogram enables us to determine only three parameters of our model. A better measurement method is to perform stepwise (or almost stepwise) strainings of the urinary bladder. One stepwise straining yields eight parameters,

provided the initial volume of the bladder is known, and more measurements on one bladder enable us to determine ten parameters. The results obtained with stepwise strainings are compatible with the model.

Samenvatting

De urineblaas werkt in twee fasen, namelijk de collectiefase en de evacuatiefase. In de collectiefase wordt de door de nieren geproduceerde urine opgeslagen in de blaas, en in de evacuatiefase wordt de opgeslagen urine via de urethra geloosd. In de collectiefase is geen energieproductie (door metabolisme) nodig, deze fase wordt gedomineerd door passieve eigenschappen. In dit proefschrift is een model beschreven dat de passieve eigenschappen van de urineblaas in de collectiefase beschrijft. Er is gebruik gemaakt van de systeembenadering. Het te onderzoeken systeem is opgesplitst in vier onafhankelijke subsystemen of blokken, waarvan er twee de geometrie van de blaas beschrijven. Het derde en vierde blok beschrijven respectievelijk de tijd- en lengte-afhankelijke eigenschappen van de wand van de blaas. Voor de afzonderlijke blokken zijn modellen gemaakt en getest. De geometrie wordt beschreven als een dikwandige bol, met een konstant weefsel-volume. De tijdafhangelijkheid van de wand van de blaas wordt beschreven met behulp van een visco-elastisch model en de lengte-afhankelijkheid wordt hierin verwerkt door de elasticiteitsmoduli mono-exponentieel van de rek te laten afhangen. Schattingen voor de parameters van de modellen zijn verkregen aan de hand van experimenten op stukjes varkensblaasweefsel uit het abattoir. Door alle blokken samen te voegen is een totaal model van de passieve eigenschappen van de urineblaas in de collectiefase verkregen. Het totaalmodel bevat twaalf parameters. De klassieke manier om de werking van de urineblaas klinisch te evalueren bestaat uit het langzaam vullen van de blaas terwijl tegelijkertijd de druk in de blaas wordt gemeten. De zo verkregen quasi-statische volume-druk relatie wordt cystometrogram genoemd. Het model beschrijft adequaat een cystometrogram in het fysiologisch bereik. Een uitbreiding van het model om een cystometrogram te "fitten" voor hogere volumina is mogelijk. Een klassiek klinisch cystometrogram stelt ons in staat om op zijn best drie van de twaalf parameters van ons model te schatten. Een goed alternatief is om de blaas stapvormig (fysisch) te rekken, en de verkregen drukresponsie te fitten met een som

van drie e-machten en een konstante. Een dergelijke meting levert schattingen op voor acht van de twaalf parameters, aangenomen dat het "ongerekte volume" van de blaas bekend is. Meerdere metingen aan dezelfde blaas leveren schattingen op voor tien parameters. Metingen werden verricht aan honden. De resultaten stemmen overeen met wat verwacht kon worden aan de hand van stripjesmetingen.

References

- Åberg, A.K.G. and Axelsson, J. (1965)
"Some mechanical aspects of intestinal smooth muscle"
Acta Physiol. Scand. 64, pp. 15-27
- Alexander, R.S. (1957)
"Elasticity of muscular organs"
in Remington, J.W. (1957)
- Alexander, R.S. (1971)
"Mechanical aspects of the urinary bladder"
American Journal of Physiology 220-5, pp. 1413-1421
- Apter, J.T. and Graessly, W. (1969)
"A relation between positive phase shift and elastic modulus enhancement
of smooth muscle"
Experientia 25-2, pp. 145-147
- Apter, J.T. and Graessly, W.W. (1970)
"A physical model for muscular behaviour"
Biophysical Journal 10, pp. 539-555
- Apter, J.T. and Mason, P. (1971)
"Dynamic mechanical properties of mammalian ureteral muscle"
American Journal of Physiology 221-1, pp. 266-272
- Apter, J.T., Mason, P. and Lang, G. (1972)
"Urinary bladder wall dynamics"
Investigative Urology 9-6, pp. 520-526
- Ausems, M.M. (1957)
"De cystometrie, haar betekenis voor het onderzoek en de therapie bij
functiestoornissen van de blaas" - Thesis
- Axelsson, J. (1970)
"Mechanical properties of smooth muscle etc."
In Bülbring, E. (1970)

Bradley, W., Clarren, S., Shapiro, R. and Wolfson, J. (1968)

"Air cystometry"

Journal of Urology 100, pp. 451-455

Brody, D.A. and Quigley, J.P. (1948)

"Some mechanical factors in the dynamics of the thin-walled, sphere viscus"

Bulletin of Mathematical Biophysics 10, pp. 25-30

Bülbring, E. (1970)

"Smooth muscle"

Edward Arnold Ltd., London

Christensen, R.M. (1971)

"Theory of visco-elasticity, an introduction"

Academic Press, New York

Coolsaet, B.L.R.A., Duyl, W.A. van, Mastrigt, R. van and Zwart, A. van der (1973)

"Stepwise cystometry of urinary bladder"

Urology 11-3, pp. 255-257

Coolsaet, B.L.R.A., Duyl, W.A. van, Mastrigt, R. van and Zwart, A. van der (1975a)

"Visco-elastic properties of the bladder wall"

Urologia Internationalis 30, pp. 16-26

Coolsaet, B.L.R.A., Duyl, W.A. van, Mastrigt, R. van and Schouten, J.W. (1975b)

"Visco-elastic properties of bladder wall strips"

Investigative Urology 12-5, pp. 351-356

Coolsaet, B.L.R.A., Mastrigt, R. van, Duyl, W.A. van and Huygen, R.E.F. (1976)

"Visco-elastic properties of bladder wall strips at constant elongation"

Investigative Urology 13-6, pp. 435-440

Coolsaet, B.L.R.A. (1976)

"De visco-elastische eigenschappen van de urineblaas"

Aggregaatsthesis, Antwerpen

Douglas, W.R. (1972)

"Of pigs and men and research"

Space Life Sciences 3, pp. 226-234

Draper, N.R. and Smith, H. (1967)

"Applied regression analysis"

John Wiley and Sons, London

Duyf, W.A. van (1974)

"Measurement of cerebral circulation, physical and mathematical aspects
in using radio-active clearance methods"

In: Ghista, D.N., Yang, W.J. and Vollenhoven, E. van

"Cardiovascular Physics" vol. II

Delft University Press

Duyf, W.A. van, Zwart, A. van der and Rikken, H. (1976)

"An electronic device for a quick analysis of exponential decay curves"

To be published

Frank, O. (1906)

"Die Analyse Endlicher Dehnung und die Elastizität u.s.w."

Annalen der Physik 21, pp. 602-608

Frank, O. (1910)

"Die Dehnung einer kugelförmigen Blase"

Zeitschrift für Biologie 54, pp. 531-532

Frank, O. (1928)

"Das aufblähen von Schläuchen und kugelförmigen Blasen"

Zeitschrift für Biologie 88, pp. 93-104

Fung, Y.C.B. (1968)

"Biomechanics, its scope, history and some problems of continuum
mechanics in physiology"

Applied Mechanics Review 21-1, pp. 1-20

Fung, Y.C.B., Perrone, N. and Anliker, M. (1972)

"Biomechanics, its foundations and objectives"

Prentice Hall Inc., Englewood Cliffs, New Jersey

- Gardner, D.G., Gardner, J.C., Lansk, G. and Meinke, W.W. (1959)
"Method for the analysis of multi-component exponential decay curves"
J. of Chem. Phys. vol. 31-4
- Glantz, S.A. (1974)
"A constitutive equation for the passive properties of muscle"
J. Bioch. Mech. 7, pp. 137-145
- Goedhard, W.J.A. (1971)
"Visco-elastische eigenschappen van de arterie-wand"
Thesis, Vrije Universiteit Amsterdam
- Harding, V. (1952)
"Über eine Methode zur Messung der dynamischen Elastizität u.s.w."
Helv. Physiol. Acta 10, pp. 482-489
- Hill, A.V. (1926)
"The viscous elastic properties of smooth muscle"
Proc. Roy. Soc. London 100, pp. 108-115
- Hill, A.V. (1949)
"The abrupt transition from rest to activity in muscle"
Proc. Roy. Soc. London 136, pp. 399-420
- Hinman, F. and Miller, E.A. (1964)
"Mural tension in vesical disorders and ureteral reflux"
Journal of Urology 91-1, pp. 33-40
- Jamison, C.E., Marangoni, R.D. and Glaser, A.A. (1968)
"Visco-elastic properties of soft tissue by discrete model characterization"
Journal of Biomechanics 1, pp. 33-46
- King, A.L. (1946)
"Law of elasticity for an ideal elastomer"
Am. J. of Physics 14, pp. 28-30
- King, A.L. and Lawton, R.W. (1950)
"Elasticity of body tissue" - In: Glaser, O.
"Medical Physics" II, pp. 303-316 - Year Book Publishers Chicago

King, A.L. and Lawton, R.W. (1971)

"The elasticity of soft body tissues"

The Scientific Monthly, pp. 258-260

Kirkegaard, D. (1970)

"A Fortran IV version of the sum-of-exponential least squares code exposum"

Danish Atomic Energy Commission, report Risø-M-1279

Research Establishment, Risø

Kondo, A. and Susset, J.G. (1973)

"Physical properties of the urinary detrusor muscle"

J. Biomechanics 6, pp. 141-151

Kuik, A.J. (1975)

"Over de haalbare nauwkeurigheid bij het schatten van de parameters van multi-exponentiële modellen"

Kandidaatsverslag Laboratorium voor Technische Natuurkunde, Delft

Kuik, A.J. (1976)

"Estimation of the parameters of a multi-exponential signal"

Afstudeerverslag deel I, Laboratorium voor Technische Natuurkunde, Delft

Kunov, H., Vachon, B.R. and Zingg, W. (1975)

"A hydraulic pouch method for assessing muscle dynamics"

Medical and Biological Engineering 13-1, pp. 64-70

Lamé, M.G. (1852)

"Leçons sur la theorie mathematique de l'elasticité des corps solides"

Paris, Bachelier, Imprimeur-libraire du Bureau des Longitudes et de L'école Polytechnique

Lanczos, C. (1956)

"Applied analysis"

Prentice Hall Inc., Englewood Cliffs, New York

Langley, L.L. and Whiteside, J.A. (1951)

"Mechanism of accomodation and tone of the urinary bladder"

Journal of Neurophysiology 14, pp. 147-152

Lee, Y.W. (1960)

"Statistical theory of communication"

John Wiley & Sons, New York

Liew, H.D. van (1967)

"Graphic analysis of aggregates of linear and exponential processes"

J. Theor. Biol. 16, pp. 43-53

Lippold, O.C.J. and Winton, F.R. (1968)

"Human physiology"

J. and A. Churchill Ltd., London

Love, A.E.H. (1927)

"A treatise on the mathematical theory of elasticity"

Cambridge University Press

Matsumoto, Y. and La Grange, R. (1973)

"Dog bladder pressure-volume relation determined from isolated strip of wall muscle, force-length curve"

Life Sciences 12-1, pp. 565-576

Mayer, C.J., Breemen, C. van and Casteels, R. (1972)

"The action of lanthanum and D600 on the calcium exchange in the smooth muscle cells of the guinea-pig, teania coli"

Pflügers Archiv 337

Melchior, S.N. (1973)

"Urodynamik"

Zeitschrift für Urologie, Heft 6, pp. 459-462

Zeitschrift für Urologie, Heft 7, pp. 521-524

Mosso, A. et Pellacani, P. (1882)

"Sur les fonctions de la vessie"

Arch. Ital. Biol. 1, pp. 97-

Nauta Lemke, H.R. van, Feikema, H., Honderd, G., Pleeging, M. and Verbruggen, H.B. (1972)

"Grondslagen van de regeltechniek" - Het Spectrum, Utrecht

Nyström, K., Bjerle, P. and Lindquist, B. (1973)

"Suprapubic catheterization of the urinary bladder as a diagnostic procedure"
Scand. J. Urol. Neph. 7, pp. 160-164

Osborne, W.A. and Sutherland, W. (1909)

"The elasticity of rubber balloons and hollow viscera"
Proc. Roy. Soc. London, Series B, 81, pp. 485-499

Rabiner, L.R. and Gold, B. (1975)

"Theory and application of digital signal processing"
Prentice Hall Inc., Englewood Cliffs, New Jersey

Ray, C.D. (1974)

"Medical engineering"
Year Book Publishers Chicago

Remington, J.W. (1957)

"Tissue elasticity"
American Physiological Society, Washington D.C.

Rose, J.G., Gillenwater, J., Attinger, F., Sim, P. and Wyker, A.T. (1973)

"Ureteral wall tension"
Investigative Urology 10-6, pp. 480-485

Ruch, T.C. and Patton, H.D. (1966)

"Physiology and biophysics"
W.B. Saunders Company, Philadelphia and London

Simeone, F.A. and Lampson, R.S. (1937)

"A cystometric study of the function of the urinary bladder"
Annals of Surgery 106, pp. 413-422

Sparreboom, D., Duyl, W.A. van, Pfaff, R. and Poelgeest, R. van (1976)

"An evaluation of the inverse Laplace transform method for the analysis
of multi-component exponential decay curves"
To be published

Späth, H. (1966)

"Algorithm 315. The damped Taylor's series for minimizing a sum of squares and for solving systems of non-linear equations"

Collected Algorithms from CACM, 315-P1-0

Stacy, R.W., Williams, D.T., Worden, T.E. and McMorris, R.O. (1955)

"Essentials of biological and medical physics"

McGraw Hill Book Co. Inc., New York

Vocke, W. (1969)

"Räumlichen Probleme der linearen Elastizität"

Veb Fachbuch Verlag Leipzig

Wesseling, K.H. and Vollenhoven, E. van (1969)

"Catheter-manometer systems"

TNO-Nieuws 24-11, pp. 603-616

Williams, J.D. (1954)

"The compleat strategyst"

McGraw Hill Book Co. Inc., New York

Winton, F.R. and Bayliss, L. (1968)

"Human physiology"

J. and A. Churchill Ltd., London

Curriculum vitae

op verzoek van de Erasmus Universiteit Rotterdam

De schrijver van dit proefschrift werd op 29 juli 1950 geboren te Rotterdam. Hij verkreeg in 1967 het einddiploma HBS-B te Delft, en studeerde in 1972 cum laude af als natuurkundig ingenieur aan de Technische Hogeschool aldaar. Op 1 mei 1972 trad hij in dienst van de afdeling Urologie van de Medische Faculteit Rotterdam, en werd als gast ondergebracht in de afdeling Biologische en Medische Natuurkunde.

Urodynamisch onderzoek werd en wordt door hem verricht in samenwerking met B.L.R.A. Coolsaet van de afdeling Urologie en W.A. van Duyl van de afdeling Biologische en Medische Natuurkunde.